Neuroethology of cooperative behavior in *Drosophila* larvae

Mark Yuryevich Dombrovski

Rostov-on-Don, Russian Federation

B.S., Moscow State University, 2012

A Dissertation presented to the Graduate Faculty of the University of Virginia in Candidacy for the Degree of Doctor of Philosophy

Department of Biology

University of Virginia

August 2019

Table of Contents

List of abbreviations

PR – photoreceptor
Rh5 – rhodopsin 5
Rh6 – rhodopsin 6
BO – Bolwig's organ
LON – larval optic neuropil
lOLP – local optic lobe pioneer neuron
glu-lOLP – glutamatergic local optic lobe pioneer neuron
cha-lOLP – cholinergic local optic lobe pioneer neuron
VPN – visual projection neuron
CP – critical period
GFS – giant fiber system
ORN – olfactory receptor neuron
TM3, **TM6B**, **CyO** – *Drosophila* balancer chromosomes
hAEL – hours after egg laying
brp – Bruchpilot (presynaptic active zone marker in *Drosophila*)
GFP – green fluorescent protein
L1-L2-L3F$_n$ – *Drosophila* larval instars (developmental stages)
VGluT – vesicular glutamate transporter
UAS – upstream activating sequence
WT – wild type
CS – Canton S (wild type *Drosophila* strain)
LacZ – β-galactosidase (used as an epitope tag)
HA – hemagglutinin (used as an epitope tag)
SEM – standard error of the mean
ANOVA – analysis of variance

Project Summary

Cooperative behavior amongst animals has been of great interest to science. However, the fundamental rules and mechanisms governing the formation, structure and interactions within social groups have proven difficult to elucidate. Neuronal, genetic and molecular rules that determine an individual's ability to belong to a particular social group remain largely unknown. Moreover, identification of short- and long-term effects of the environment on the genes, circuits and behaviors that affect sociality has been a task of great complexity. The major reason behind it is a lack of a laboratory model system available in conditions that would permit to easily manipulate the behavior, physiology and genetics of an individual, thereby allowing to evaluate its contribution to organization and stability of a social structure. The main message of my thesis is an establishment a new neuroethological experimental model system that features cooperative foraging behavior emerging among larval *Drosophila melanogaster*. The proposed model system has several advantages. It involves a complex behavior with a social component that occurs in natural conditions, which develops during a restricted time window, and therefore can be used to address all of the abovementioned questions. At the same time, it allows to use a large array of molecular and genetic tools available for fruit fly thereby making it possible to implement an integrative multidisciplinary approach. Throughout my work, tools and methodology adapted from behavioral neuroscience, developmental and molecular neurobiology and

evolutionary biology were used to sequentially dissect various aspects of this emerging cooperative behavior model.

The first part of my work describes mechanistic features and behavioral aspects of cluster-like digging structures formed by *Drosophila* larvae in the liquefied processed food (Figure 1A), where they engage in highly synchronized digging movements. On a basis of a directed genetic screen we showed that vision serves as a crucial sensory modality for formation and stability (thus providing an example of a novel type of photobehavior in fruit fly larvae). Next, we investigated a contribution of an individual to overall group stability and proposed a mechanism for group cooperation. Using customized tracking software, we identified that individual larvae are able to use visual cues to follow their immediate neighbor's movements and therefore maintain minimal time disparities within a cluster to support integrity of the digging structure (Figure 1B). Moreover, we also demonstrated that this trait requires prior visual and social experience during a restricted developmental period. Therefore, we characterize clustering as a learned visually guided cooperative behavior and hypothesized that its emergence is

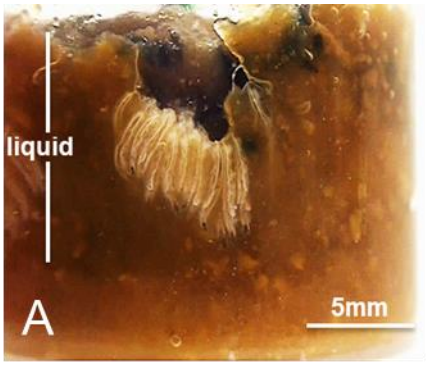

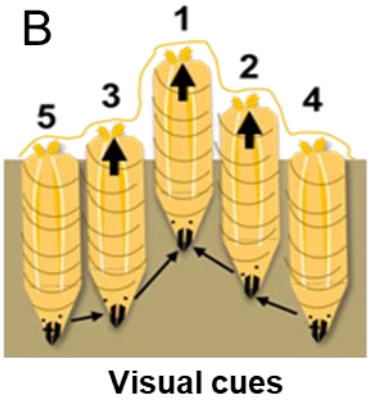

Figure 1
A. Cooperative larval clusters emerging in liquid food
B. Proposed model for visually guided intra-cluster cooperation

associated with experience-dependent plasticity in the underlying neuronal circuits.

The second part of my work originates directly from our previous findings and delves deeper into identifying specific circuits of the larval visual system underlying cooperative behavior. I find that synaptic plasticity that occurs in these circuits making them susceptible to experience-dependent rearrangements. It has been established that larval visual system comprises two parallel input pathways originating from Rh5- and Rh6-photoreceptors converging onto a set of lOLP interneurons (Figure 2). Using a combination of behavioral, genetic and physiological approaches we show that, while Rh5 pathway is responsible for general light-dark discrimination, Rh6-lOLP pathway acts as a movement-detecting module that is specifically implicated in visually guided cooperation during clustering behavior. Moreover, we further demonstrate that Rh5 pathway represents a hard-wired circuit, while Rh6-lOLP pathway is susceptible to experience-dependent pre- and postsynaptic morphological and functional plasticity, thereby serving a cellular substrate for larval social learning that occurs during a critical period early in development.

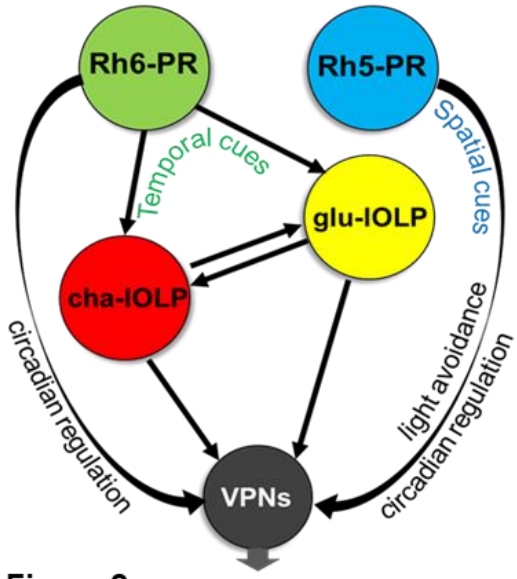

Figure 2
Schematic view of larval visual circuit

The final part of my work looks at ecological and evolutionary role of clustering behavior. We hypothesize that engagement into socially foraging groups may have an evolutionary advantage over solitary digging. We demonstrate that in conditions of high population density when access to food resources is limited and the level of competition is high, clustering animals display greater fitness that comes as a result of increased duration of the larval stage. This finding justifies the importance of early social learning that determines group membership in the future to provide trophic benefits (Figure 3).

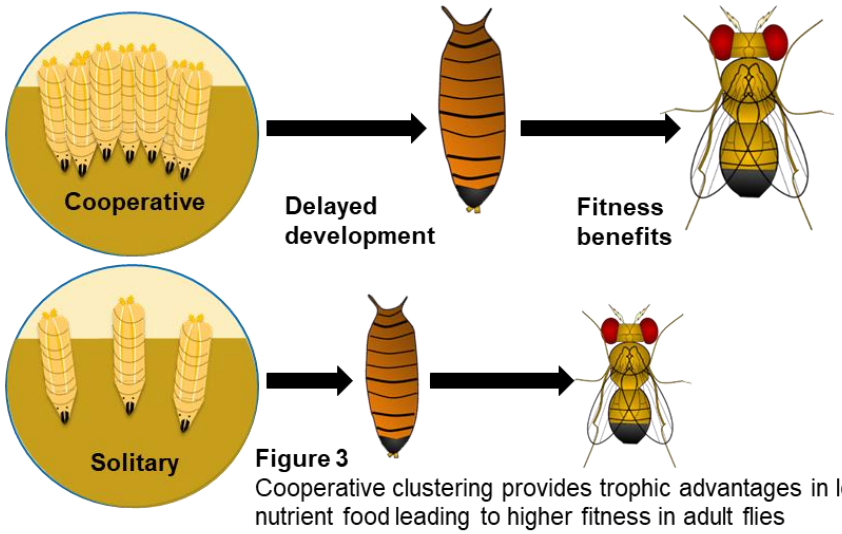

Figure 3
Cooperative clustering provides trophic advantages in low-nutrient food leading to higher fitness in adult flies

In summary, we characterize a novel type of visually guided collective behavior in fruit fly larvae that requires sensory input during a critical developmental window, provide an example of how social environment promotes the emergence of cooperative behavior on a cellular level, and suggest an evolutionary advantage that supports larval cooperative structures. This experimental model system creates a framework for further addressing fundamental questions in neurobiology and ecology, answers to which are yet to be found.

Acknowledgements

I would primarily like to thank my mentor Barry Condron for his invaluable help and support throughout my 4-year stay in his lab. I am forever grateful that he made a decision to entrust me, a newly recruited graduate student, one of the big projects emerging in the lab that I started working on and that has yielded in great results, including two high-impact publications and two more papers currently in preparation, all of which have formed the basis of my thesis. Barry has proved to be a very attentive, understanding and demanding advisor who kept coordinating the course of my research, but at the same time gave me the freedom of choice and action where it was necessary and beneficial for my growth as a scientist. His reasonable equanimity and composure in solving many difficult tasks never ceased to amaze me, and Barry's advice and recommendations have proved very valuable to me in situations where everything seemed to be going badly and not working properly, which is an unpleasant but integral part of a graduate student's life. It is important to mention that Barry has always highlighted the importance and supremacy of implementing a purely scientific approach and critical thinking to any problem, which is something that defines a true scientist regardless of the field he works in. This is one of the most valuable things that I learned over the years spent in Barry's lab and hope to maintain and take advantage of this knowledge throughout my career. Overall, it has been an incredibly rewarding and enjoyable experience for me to work under Barry's supervision for the past 4 years.

I would also like to thank members of my thesis committee: Ali Guler, Dorothy Schafer, Dan Meliza and Sarah Siegrist have all provided me with insightful feedback and discussions full of constructive criticism during my Qualifying Exam and subsequent Committee Meetings, thus largely determining and coordinating the course of my research. Importantly, each of them was always supportive and willing to kindly share advice and recommendations in situations when I needed help. In this regard, I would like to specifically highlight the role Dorothy Shafer has played in my life and career. Being a DGS during my recruitment to the UVA, she largely contributed to me making a final decision to join the Department of Biology at UVA. Later on, she helped me a lot with accommodation and organizing my life during my first week in Charlottesville, for which I am extremely grateful.

Many faculty members at the Department of Biology and outside it have provided me with much help and support throughout my stay in Charlottesville. I would like to thank Chris Deppmann, Jay Hirsh, Alan Bergland, George Bloom, Robert Cox, Iggy Provencio, Tony Spano, JC Cang, Adrian Halme, Michelle Bland and many others for sharing valuable advice, recommendations and resources.

I value and highly appreciate the help of all Condron lab members that I had a chance to interact with during my stay in the lab. It was a delight to work alongside with everyone, and many current and former lab members have made significant contributions to research I have been working on. Undergraduate students Elizabeth Schott, Nick Hogan, Leanne Poussard, Kamilia Moalem and Hunter Shelton, as well as lab technicians Rives Kuhar and Allie Mitchell have

been acknowledged as co-authors in publications that emerged from our lab in the last 4 years. I am also grateful to Andrea Vaccari from the Department of Electrical Engineering for his help with software design and recommendations.

Finally, I would like to thank my friends and my family in the United States, Russia and Israel who have been an essential part of my non-scientific life during the past 5 years and proved to be sources of inspiration and motivation for my work. All of my current results and achievements would have been impossible or meaningless without their love, support and appreciation.

Chapter 1

Introduction

Critical developmental periods: what can be learned from *Drosophila*?

Key principles and classic models of critical periods

Experience-dependent synaptic plasticity is a complex process inherent to a nervous system that allows it to stably store variable environmental information so as to guide appropriate future behavioral responses [1,101]. Certain parts of the brain, such as the mammalian hippocampus and mushroom bodies in arthropods, remain susceptible to experience-dependent rearrangements throughout an animal's life [92,103,164]. In contrast, some types of plasticity are spectacularly restricted to a specific time, a critical period, that very often occurs early in postnatal development and is manifested by exceptional sensitivity of the brain to external sensory experience, resulting in underlying circuits being irreversibly shaped by environmental input [18,106]. The key aspects to plasticity taking place during a critical period is that it has distinct temporal points of onset and termination, requires a particular type of sensory experience and yields a robust phenotype that remains unchanged for the rest of animal's life. This can vary from stereotyped patterns of motor behavior to complex social traits that require the

engagement of multiple sensory modalities [18,106]. Perhaps one of the best described phenomena illustrating these principles is imprinting, a form of learning in which a young animal acquires characteristics of a certain stimulus to further adjust its behavioral responses to it, therefore ethologically integrating itself into a favorable social environment with subsequent benefits in survival and reproduction [112,201]. A classic example of imprinting features newly hatched bird chicks that narrow down their social attachment to the first object they are visually exposed to [23,146]. Food and prey imprinting have been observed in reptiles and invertebrates, where early visual [52], olfactory [28,176] or gustatory [27] familiarization with a particular alimentary stimulus consolidates and secures foraging and hunting habits for a lifetime. Finally, social behavior often serves to help aggregate sibs which are most similar genetically [64]. Early observations of conspecifics with their intrinsic characteristics of appearance and behavior necessary for subsequent establishment of mating preferences has been described as sexual imprinting in birds [16,111,114], a particular form of which is argued to be inherent to humans [241]. Apart from classic imprinting featuring examples of fundamental behaviors like feeding, mating and predator escape, more complex socially relevant traits that naturally occur in the animal kingdom are also susceptible to emergence during critical developmental periods. These embrace social interactions between individuals in multiple mammalian taxa [66,76] including development of speech perception [239] and acquisition of new languages in humans [73,93,110], as well as general integration into a social environment [20]. These processes likely result from cumulative critical periods

representing heightened sensitivity to experience of multiple sensory systems. However, all of the above models serve only descriptive and observational purposes. At the same time, molecular and cellular mechanisms that control timing, duration and closure of restricted periods associated with increased experience-dependent plasticity in early postnatal life have yet to be determined [96]. Assessment of the relative contribution of genetics and environment to plasticity in the brain, understanding complex interplay between structural and functional remodeling of neuronal networks as well as the degree of reversibility of these changes and its temporal dynamics require deeper investigation. This becomes especially important in light of understanding the nature of pathological processes that specifically occur during experience-sensitive periods in the nervous system development [152] and cause life-term consequences for brain function including learning disabilities, schizophrenia, autism and other complex psychiatric disorders [131,138,148]. Being able to use this knowledge to genetically and pharmacologically manipulate the course and duration of a critical period might have an enormous therapeutic potential for a variety of developmental cognitive disabilities, and identification of cellular and molecular targets for these manipulations now becomes one of the top priorities for translational neuroscience [162]. Moreover, an opportunity to restore adult brain sensitivity to environmental input might also contribute to enhancement of recovery process from brain injuries and stroke that is severely limited due to restrained levels of plasticity in the aging brain [97,172]. A lot of insights over the last decades came from model systems looking at experience-dependent plasticity in higher-order brain regions of

vertebrates. Thus, development of mammalian visual cortex is tightly associated with critical periods for ocular dominance plasticity and binocular matching [68, 89,142], during which a lack of proper sensory input from one eye results in a dramatic and irreversible shift in ocular dominance leading to predominance of an open eye inputs into the cortical cells and permanent loss of binocular vision [105,240]. Similarly, rodent auditory cortex was also shown to have a critical developmental period for structural and functional maturation of a frequency map which is sensitive to external acoustic input [35]. Another great example is experience-dependent plasticity in the auditory components of songbirds during early vocal learning [167,168], where the original memory of a “tutor” song is being acquired within a limited sensory critical period and then gradually matched with a proper vocal output later in development [22]. For both model systems, cellular substrates and circuit mechanisms [38,151,199,233,244,245] as well as particular molecular determinants [134,187,226] underlying developmentally restricted plasticity were identified, including ones that regulate specific timing of a critical window opening [56,104]. However, the complexity of *in vivo* mammalian and avian models has slowed progress in further elucidating molecular and circuit mechanisms underlying experience-dependent plasticity and bringing these mechanisms together. These limitations are becoming more critical with the growing opportunity to use sophisticated genetic and molecular manipulations with a simultaneous assessment of complex behaviors including social interactions between individuals. A simpler invertebrate model of a critical period is of great value to this area of study.

Critical developmental windows in *Drosophila*

Here we describe a set of critical windows occurring at different developmental stages in *Drosophila*, a genetically tractable and experimentally accessible model organism displaying an array of complex behaviors. Recent advances in *Drosophila* neurobiology have developed an amazing set of tools and techniques that allow ultra-specific targeting of individually identifiable neurons with transgenic drivers library [116], assessment of their functional connectivity [37,69] and manipulating activity *in vivo* using optogenetics [113] and other sophisticated tools [173]. These opportunities are coupled with a continuing work targeted at generating precise maps of *Drosophila* brain circuits [170,219] including full or partial reconstruction of an entire brain connectome [218,243,247]. All of this allows to correlate sophisticated data in molecular biology and cellular physiology with high-throughput behavioral readout using fruit fly as a model system, therefore building an integrative neuroethological model of experience-dependent plasticity that occurs at critical developmental stages.

Embryonic stage

Starting from embryonic stage, *Drosophila* provides examples of how sensory input within a limited time window is required to sculpt a functional circuit (Table 1). Thus, a great example is development of motor circuits required for larval peristaltic locomotion [132]. Several studies have identified that, while circuits responsible for crawling develop independently of any external sensory

input during embryogenesis, its maturation into a functional sensorimotor circuit responsible for the actual locomotion pattern (speed and polarity of movements) is hugely affected by a feedback from a set of sensory neurons conveying sensory information of the animal's own movements [212]. Moreover, later work showed that inhibition of synaptic transmission between sensory chordotonal organs (ChO neurons) and motor neurons for only a short time frame in late embryonic development (16-20h AEL) is sufficient to cause profound and irreversible effects on locomotion seen in 2nd and 3rd larval instars [77]. This serves a classic model of experience-dependent plasticity occurring in a narrow critical developmental window. Importantly, this time period coincides with a time when ChO sensory neurons develop their axon terminals [132], indicating that critical period plasticity might imply fine-scale synaptic refinement process that occurs in an activity-dependent manner. In support of this notion, several studies have shown that endogenous activity in developing motor networks [50] and neuromuscular junctions [115] during critical periods was necessary for synaptic development and proper circuit function. Consistent with that, manipulations with levels of neuronal activity during restricted periods of embryogenesis were shown to affect seizure-like phenotypes in adult animal [81], therefore largely contributing to establishment of a fruit fly model of epilepsy. Although attempts were made to identify cellular and molecular mechanisms regulating neuronal excitability and structural homeostasis during embryogenesis [160,228], further assessment of molecular determinants underlying synaptogenesis in *Drosophila* embryonic models might be of great value to translational research, considering the relevance of circuit

assembly and refinement during critical developmental periods for understating human neurodegenerative disorders [57]. In particular, growing evidence of the role of exosomes in synaptic development [107], including rapidly emerging evidence about the role of Arc protein in *Drosophila* for exosome-dependent intercellular signaling [10,171] might represent one of the central topics for future investigation in this field. Finally, considering the fundamental role of accurate timing and sequence of cellular and molecular events occurring during embryonic stage, there is no surprise that a multitude of key transcription factors that regulate embryonic patterning, and segment polarity work in very short and temporally restricted developmental windows [51,209], and this high temporal precision makes any rearrangement an irreversible and critical event. In addition, distinct neural maps such as the myotopic map develop within specific developmental windows [135]. However, little or no evidence of any sensory and neural input involved in these processes.

Pupal stage

Pupal development in *Drosophila* is also manifested by wide scale rearrangements involving formation of neuronal circuits that specify simple and complex behaviors in the adult animal, many of which are restricted to specific critical periods as well (Table 1). Development of giant fiber system (GFS) that mediates escape response in *Drosophila* starts during pupal stage and represents an interesting model in this context. Temporal pattern of synaptogenesis between the giant fiber axon and a descending motor neuron was examined with high

precision [161], suggesting that a particular step in synapse formation (maturation of a growth cone) might be rate-limiting for this process, occurs in a critical time window and requires the function of a specific axon guidance molecule [161]. Overall such an observation is not surprising considering the robustness of a resulting behavioral response, but this may draw more attention to investigation of temporal developmental patterns of other components of GFS. Visual inputs into the giant fiber originate in the lobula and lobula plate and include 2 classes of neurons that are responsible for ultra-sensitive looming detection [3,130], which have a unique anatomical structure that corresponds to their receptive visual field. These neurons in turn receive directionally selective inputs from ascending motion-sensing cells [130]. Therefore, an upstream part of the GFS represents a highly sophisticated circuit that perceives angular size and speed information with great precision in order to determine spike timing in the giant fiber and produce a robust escape response [3]. Whether formation of such complex system is experience-dependent and requires specific visual stimulation during development remains unknown and will be investigated. In general, development of *Drosophila* adult visual system that starts during late larval and peaks during mid-pupal stage has been used as a very common and convenient model to study cellular and molecular mechanisms of circuit formation, synaptic plasticity [210] and synaptic specificity [185,192]. At the same time, very little is still known about the role of sensory experience during visual system development and potentially relevant critical periods. More than 20 years ago work by Heisenberg and colleagues revealed that not only does exposure to light affect the size of such structures in

Drosophila brain as mushroom bodies [95], central complex and optic lobe [14], but this effect is dramatically limited to the first day of post-eclosion life [15], suggesting it to be a critical period for neuropil development. Since then, not many advances have been made in investigating the role of critical periods and experience-dependent plasticity in developing and mature visual system of the fly, as well as understanding keen mechanisms governing the above processes and their behavioral consequences. Similarly to embryonic stage, formation of a highly sophisticated structure like visual system of an adult fruit fly organized in distinct layers and columns requires temporally specific function of protein regulators on the earliest stages of development that irreversibly determine cell fate, which occurs in a restricted period but does not rely on any sensory feedback. This was shown for the function of *sevenless, bride of sevenless* and *seven-up* genes in developing ommatidia during R7 photoreceptor specification [26,99,232]. Further work demonstrated that once all cell types are formed, the connectivity pattern and synaptic specificity is also established in a sensory input-independent manner [98]. At the same time, functional aspect of circuit connectivity of the fly visual system in regard to sensory experience has barely been addressed in any studies. Only recently Akin and colleagues [5] demonstrated that cell-type specific spontaneous network activity is inherent to the developing fly visual system during late pupal stage, which, interestingly, still does not require sensory stimulation and occurs after the end of synaptogenesis in all layers [5]. Therefore, functional relevance of such activity is still to be determined. It is likely to be inferred from looking at integrative sensorimotor circuits underlying complex visually guided behaviors

from a developmental perspective, such as the study by Hirsch and colleagues [100] showing that light deprivation in newly eclosed flies has irreversible effects on aspects of their visual preferences. Therefore, similarly to maturation of larval locomotor circuits during embryogenesis [212], spontaneous activity in the developing adult visual system [5] might only be a small part of general synaptic scaling process involving sensory inputs that become active only in the adult fly, and various downstream motor output systems, such as ones described for the looming response-escape pathway [130,161] and many other photobehaviors seen in adult *Drosophila*. Determination of a male- and female-specific sexual behavior is a process that also occurs during early-mid pupal stage and can be of a great value for understanding molecular factors that regulate onset and closure of critical periods. Activity of sex-specific splice variants of *transformer* (*tra*) and *fruitless* (*fru*) genes in females [9] and males [53,140], respectively, during a restricted period of pupal development was sufficient to irreversibly program future courtship behavior in a sex-specific manner, while ectopic expression of male-specific *fru* in females, as well as downregulation of *tra* expression in females, resulted in emergence of an altered courtship behavior in adulthood including reversed and mixed sexual preferences [9,53]. Importantly, sex-determining transcription factors only affect functional maturation of an underlying circuit, while its structural assembly and establishment of connectivity pattern occurs independently [140]. In addition, this functional modulation does not directly initiate behavior, but rather creates a potential for its emergence in the future, which in

turn is triggered by an encounter with a corresponding stimulus within a favorable environment.

Adult stage

Early post-eclosion stage represents another crucial developmental period important for regulation of complex behaviors through irreversible modulation of underlying circuits function (Table 1). It is characterized by increased sensitivity to external stimuli that come directly from the environment or being relayed through its effect on animal's internal state. Thereby it allows to understand the intersections between sophisticated behaviors that are inherent to an adult fruit fly. Hence, functional relationship between early adult sleep and sexual behavior was revealed by Kayser and colleagues [122]. Juvenile flies deprived from their normally increased duration of sleep displayed an irreversibly impaired development of a brain region responsible for courtship with corresponding behavioral deficits. Interestingly, although circuit mechanisms causing prolonged sleep in newly eclosed flies were dissected (CREB-dependent late onset of dopaminergic neuron activity that inhibits sleep-promoting region in fan-shaped body) [122], specific links between sleep and courtship remain unknown. Aside from courtship, proper sleep throughout a critical early post-eclosion stage was shown to regulate normal short-term memory and response inhibition [196]. Regulation of sexual behavior in fruit flies is further complicated by findings that revealed a critical developmental period for courtship dominance in immature male flies who are susceptible to experience-dependent behavioral alterations upon

exposure to pheromones derived from adult males [213,214]. In addition, targeted and temporally restricted expression of female splice variant of *tra* gene in juvenile male flies turned out to be sufficient for life-long production of female pheromones, which did not reverse their courtship preferences but elicited homosexual courtship from other males, serving a determinant of individual's sexual identity [70]. Therefore, development of courtship behavior in *Drosophila* can be regarded as a multi-stage process integrating a complex interplay of a hierarchy of sex-determining genes function in specific circuits and within a critical period during pupal stage, environmental conditions during this critical stage, and early post-eclosion sensory experience required to initiate the behavior. All these findings establish a broad framework for future research aimed at investigation of cellular and molecular aspects underlying developmental intersections between such complex and socially relevant aspects of *Drosophila* ethology as sexual behavior, sleep and multiple forms of associative learning. Social experience was shown to play an important role for the developing mushroom bodies in young flies during first 2 weeks post-eclosion. Interestingly, it could be discriminated from other types of sensory input such as general exposure to light [223]. Hence, interacting young flies displayed a higher number of Kenyon Cell (KC) axons compared to animals reared in isolation since eclosion, suggesting that some regions of the fly brain responsible for memory and learning undergo constant rearrangements during early life. This was further supported by work of Heisenberg et al. [95] which showed that overall KC fiber volume was affected by the sex of a young fly social partner and was significantly higher in heterosexual pairs [95]. These intriguing

observations suggest deep intersections between sexual behavior and early visual and olfactory learning integrated in higher-order processing centers in *Drosophila* brain and require further experiments to reveal the underlying mechanisms of experience-dependent plasticity.

Another good example of an experience-dependent circuit modifications during a critical period is seen in the young adult fly olfactory system. Olfactory receptor neurons (ORNs) conveying sensory information from specific odorants are classically considered to form a hard-wired stereotyped connectivity map with corresponding olfactory glomeruli through a set of interneurons and projection neurons [49]. However, multiple studies have revealed the susceptibility of this network to structural and functional remodeling during critical periods in young flies, long after the end of synaptogenesis. Thus, plastic changes followed by an imprinted behavioral adaptation were revealed in DM2 and V glomeruli when juvenile flies were exposed to benzaldehyde [54]. Similarly, early excessive exposure to CO_2 during a critical window leads to a reduction in behavioral response through an increase in sensitivity of a local interneuron and reversible volume increase in the CO_2-specific glomerulus [183]. Moreover, stimulation with a specific odor during an early critical period results in altered connectivity between ORNs and corresponding glomerulus, presumably through synapse elimination and axon retraction [88]. Importantly, the loss of innervation remains reversible within the critical period time frames but not outside it. An activity-dependent nature of synaptogenesis in olfactory system was supported by loss of innervation resulting from blocked output from ORNs and downregulation of NMDA receptor

activity in glomeruli [88]. Therefore, experience-dependent remodeling of *Drosophila* olfactory system serves an excellent model for deeper understanding developmental transitions between plastic and hard-wired parts of the circuitry underlying complex behavioral responses and may be relevant for human neurological diseases like fragile X syndrome [57,58] and other disorders involving developmental intersections between early sensory experience and social behavior [59,148,152].

Larval stage

However, despite the relatively small size of the adult fly brain with about 200,000 neurons it is formed by, its complexity might create various obstacles and complications when addressing the abovementioned questions. In this regard, a larval brain comprising two orders of magnitude less cells may seem a more attractive and accessible model. Indeed, quite a few studies have reported full connectome reconstructions of multiple regions in larval brain including olfactory circuit [16], visual system [136] and mushroom bodies [65]. Even more importantly, several successful attempts were made to superimpose the full functional architecture of large centers in *Drosophila* larval brain on the existing structural data [109,133,153]. This includes those responsible for complex learned behaviors [186], which among other things has facilitated the process of dissecting mechanisms underlying critical period plasticity in these systems (Table 1). Perhaps the most well-described and recognized example of a temporally restricted process occurring during larval stage is critical weight assessment,

which represents an important checkpoint in development that determines whether and when metamorphosis will occur depending on the nutritional state of an animal [46,155,157]. A complex but temporally precise interplay between insulin, ecdysone and juvenile hormone signaling reflects nutrient availability and dictates the exact time of critical weight achievement, which becomes a turning point that delineates differential effects of similar environmental factors on animal's future: while malnutrition or starvation before the critical point can extend pupariation and even lead to larval deterioration, post-critical weight starvation only affects animal size but not survival [46,155,157]. Therefore, although not involving sophisticated neuronal circuits and complex behavior, it is great system to study critical time windows in context of environmental impact and precise cellular and molecular mechanisms that regulate opening and closure of critical periods in general. A more canonical example is the regulation of a transition from foraging to wandering in larvae. This rapid behavioral switch occurs in late 3rd instar animals and is characterized by cessation of feeding and onset of a preparation to metamorphosis, but its proper timing is regulated during a critical window in early 3rd instar termed Terminal Growth Period after the assessment of critical weight and before the start of wandering [4,238]. A sensory input from PPK1 neurons during this period is vitally required for the foraging-wandering transition to occur in future. Thereby larvae are thought assess mechanical properties of the surroundings during so-called surfacing behavior, which serves the purpose of making sure the environment is not too dry and will not result in desiccation during pupal stage [117]. Similarly to critical weight assessment, these simple behavioral

responses are consistent with the notion of a larval stage primarily focused on feeding and ensuring a safe transition to adult animal, and it might seem that these basic needs do not require any sophisticated ethology. Nevertheless, the first example of a socially relevant behavior that requires learning during a critical period has been recently documented for *Drosophila* larvae [60,63]. In crowded conditions and liquid food early 3rd instar larvae form cooperative digging clusters that persist for several days until animals exit food for pupariation. Interestingly, cluster membership requires prior social experience during late 2nd-early 3rd instar, which therefore represents a critical developmental window during which animals need to undergo unsupervised learning with their peers in order to later participate in group behavior [60]. One remarkable trait inherent to clusters is that larvae use visual cues to synchronize their digging movements with immediate neighbors, which becomes a rate-limiting step for cooperation. This is of particular interest, because an earlier study has revealed that complex “social” vision and ability to recognize movements also emerges among fruit fly larvae during a critical stage on the border of 2nd and 3rd larval instar stages and requires exposure to other moving larvae [119,200]. Further work by Dombrovski and colleagues [61] has established a connection between complex larval vision and clustering by showing that participation in cooperative digging is associated with significant structural and functional changes in a specific pathway within larval visual system that is thought to detect temporal light signals [61]. Importantly, these plastic changes mostly occur at early 3rd instar larvae, while sensitivity to general light stimuli and complex visual cues is significantly reduced outside this period [61]. This implies that

experience-dependent plasticity in the visual system might be the key factor that determines larval membership in group foraging behavior, and animals acquire an ability to visualize complex moving patterns during the sensitive critical period. How exactly this process occurs on a cellular and molecular levels, what determines the onset and termination of sensitivity to visual experience, and whether other sensory modalities like mechanosensation [169] in larvae are susceptible to such forms of social plasticity, remains largely unknown. Interestingly, other studies have revealed the presence of experience dependent structural and functional plasticity in parts of *Drosophila* larval visual system responsible for circadian regulation [246], including ones that happen during a critical period and induce irreversible behavioral changes in adult animals [195]. This might imply that plastic visual circuit rearrangements that determine larval sociality might have implications in the adult flies as well. Taking advantage of a fully reconstructed connectome of a larval visual system [136], these questions are likely to be addressed in the nearest future.

Evolutionary significance of critical periods

Apart from dissecting molecular and circuit mechanisms that control initiation, termination and duration of plasticity inherent to critical developmental periods, understanding evolutionary significance of early imprinting is of big importance well. An open question is whether irreversibly sculptured circuits serve as inevitable limitation and consequence of high complexity of a developing brain, or is it an evolutionary adjustment that gives undisputable advantages over life-

long plasticity in specific environments. Another fundamental question in neurobiology is how such permanent circuit changes functionally integrate with the intrinsic flexibility and variability of sensory and motor systems whose responses are modulated by dynamic environmental conditions and internal state of an animal. Recent studies in *Drosophila* that might shed more light on this topic demonstrate how innate sensory preferences can be modulated and even reversed by a change in internal state caused by multisensory integration of several stimuli converging into a circuit node that in turn produces a context-dependent behavioral response [128,184]. This includes rather simple switches that momentarily change valence of visual, olfactory or gustatory stimuli [39,55,239] along with more profound long-lasting changes in socially relevant behaviors [34,102,237]. It allows animals to modify their behavioral responses according to environmental cues and current vital demands. However, such immediate state-dependent modulation might only be advantageous when an animal is naturally exposed to a simple binary choice of action and a limited set of possible stimuli. This notion is further broadened by studies demonstrating that sometimes competing internal states may shift the balance between antagonistic sensory drives forcing an animal to make risky decisions which, however, may be critical for survival [118,139]. Therefore, it justifies the flexibility of such rapid binary response systems. Moreover, the cost of making a wrong behavioral choice is restricted to a single animal and might often be outweighed by an unconditional fitness advantage at relatively low risk of failure due to robustness and unambiguity of a stimulus.

The next level of relationship between environmental inputs and behavioral responses is seen when higher-order brain regions like mushroom bodies act as complex switch panels that are able to redirect the same signal onto different behavioral output circuits [44]. This happens after a process of associative learning has occurred and a given stimulus was assigned with a valence [11]. Such evolutionary mechanism generates higher variability in behavior and broadens animal's potential to adjust to various environmental conditions. From physiological perspective it is coupled with unlimited degree of plasticity that lasts throughout lifetime. However, enhanced flexibility comes at a cost of increased chance of creating a wrong association followed by an unsafe decision. In other words, opportunities to easily change valence of a sensory input allow a high degree of flexibility in a changing environment but are more error-prone and might prove more costly for an individual's survival.

Importantly, all of the examples mentioned so far feature only functional modulation of circuit outputs using aminergic or peptidergic stimulation to alter strengths of synaptic connections and levels of neuronal excitability without having any short- or long-lasting consequences for connectivity [128]. At the same time, deep changes in the environment accompanying speciation can lead to rapid structural rearrangements in circuits that were considered hard-wired under previously unchanged conditions, such as fly olfactory system [13]. These modifications originate from molecular changes in olfactory receptors followed by adaptations is circuit patterning and corresponding behavioral phenotype.

Thus, a choice between irreversible structural plasticity restricted in time as opposed to more flexible model of functional circuit modulation by internal state and ongoing conditions becomes a question that should be addressed primarily in terms of opportunity costs and trade-offs rather than technical issues. Indeed, examples of early imprinting in arthropods allow to understand why this particular form of plasticity was evolutionary preferred for individual species over constant circuit modifications that reflect recent and ongoing experience during lifetime. Food imprinting was shown inherent to newly hatched cuttlefish [52], spiders [172] and even predatory mites [189]. In all cases, visual exposure to a certain type of prey resulted in a life-long preference in foraging behavior; importantly, sensory presentation occurred without reinforcement, was limited to a narrow developmental window and the effect persisted into adulthood, this supporting this plasticity to be equivalent to well-described imprinting in vertebrates [201]. In abovementioned examples, an early formation of a highly stereotyped behavioral response is fully justified by a fundamental nature and importance of foraging behavior for the young animals representing species that do not implement parental care and supervision. In other words, for these particular environmental conditions early brain maturation gives unambiguous ecological advantages from an individual's standpoint, making a hard-wired circuit formation enshrined in evolution.

Overall, this implies that a thin balance between structural and functional tuning of circuits exists as a species- and environment-specific evolutionary adaptation. It reflects a dynamic equilibrium between a current demand for

enhanced adaptability and a concomitant tradeoff in survival chances for an individual or increased metabolic expenditure required for structural plasticity. Moreover, stability and predictability of critical period-derived robust behavioral responses become even more relevant for social animals who share responsibilities within groups, where a cost of making a mistake increases dramatically. This is likely the case for a model system we focus on featuring critical periods for clustering and motion-sensing in *Drosophila* larvae [60,61,200]. Indeed, these studies suggest that stability of social digging clusters representing synchronized and organized ensembles requires equal contribution from every single member, and an introduction of a defector causes a dominant-negative effect leading to a cluster breakdown [60,61]. From an ecological standpoint it means that a mistake made by a single animal could prevent the entire group from accessing benefits of cooperative behavior, with potentially negative consequences for fitness in adulthood. Hence, an increased cost of an error in this ecological paradigm becomes outweighed by early social imprinting of a proper behavioral response which reduces the probability of such an error to zero, while a persisting plasticity would be a clear drawback in this particular case. Importantly, critical period for social clustering temporally correlates with a critical weight assessment [154,155]. Therefore, a binary lifestyle choice made by an early 3rd instar larva to be a social or a single forager is also highly entangled with current balance of metabolic supplies and demands that in turn determine animal's developmental trajectory. In addition, early acquisition of a particular behavioral

pattern might play a role in segregating larvae of different species and even conspecific populations.

In summary, a model system featuring larval cooperative digging clusters takes advantage of accessible fruit fly genetics and connectomics and enables to further elucidate circuit mechanisms and key molecular determinants that operate the flow of experience-dependent critical period plasticity. Complexity of clustering behavior implies multisensory integration required for its emergence and control, which creates a framework for future and ongoing studies investigating cellular and molecular mechanisms of vision [21,109], mechanosensation [169] and sensorimotor control of feeding [153] related to larval social behavior. Thus, we demonstrate how a relatively simple model system allows to address fundamental questions in neurobiology and may serve as translational research leading to better understanding of mammalian models of plasticity and associated human disorders

<u>Table 1:</u> List of critical developmental periods inherent to *Drosophila*

	Critical stage	Resulting behavior/trait	Sensory experience
Embryo 	16-21h AEL	Functional development of sensorimotor circuits underlying locomotion (Frequency and polarity of peristaltic waves etc.)	Feedback from sensory neurons
	11-19h AEL	Induction/rescue of seizure-like behavior in postembryonic stages	Increase in excitation/inhibition of activity in dorsal motor neurons (aCC/RP2)
Larva 	Early L3F1 (72-84h AEL)	Movement recognition Cooperative foraging group membership	Visualization of moving objects and other larvae (Potentially mechanosensation)
	Late L3F1 (80-90 hAEL)	Onset and time of metamorphosis	Critical weight assessment Sensing nutrient availability through insulin signaling in PG cells with subsequent ecdysone secretion
	L3F1-L3F2 (72-120h AEL)	Altered circadian regulation during adult stage	Exposure to ethanol
	L3F2 (100-120h AEL)	Transition from foraging to wandering behavior in late 3rd instar	Sensory input from class IV multiple-dendritic nociceptor neurons Assessment moisture levels through surfacing behavior
	L3F2 (96-120h AEL) *strongest phenotype	Development of circuit (dendritic arbors of ventral lateral neurons) underlying circadian entrainment	Exposure to normal light/dark cycle

Pupa 	Late larval-early pupal stage	Ommatidia development (R7 cell sensitive to UV light and other cell types)	Expression of *sevenless* gene encoding a receptor tyrosine kinase; subsequent interaction with *boss* gene product on the surface of a neighboring cell
	24-48h APF	Synaptogenesis between giant fiber and motor neurons; development of proper looming escape response	Function of semaphorin Sema1a during transition from a growth cone into a mature synapse
	24h before – 48h APF	Development of proper sexual behavior and preferences	Temperature-sensitive expression of *tra* gene
	55h APF – eclosion	Maturation of sensorimotor circuits underlying visually guided behaviors **(TBD)**	Spontaneous network activity in developing visual system
Adult 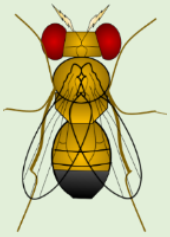	0-24h after eclosion (primary) 24-120h (secondary)	Development of lamina and other components of optic lobe	Dark rearing during primary phase irreversibly decreases neuropil size Normal light conditions during secondary phase affect lamina size
	0-36h after eclosion	Maturation of courtship circuitry (through proper development of VA1v olfactory glomerulus) and behavior	Increased duration of sleep in young flies, resulting from suppressed activity of wake-promoting DA neurons with input into dorsal Fan-shaped body
	0-24h after eclosion	Deficits in short-term memory and visual associative learning	Sleep deprivation

	0-72h after eclosion	Synaptogenesis in the antennal lobe Induction of circuit rearrangements (innervation of olfactory glomeruli by olfactory sensing neurons) underlying behavioral response to certain olfactory stimuli	Exposure to specific odorants Plasticity requires glutamatergic transmission through NMDA receptors
	Early post-eclosion (0-5 days)	Courtship dominance	Social interactions with mature males
	12-48h after eclosion	Production of sexually specific hydrocarbons; determination of animal sexual identity	Proper ubiquitous expression of *tra* gene
	Early post-eclosion	Visually guided choice behavior	Light deprivation
	2 weeks after eclosion	Determination of Mushroom body volume (primarily through changes in Kenyon Cell fiber number)	Social experience

Chapter 2

Cooperative behavior emerges among *Drosophila* larvae

Authors:

Mark Dombrovski[1], Leanne Poussard[1], Kamilia Moalem[1], Lucia Kmecova[1], Nic Hogan[1], Elisabeth Schott[1], Andrea Vaccari[2], Scott Acton[2] and Barry Condron[1,3,*]

Author affiliations:

[1]Department of Biology

[2]Department of Electrical and Computer Engineering

University of Virginia, Charlottesville, VA 22901, USA

[3]Lead Contact

*Correspondence: bc4f@virginia.edu (B.C.)

Published as a research paper:

Dombrovski, M., Poussard, L., Moalem, K., Kmecova, L., Hogan, N., Schott, E., Vaccari, A., Acton, S. and Condron, B., 2017. Cooperative behavior emerges among Drosophila larvae. *Current Biology*, *27*(18), pp.2821-2826.

https://doi.org/10.1016/j.cub.2017.07.054

Highlights

-cooperative feeding groups emerge among fruit fly larvae

-cooperation requires visually guided inter-larval coordinated movements

-stable membership in cooperative groups requires experience

Keywords: Drosophila, vision, cooperation, behavior, learning

Dombrovski *et al*. report that in liquid food, groups of *Drosophila* larvae cooperate so as to dig more effectively. This cooperation requires visually guided coordination of movements and stable membership within a group is enhanced with experience.

Summary

Spectacular examples of cooperative behavior emerge among a variety of animals and may serve critical roles in fitness [6,166]. However, the rules governing such behavior have been difficult to elucidate [166]. *Drosophila* larvae are known to socially aggregate [63,242] and use vision, mechanosensation, and gustation to recognize each other [119,149,169,200]. We describe here a model experimental system of cooperative behavior involving *Drosophila* larvae. While foraging in liquid food, larvae are observed to align themselves and coordinate their movements in order to drag a common air cavity and dig deeper. Large-scale cooperation is required to maintain contiguous air contact across the posterior breathing spiracles. On the basis of a directed genetic screen we find that vision plays a key role in cluster dynamics. Our experiments show that blind larvae form fewer clusters and dig less efficiently than wild type and that socially isolated larvae behave as if they were blind. Furthermore, we observed that blind and socially isolated larvae do not integrate effectively into wild type clusters. Behavioral data indicate that vision and social experience are required to coordinate precise movements between pairs of larvae therefore increasing the degree of cooperativity within a cluster. Hence, we hypothesize that vision and social experience allow *Drosophila* larvae to assemble cooperative digging groups leading to more effective feeding and potential evasion of predators. Most importantly, these results indicate that control over membership of such a cooperative group can be regulated.

Results and Discussion

Drosophila larvae form cooperative feeding clusters in liquid food

After a few days of feeding in agar-molasses food vials, *Drosophila* larvae liquefy the upper food layer. To reach the deeper and potentially higher quality food, single larvae make brief dives and breathe through an air tunnel created by their descent. Such tunnels, though, can easily collapse or be destroyed by the passage of other larvae. Cooperative behavior emerges within groups of larvae as a more efficient way of digging. Under crowded conditions, wild type Canton S (CS) larvae congregate to form organized groups, termed here ‘clusters’, all oriented with their breathing spiracles directed up and their heads down, and make coordinated dives (Figures 1A, S1A, Movie S1). By pulling a large common meniscus, they can often continue feeding at the lower half of the vial for many hours before group breakups occur (Figure 1B). All observed cluster breakups occur when access to air is lost. This coherent motion is observed to rise and fall a few body lengths every few minutes and animals appear to be moving closely together (CS clusters move 1.12±0.22mm every 176±44s; N=37, see Figure S1B). As this appears to be a model example of cooperative behavior, further experiments were carried out to examine its properties.

Directed genetic screen reveals the role of vision in clustering

Clusters were defined as groups of more than 4 larvae pulling a meniscus down more than half a body length from the surface (Figure 1A). In a vial, clusters are quantified when pressed against the clear plastic where only the front row of larvae is counted. Clusters can be identified from above as a cavity. A cluster in a vial is estimated to contain 10-100 larvae. In vials with about 50 egg-laying adults, cluster frequency was measured using the average number of clusters per vial, against the vial side, counted 3 times a day, and assayed over 4 weeks. Cluster frequency was measured over two weeks and compared to the depth of liquefaction (Figure S1C), which was measured by evaluating the darkening of the agar (Figure 1A). Clustering was observed to closely correlate with the liquefaction depth and to decrease after 2 weeks as vials began to dry out (Figure S1C and S1D). To further understand the dynamics of clusters that form and breakup continuously in vials, we conducted a directed genetic screen and quantified the clustering properties of several mutants using the parameters described above (Figure 1C shows the average clustering frequency for each mutant). The results show that a transgenic control background, Rh5-GAL4 and the smell-blind mutant *orco*^{1} both clustered with frequencies similar to CS whereas the morphological mutant *tubby*, which has a round body shape, failed to cluster. The mechanosensory mutant *nompC* clustered less frequently as did three independent blind mutants, norpA^{P41}, GMR-hid1 and GMR-hid2. This means that vision and mechanosensation play important roles in clustering. Gustation [149] and IR-class olfaction [17] were not tested. In addition, vials of CS, cultured in the

dark, also clustered less frequently (Figure 1C). Because of experimental tractability, the contribution of vision to clustering was chosen for further study.

Properties of clusters in pre-processed vials

To control for the process of food liquefaction and for larval number, agar vials were “pre-processed” with about 100 CS larvae produced over 24hrs from 50 adults, and incubated up to the time when pupation started. Vials were frozen for 24hrs so that all resident larvae died. This produced a vial with about 50% liquefaction. Adding 200 second instar (L2) larvae back to such a “pre-processed” vial produces robust clustering (Figure S1D). Clustering frequency was found to peak at the end of the larval stages, independently of the age at which animals are added, and also depends on the number of larvae added (Figure S1E). The contribution of vision was reexamined using these “pre-processed” vials and cluster formation frequency was again greatly reduced in visually impaired larvae (Figure 1D). Compared to wild type CS, two transgenic *white*-minus backgrounds (GMR-GAL4 & UAS-NaChBac) clustered normally. Crossing two of these backgrounds produces larvae that are visually compromised due to excess activity in visual neurons [165]. Blocking vision using UAS-NaChBac resulted in few clusters (3 clusters out of 3 vials observed over 4 weeks, with resulting frequency per vial = 0.05±0.03, N=58). Decreased clustering was also observed in two independent lines where photoreceptors were ablated (GMR-hid1, 2) as well as in blind $NorpA^{P41}$ mutants and in wild type CS reared in the dark (Figure 1D). These results support a role of vision in clustering behavior. We measured digging

movement frequency of CS larvae in the light and in the darkness (Figure S1F). Our data indicate that no significant differences in the number of backward digging movements per minute are observed between two groups of larvae. Therefore, the absence of light does not affect general digging activity in larvae, but at the same time causes alterations in clustering. Interestingly, we observed that once clusters have formed in visual mutants, they tend to survive just as long as wild type (Figure 1E). However, the distribution of cluster life spans, for wild type and blind larvae, is a skewed distribution, indicating a more complex dynamical process (Figure S1F). Given that visually compromised larvae have reduced cluster frequencies but similar cluster life spans, when compared to wild type, vision appears to be important for cluster initiation.

Properties of clusters in 2D

While clusters in vials probably represent a closer experimental model to how this behavior occurs naturally on rotting fruit, only the front row of larvae of a cluster can be imaged in this experimental scenario (Movie S1). In addition, because not all larvae can be monitored, the percentage in clusters or average digging depth cannot be measured. To visualize all larvae and obtain these measurements, 2D configuration was developed (Figure 2A). 30 larvae from a “pre-processed” vial are added to “pre-processed” liquefied food sandwiched between two glass slides (see Figure S2A for a general outline of experimental setup). Clusters form within minutes (Movie S2) and both wild type and blind (GMR-hid1) larvae in 2D configuration show similar movements as those in vials

(Figure S2B). However, similar to vials, few clusters form for blind larvae (GMR-hid1). Cluster formation was quantified for 2D by measuring percentage of larvae in clusters. Digging depth was also measured by calculating the average depth of all larvae in the food. Digging depth and average cluster membership is reduced for blind larvae when compared to wild type (Figures 2B, S2C, S2D). However, similar to vial-formed clusters, blind clusters, once formed, survive about as long as wild type (CS: 363±139min N=20; GMR-hid1: 241±184 N=36, P=ns, see Figure S2E). As clusters tend to breakup when the sides of the tunnels collapse, lifespan is probably also dependent on the mechanics of the food in addition to larval coordination.

Clustering improves with prior visual experience

In previous experiments larvae were found to go through an early third instar critical period in which they acquire visual recognition of movements of other larvae [200]. To test the role of early visual experience in clustering, larvae were isolated at L2, grown up to the middle of L3 and grouped in the 2D apparatus. These isolated larvae rarely cluster when compared to their socially reared sibs (Figures 2B, S2C). As isolation could affect either visual or mechanosensory development, we performed two specific critical-period rearing experiments to distinguish between the two possibilities. First, CS larvae we reared in “pre-processed” vials in complete darkness until late L3 stage and then tested for clustering. This approach would allow larvae to obtain mechanosensory-based but not visual experience. When these larvae were tested, both percentage of larvae in clusters

and digging efficiency were reduced (Figures 2B, S2C), but not to the level of total isolation. We next tested group rearing in a thin layer of processed food in a Petri dish and in the light. This preserves all conditions of a processed vial except that the flat arrangement means that clustering cannot happen and larvae should lack group mechanosensory experience. These animals also showed reduced digging and percentage of larvae in clusters but at a more moderate level (Figures 2B, S2C) than visually deprived larvae. This indicates that the group experience likely involves both mechanosensory and visual component, though the impact of the latter seems to be more significant. To further examine the role of vision and experience on clustering, individual larvae from wild type clusters, blind larvae (GMR-hid1) or those reared in isolation, were labeled with food-coloring (Figure 2C) and placed into preformed 2D wild type or blind clusters. All larvae almost immediately joined a cluster over which they crawled. Once in a cluster, the labeled larvae were followed to determine how long they spent as members. Wild type larvae spent more time in wild type clusters than did any of the other combination indicating that vision and experience contributes to more stable cluster membership (Figure 2D). The role of vision raises the hypothesis that general cluster stability is related to how individual larvae use sensory cues to coordinate their movements in relation to each other. We therefore further examined the dynamics of individual larvae in clusters.

Role of inter-larval coordination in clustering

Higher resolution videos of neighboring larvae were examined to extract information about the movements between individuals. To analyze larval movements, head and tail position in time were determined using ImageJ kymograms, which allowed identifying positions of larval front and rear ends (see Figures S1B, S2B, S3A). A Python-based machine vision for larval tracking was used to measure positions over time (see Figure S3E). The infrequent and smaller contractions during the downward motion are contrasted by longer and vigorous contractions during the backward crawling (see rising and diving phases in Figure 3A). In backward crawling, larvae move about 1/3 of their body lengths in each contractile cycle (see kymogram in Figure S3A, and Movie S3). Because of this, only upward movements were analyzed. The first objective was to determine whether the backward larval locomotion cycle was different between single larvae and those in clusters and how vision affected this movement. Locomotion cycles were measured, in 2D and 3D, for single larvae, pairs, and clusters. Visually impaired larvae (GMR-hid1) were also examined in 2D clusters. Each upward locomotion cycle, just over 2 seconds long (Figure S3B), was observed to be consistent across genotypes, numbers of larvae, and spatial configuration. The contraction cycle can be subdivided into a compression phase, in which a contractile wave begins at the anterior thorax and moves posterior and ends with spiracle withdrawal (Figure S3B), followed by upward extension, and finally a variable delay before the next cycle. When compared to 2D grouped larvae, times are similar except that 3D grouped compression and extension phases are faster

(Figure S3C). This might be related to the fact that in 3D, larvae are moving more against each other and less against the glass surface as in 2D configuration. Visually compromised individual larvae have the same contractile parameters as CS. Finally, in a free-range crawling test in a 10cm Petri dish with no distinct visual cues [200], visually compromised larvae move the same distance as CS (Figure S3D). The conclusion from these experiments is that visual function does not measurably affect locomotion and that the general backward locomotion cycle is not affected by vision, group size or the spatial environment.

To measure how closely larvae coordinated their movements, the posterior positions of individual larvae were tracked. In 3D vial clusters, only larvae of the front row were tracked, while the 2D configuration allowed tracking of all larvae simultaneously (Figure S3E). The timing differences of spiracle retractions between three adjacent larvae were measured in runs of 2-3 backward contractions. The differences in timing of spiracle contraction for wild type larvae were compared between the middle larva and its left and right neighbor (Figure S3F). As a negative control where no temporal linking is expected, the timing differences between three single larvae, spaced out and undergoing backward locomotion, were measured. The average time difference, expressed as a fraction of the 2-second normal contraction cycle time, was plotted for different pairs as a relative temporal difference. For the separated control, the smallest time difference between two of the three neighbors was chosen and corresponds to about 1/3 of a cycle with high variation (Figure S3F). In contrast, the closest neighbor in time for 2D and 3D clusters is significantly less than the control. While one neighbor is

paired closely in time, the other neighbor is no more paired than the negative control. This suggests that for any larval contraction, only one other larva, either to the left or to the right, is closely following in time with its own contraction. When the same measures were performed for the blind (GMR-hid1) larvae, no significant differences were observed between negative control (spaced larvae) and any combination of the neighbors (Figure S3G), suggesting that vision plays a key role in regulating close timing between neighbor contractions. Larval coordination was further measured for 3D clusters of different genotypes using the same method (Figure 3B). Compared to CS, visually compromised larvae (GMR-GAL4>UAS-NaChBac) show over twice the time delay and blind $NorpA^{P41}$ mutants are indistinguishable from the spaced control. The background strains are not different from CS (GMR-GAL4 and UAS-NaChBac). When imaged with a dim red light, which *Drosophila* larvae do not sense, CS larvae are as uncoordinated as their blind counterparts (Figure 3B). These data again suggest that larvae are dependent on vision to match the timing of contractions between larval pairs. Similar measures were performed for 2D clusters and results were consistent with previous data (Figure 3C). Importantly, wild type larvae reared either in isolation or in the darkness are also as uncoordinated as the blind counterparts, while larvae reared in a thin layer of food show no significant differences with the wild type (Figure 3C). This indeed suggests that prior visual rather than mechanosensory experience is specifically important for neighbor movement coordination. We next analyzed the timing differences for transplanted larvae. CS larvae transplanted into CS are indistinguishable from non-transplanted CS larvae within clusters (Figure

3C). Transplanting does not change this temporal coordination. However, all other combinations breakdown this coordination. This indicates that coordination of timing is likely a mutually timed behavior and requires two-way signaling between any larval pair. To further examine the relationship between movement coordination and cluster formation, we have measured the relationship between time disparities and percentage of larvae in clusters as well as cluster residing time (Figures S3H and S3I). Our data show that these parameters are closely related, indicating that high coordination of neighbors' digging movements determined by visual cues is a key to cluster size and stability.

Our experiments show that clustering emerges at late stages of larval development and requires, among other senses, vision and social experience. Clustering may serve a number of functions in larvae. The simplest role is to dive to better food when the surface has become liquefied. This is a likely scenario on rotting fruit where the complex and dynamic microbial milieu can both influence and be managed by *Drosophila* larvae [71,207]. Larval clustering may serve to tightly manage certain microbial communities into distinct beneficial patches, which might also provide an organizational role, or stigmergy [85,143,179]. The sharing of these constructed patches should require some cooperation such that the generated common resource is appropriately distributed [6,85,166]. Finally, up to 90% of wild *Drosophila* larvae can be infected with parasitoid wasp eggs [74] and digging depth provides protection from these lethal attacks [31,32]. Cooperation provides a clear way to dig deeper and is therefore likely to provide a selective advantage in avoiding parasitoid wasps.

The larval visual system, while simple, can visually recognize the movements of other larvae [119,200] and this might be a more general mechanism for social interaction in the same manner as mechanosensation [169,178]. Indeed, both experimentation and modeling indicate that relatively simple insect circuits are capable of complex visual recognition [182]. Larvae likely also use the movement of the meniscus as a signal between neighbors but probably employ faster visual cues to make the process more robust. The specific role of mechanosensation in clustering has yet to be delineated. It is not clear why each larva is coordinated with only one neighbor but it might be based on the simplicity of the cueing. If a larva initiates a locomotion cycle based on whichever neighbor moves first, and given a variance to its cycle length, then there should be a tendency to switch the cueing neighbor between cycles. This might also have the advantage of broadly distributing the phase-locking between larvae and create a more synchronous movement. The development of methods to image and measure individual movements in large clusters will likely shed light on global correlations between larvae. Socially learned visual behavior could also match the sensory input to lighting conditions as well as the locomotor signatures of nearby larvae. Such a filter would serve to link cluster membership to only those larvae who were together during a distinct developmental period. Membership likely requires a matched motor profile, therefore providing a means to select for the same species or even sibs. This could provide a mechanism of excluding potential cheaters who would try to gain from any profit of cooperative behavior but do not

want to contribute to the labor [191]. Further study of this model should provide a unique perspective of the fundamental rules of cooperative social behavior.

Author contributions

Conceptualization & Methodology: B.C.,M.D.,A.V.; Investigation & Data collection: B.C.,M.D.,N.C.,E.S.,L.P.,K.M.,L.C.; Data analysis: B.C.,M.D.; Writing, reviewing and editing: B.C.,M.D.,A.V.,S.A.,N.C.,E.S; Funding acquisition: B.C.,S.A."

Acknowledgements

We thank the Bloomington Stock Center (NSF DBI0,841,154) for providing fly stocks. We thank Jay Hirsh, Sarah Siegrist, Chris Deppmann, Ali Guler, B. Rimstone and members of the Condron and Acton labs for providing advice and comments. We thank Robert Radifera for advice about photography and Ray Keller for advice about group mechanics. This work was supported by NSF Grants CRCNS1010333 (BGC), ABI1062433 (SA and BGC), the Hobby Foundation (SA and BGC) and the Jefferson Scholars Foundation (MD).

Materials and Methods

Contact for reagent and resource sharing

For further information regarding the any resources and reagents please contact Barry Condron (bc4f@virginia.edu).

Establishing clusters in vials with adults

For food vials, 25mm x 95mm polypropylene vials were filled with standard Caltech food mixture (1000ml molasses, 14000ml H_20, 148g agar, 1000ml corn meal, 412g Bakers Yeast, 225ml Tegosept, 80ml propionic acid). About 50 adult Canton S (CS) flies were added to each vial and vials were kept at 22°C, 30% humidity, in constant fluorescent lighting conditions. Vials were left undisturbed except for a gentle turning 3 times daily to count clusters. Clusters were counted, blind to the genotype, for 4 weeks during which at least 2 generations of adults were produced. The liquefaction of the food was measured by a distinct darkening of the agar (see Figure 1A) and this was confirmed to be liquid in a set of test vials by tilting and examining the flow. The change in the texture, while comparing well to measuring liquefaction by tilting the vial, was preferred since the latter method disturbs and breaks up clusters. The height of the discolored region was measured and compared to the total height of the food and levels expressed as a percentage.

Establishing clusters in “pre-processed” vials

For “pre-processed” vials, 50-100 CS adults were placed in a vial with fresh food for 24hrs, removed, and larvae were allowed to feed for 8 days. Once larvae have left food and pupated, vials were frozen for at least 24hrs. Egg plate larvae collected over 24hrs were staged to second instar and 200 were transferred to a

thawed vial with a dental pick. Vials were left largely undisturbed in constant fluorescent lighting, 22°C, 30% humidity, for up to 10 days. Clustering frequency measures were averaged over days 3, 4 and 5 after loading of L2 larvae.

Establishing 2D clusters

“Pre-processed” food was placed between two glass slides (70x38x1mm) with 1mm modeling clay spacers, held in place and upright with two 2” binder clips. Larvae were scooped out from a cluster, washed with water, and 30 placed into the stop of the 2D apparatus. In initial pilot experiments, fresh food was placed in the lower half of this arrangements in order to simulate a vial more completely. However, the presence of fresh food is not required to establish clusters. To measure digging distance, the distance from the top was measured for all 30 larvae at 10hrs after loading and averaged. As for vials, clusters were defined as groups of 4 or more aligned larvae, more than half a body length into the food but in addition, going through at least one upward movement. Likewise, the membership in a cluster or not was determined for every larva every 5’, data from all 30 larvae were averaged and used to determine the percentage cluster membership. As a single metric for a cluster, the average of these measures was determined between 25’ and 125’ after apparatus loading.

Transplanting larvae into 2D clusters

Larvae were placed in blue-food-colored “pre-processed” food for 30’ and then washed with water before being placed over an established cluster in the 2D apparatus. In general, larvae can be followed within a cluster for a few hours before the labeling dye is fully voided.

Photography

For general cluster dynamics, movies were recorded on an iPhone 4s at full resolution and 1 frame/10” using “Lapseit” software. For high-resolution recordings, a Nikon D3100 CMOS camera, with 50mm lens and fitted with a Raynox Macroscopic 4x lens was used and videos (1920x1080 pixels) were recorded at 24Hz. For dim lighting, an infrared light was used with the same camera. General video analysis was done with iMovie followed by ImageJ and customized Python-based software.

Quantification and statistical analysis

Unless otherwise stated, data is quantified as averages and error bars represent the SEM. Statistical significance was calculated by ANOVA using Tukey’s method: *P<0.05; **P<0.01; ***P<0.001.

Segmentation and tracking

Computer segmentation and tracking were conducted on the recorded videos using customized Python software, which is available upon request. The application allows the user to identify several regions to be concurrently tracked, typically larval tails or heads. Once regions are identified, the software used a rectangular window centered on the selected areas to build spatiotemporal templates for each region by stacking the tracked data from 30 consecutive frames (Figure S3E). The templates, obtained by evaluating a weighted average of the temporal stack of the windows and favoring most recent times, are then used to track the selected regions as they move within the frame [22]. The absolute position of each template with respect to the frame as well as the relative position between all the templates is used to measure the location of each larval posterior and its relative placement with respect to that of the neighbors over time

Data and software availability

Python code for larval tracking software Is available at the following link:

https://github.com/avaccari/DrosophilaCooperative

Key resources table

Reagent or resource	Source	Identifier
Experimental model: fly strains		
GMR-hid^{G1}	Bloomington stock center	Cat#5771
GMR-hid^{SS1}	Bloomington stock center	Cat#5248
norpA^{p41}	Bloomington stock center	Cat#1951
nompC3	Bloomington stock center	Cat#42258
GMR-GAL4	Bloomington stock center	Cat#8605
UAS-NaChBac	Bloomington stock center	Cat#9466
UAS-mCD8::GFP	Bloomington stock center	Cat#5137
Rh5-GAL4	Bloomington stock center	Cat#7458
orco^{1}	Bloomington stock center	Cat#23129
tubby	Bloomington stock center	Cat#624
Canton S	Ed Lewis, Caltech	N/A
Software and algorithms		
Software (Python) for larval tracking	This paper	N/A
ImageJ	NIH	v1.6.0_24 (32-bit)

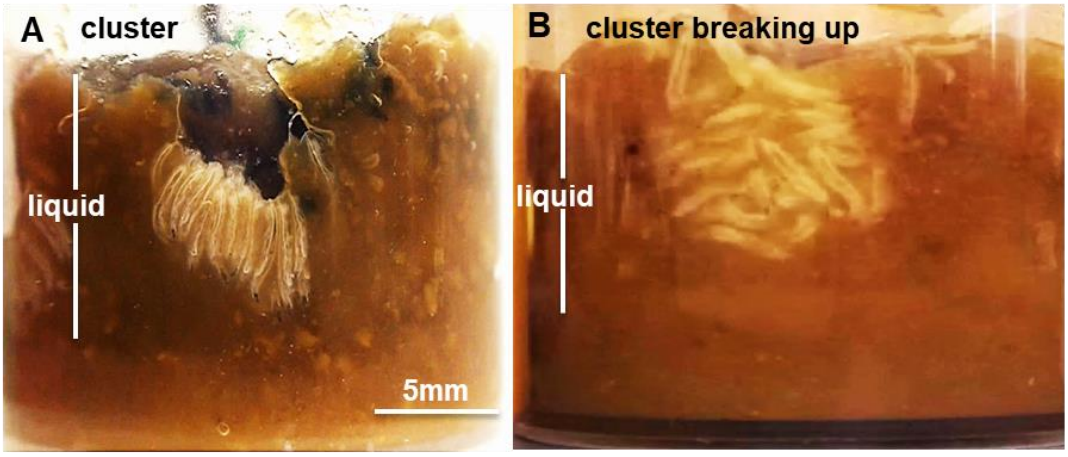
A
cluster
liquid
5mm
B
cluster breaking up
liquid

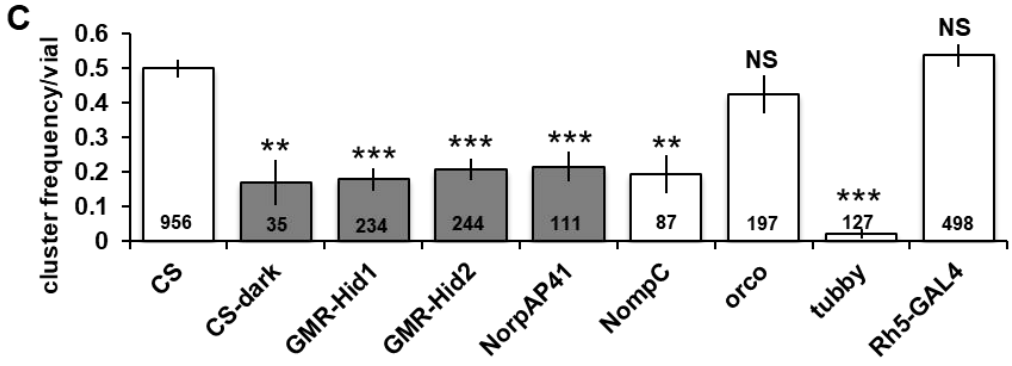
C
cluster frequency/vial
0.6
0.5
0.4
0.3
0.2
0.1
0
956
35
234
244
111
87
197
127
498
**
***
***
***
**
NS
***
NS
CS
CS-dark
GMR-Hid1
GMR-Hid2
NorpAP41
NompC
orco
tubby
Rh5-GAL4

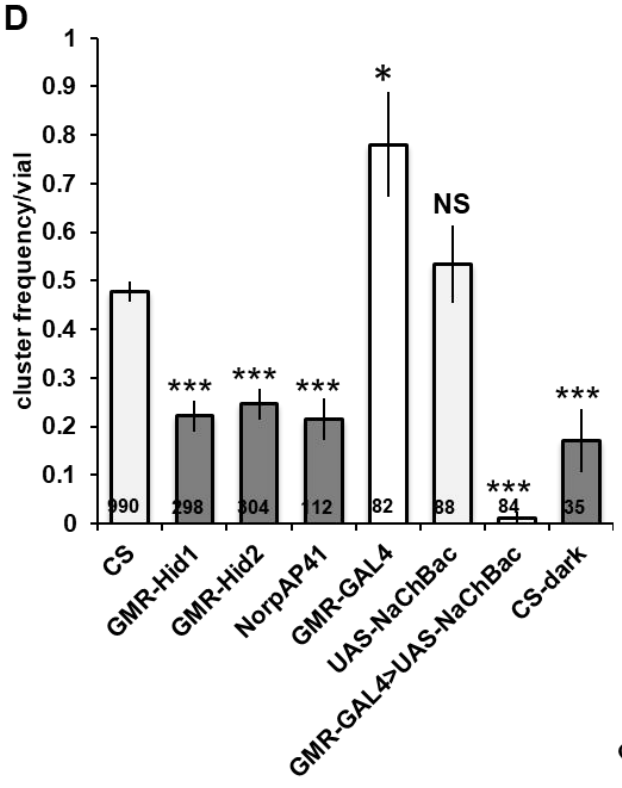
D
cluster frequency/vial
1
0.9
0.8
0.7
0.6
0.5
0.4
0.3
0.2
0.1
0
990
298
304
112
82
88
84
35
***
***
***
*
NS
***
CS
GMR-Hid1
GMR-Hid2
NorpAP41
GMR-GAL4
UAS-NaChBac
GMR-GAL4>UAS-NaChBac
CS-dark

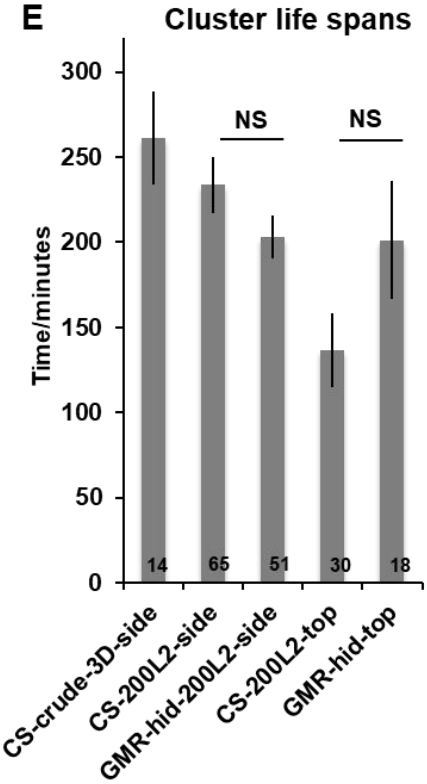
E
Cluster life spans
Time/minutes
300
250
200
150
100
50
0
14
65
51
30
18
NS
NS
CS-crude-3D-side
CS-200L2-side
GMR-hid-200L2-side
CS-200L2-top
GMR-hid-top

Figure 1. Vision is required for clustering

(A) Typical larval cluster. All larvae feed with heads down to the edge of the liquid phase (darker layer) and breathing spiracles at rear and inserted into the air cavity. A typical cluster will have 10-100 larvae and can last for many hours.

(B) A larval cluster rapidly breaking up when larvae lose access to air.

(C) Summary of cluster frequency (measured for “crude” vials in the original directed genetic screen), averaged for days 5 to 25 after hatching, for a number of genotypes. The bars represent the average and errors bars represent the SEM. Number of observations is shown in bold numbers for each genotype. Statistical significance was calculated by ANOVA using Tukey’s method for 1C to 1E: *P<0.05; **P<0.01; ***P<0.001.

(D) Summary of cluster frequency after 200 L2 larvae are placed in a pre-processed vial. Indicated are the averages and error bars represent the SEM. Number of observations is shown in bold numbers for each genotype.

(E) Summary of cluster life spans, measured for “crude” vials and “pre-processed” vials (both wild type and blind GMR-hid1 larvae, including side- and top view). Cluster life span time and error were derived from average clustering frequency Indicated are the averages and error bars represent the SEM. Number of observations is shown in bold numbers for each genotype and condition.

See also Figure S1

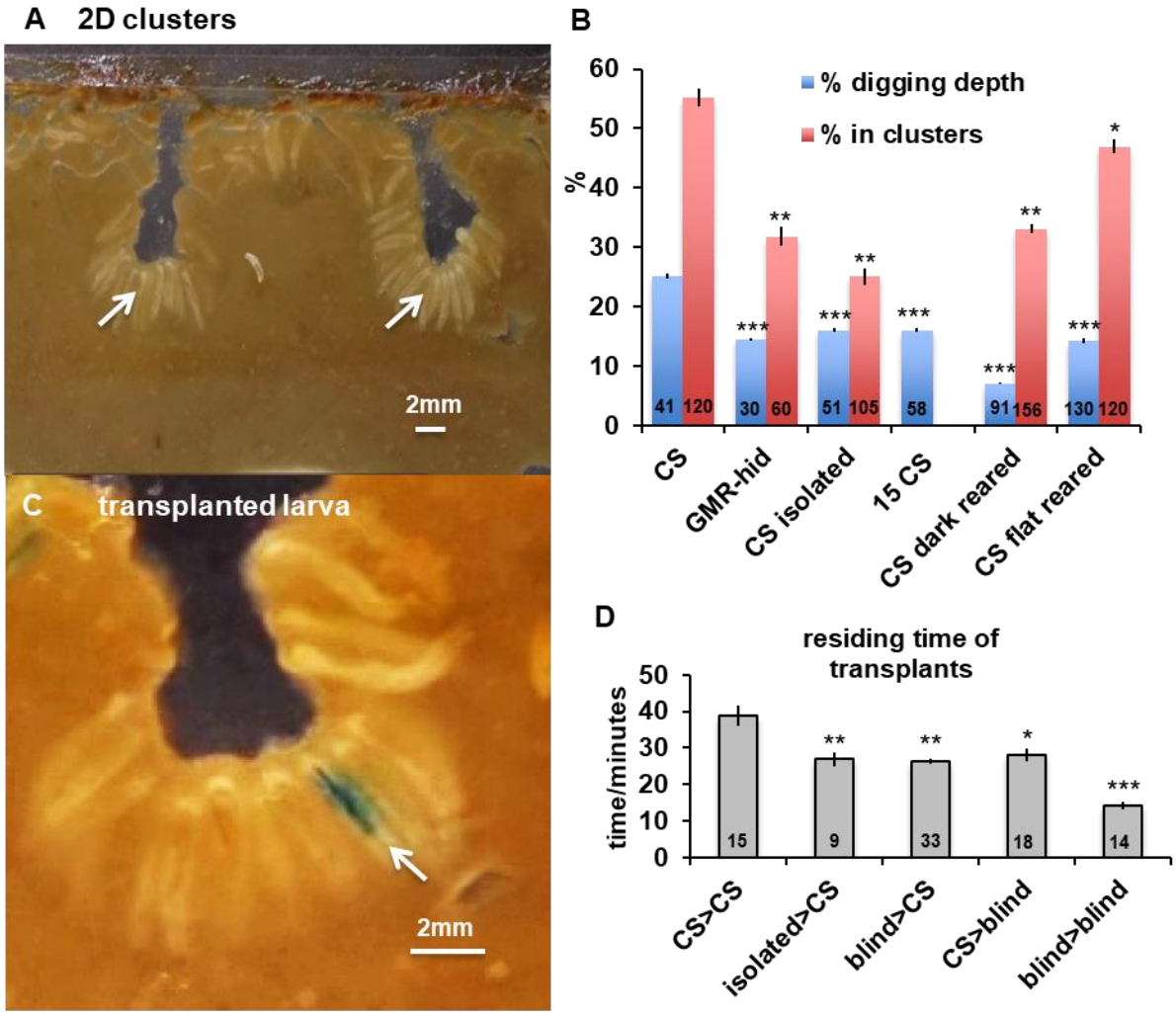

Figure 2: Properties of 2D clusters

(A) An example of a larval cluster in a 2D configuration. Two wild-type clusters (indicated with arrows) form within an hour after transplantation in “pre-processed” food.

(B) Properties of clusters in 2D configuration. Blue bars represent the average digging depths of 30 or 15 wild type larvae, blind (GMR-hid1) larvae and wild type larvae that were flat reared, dark reared or reared in isolation. Depths are expressed as percent distance into 38mm of preprocessed food averaged over all larvae. Both blind and isolated larvae, as well as larvae reared in darkness and a

thin layer of food display reduced digging efficiency similar to 15 wild type larvae. Red bars represent cluster formation efficiency expressed as percentage of larvae in clusters. Both blind and isolated wild type larvae, along with larvae reared in the darkness and in a thin layer of food display significantly reduced percentage of larvae in clusters. Indicated are the averages and error bars represent the SEM. Bold numbers represent the number of measures. Statistical significance was calculated by ANOVA using Tukey's method: *P<0.05; **P<0.01; ***P<0.001.

(C) Example of a single larva transplantation experiment. Individual larvae of different genotypes were placed in blue food-colored "pre-processed" food, then washed with water and placed over an established cluster of a given genotype in the 2D apparatus.

(D) Residing time of transplants. Individual larvae of a given genotype were transplanted into a cluster and their residing time was measured. Wild type into wild type is the most stable combination. Indicated are the averages and error bars represent the SEM. Bold numbers represent the number of measures. Statistical significance was calculated by ANOVA using Tukey's method: *P<0.05; **P<0.01; ***P<0.001.

See also Figure S2

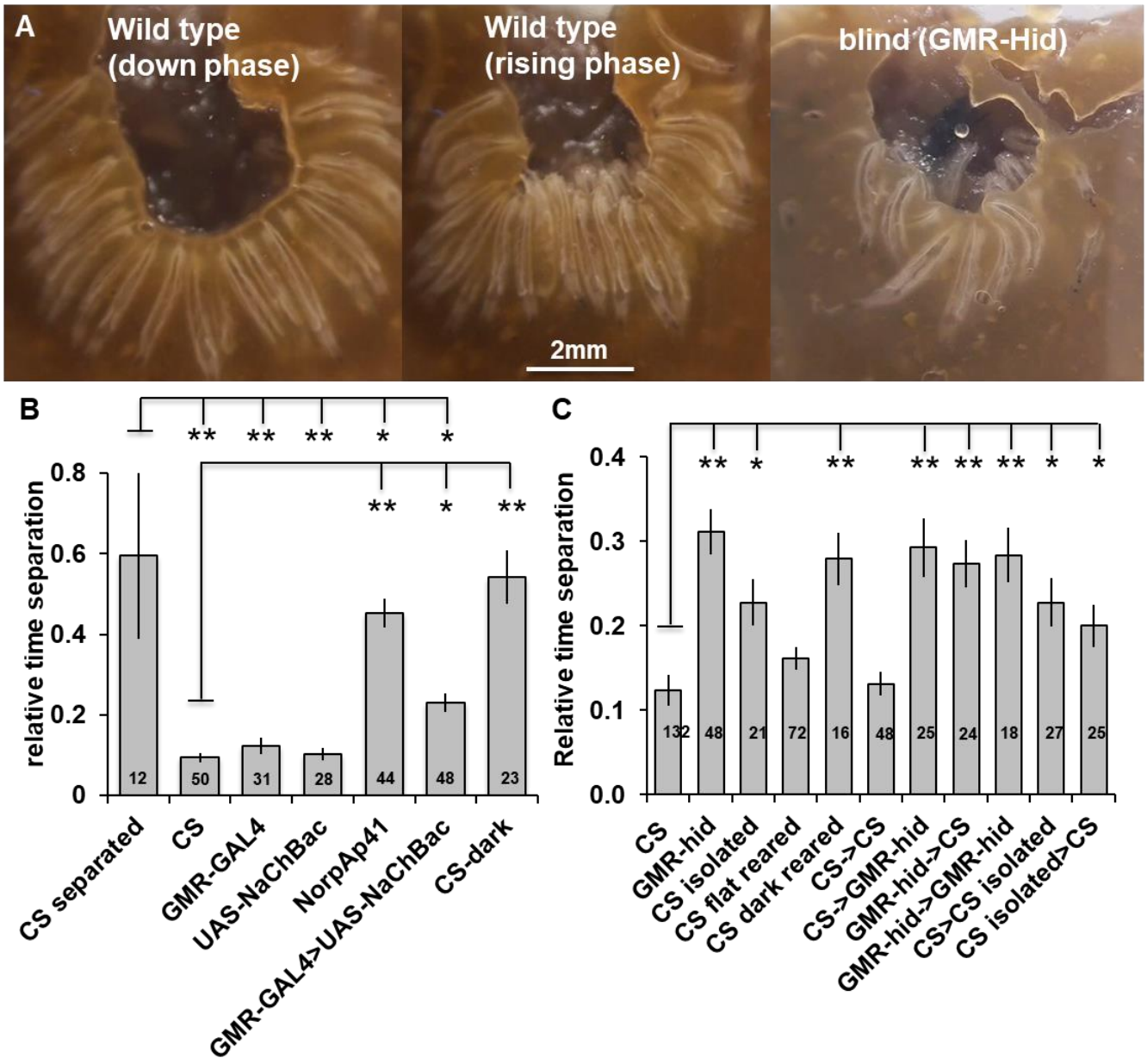

Figure 3. Inter-larval coordination within clusters

(A) Different phases of larval coordinated movements within a cluster. During the down phase (left panel), larval spiracles pull the meniscus. During the rising phase (middle panel) occurring every 2-4 minutes larvae shuffle up alongside each other by exhibiting coordinated backward contractions. Visually impaired (GMR-hid1) larvae form smaller clusters with poorly coordinated movements (right panel).

(B) Measures of the timing of spiracle contractions between individual larvae in 3D clusters in “pre-processed” vials (samples were measured in the front end of a

cluster in a vial). In each case, three adjacent larvae were chosen and for each contraction of the middle larva, the next contractions of the left and right neighbors are measured. Indicated are the averages and standard errors with numbers of measures shown in bold. As a negative control, “CS separated” represents three separated and independently backward-crawling larvae in a vial, and the timing shown is the closest to the middle animal. Visually impaired larvae ($NorpA^{P41}$, conditional mutants GMR-GAL4>UAS-NaChBac and wild type in the darkness) all display significantly increased time disparities between neighbors’ movements. Indicated are the averages and error bars represent the SEM. Statistical significance was calculated by ANOVA using Tukey’s method: *P<0.05; **P<0.01; ***P<0.001.

(C) Measures of the timing of spiracle contractions between individual larvae in 2D clusters. All measurements were performed using the same approach described for figure 2B. Consistent with data from 3D clusters, visually impaired larvae (GMR-hid1) display significantly increased time disparities, and so do wild type larvae grown in isolation or reared in the darkness. Larvae reared in a thin layer of food display an intermediate phenotype. In addition, same measurements were done for individually transplanted larvae (same combinations described in figure 2D). CS larvae transplanted into CS clusters behave the same way as non-transplanted CS, while all other transplant combinations display significantly decreased time disparities. Indicated are the averages and error bars represent the SEM. Statistical significance was calculated by ANOVA using Tukey’s method: *P<0.05; **P<0.01; ***P<0.001.

See also Figure S3

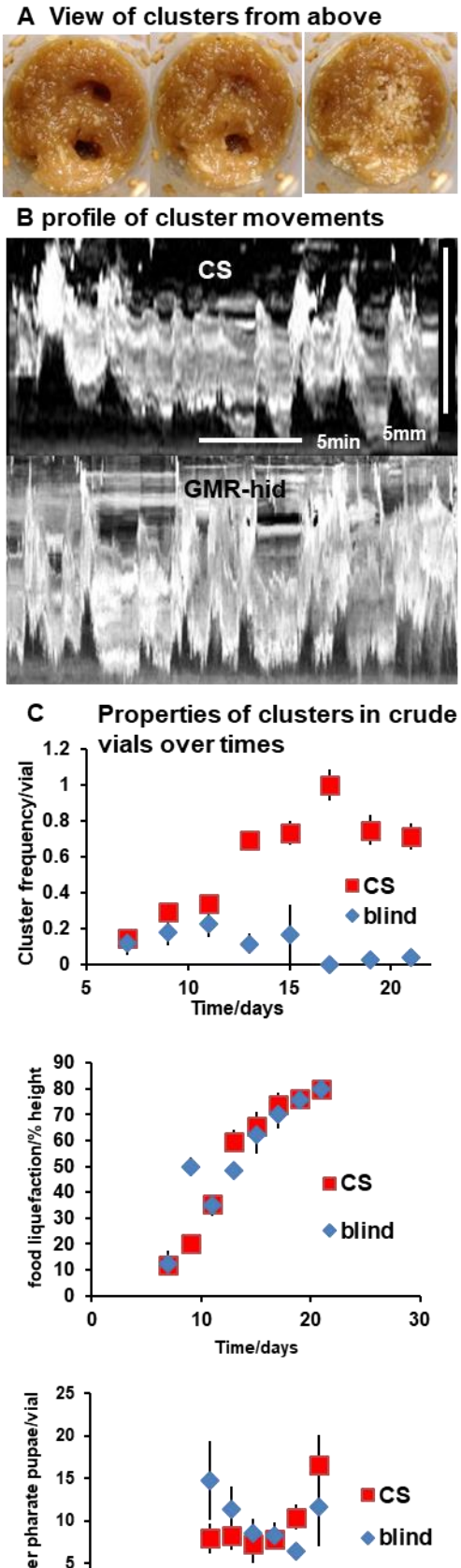
A View of clusters from above
B profile of cluster movements
CS
5min
5mm
GMR-hid
C Properties of clusters in crude vials over times
Cluster frequency/vial
Time/days
CS
blind
food liquefaction/% height
Time/days
CS
blind
Number pharate pupae/vial
Time/days
CS
blind
D Properties of clusters in pre-processed vials
effect of stage of added larvae
eggs
added at L2
added at L3F1
added at L3F2
cluster frequency/per vial
L1
L2
L3F1
L3F2
L3F3
L3F3+1
L3F3+2
L3F3+3
L3F3+4
L3F3+5
time/estimated stage of development
effect of number of L2 larvae added
100
200
400
cluster frequency/per vial
time/days after addition of L2's
E Distribution of cluster life spans
GMR-hid 200L2
CS 200L2
frequency, %
Time, minutes
F Larval digging activity in the dark
NS
Backwards compression cycles per minute
25
22
CS in the light
CS in the darkness

Figure S1. Related to Figure 1

S1A: View of wild type clusters from above. Cluster formation is associated with the formation of a cavity in liquefied food 10-20 mm in depth allowing access to air for clustering larvae. Once the cavity wall collapses and access to air is lost, the cluster immediately breaks up (see Video S5).

S1B: Kymogram of a cluster displaying temporal profile of cluster movements for wild type and blind (GMR-hid1) larvae.

S1C: Properties of cluster in "crude" vials over time. Cluster frequency (top panel) highly correlates with food liquefaction (middle panel). Bottom panel shows the rate of pharate pupae appearance in vials with wild type and blind (GMR-hid1) larvae. The data points are the averages with standard error bars.

S1D: Top panel. Properties of clusters in pre-processed vials. Clustering peaks at the end of larval stage independently of the age at which animals are added (time on the X-axis is an estimated larval stage after transplantation). Bottom panel: cluster frequency is dependent on the number of larvae added. Adding 100 larvae results in poor cluster formation, while adding 400 results in a more complex temporal profile. Adding 200 larvae results in a more distinct clustering peak 3-4 days after addition and was chosen for further experiments.

S1E: Frequency distribution of cluster life spans for wild type and blind (GMR-hid1) larval clusters, 200 L2 larvae in "pre-processed" vials).).

S1F: Measurements of larval digging activity in light and darkness. For wild type larvae clustering in pre-processed vials, the number of backward compression cycles per minute was measured either in light or in the darkness. Our data suggest that presence or absence of light does not affect larval backward digging activity. Indicated are the averages and error bars represent SEM. Statistical significance was calculated by ANOVA using Tukey's method: *P<0.05; **P<0.01; ***P<0.001.

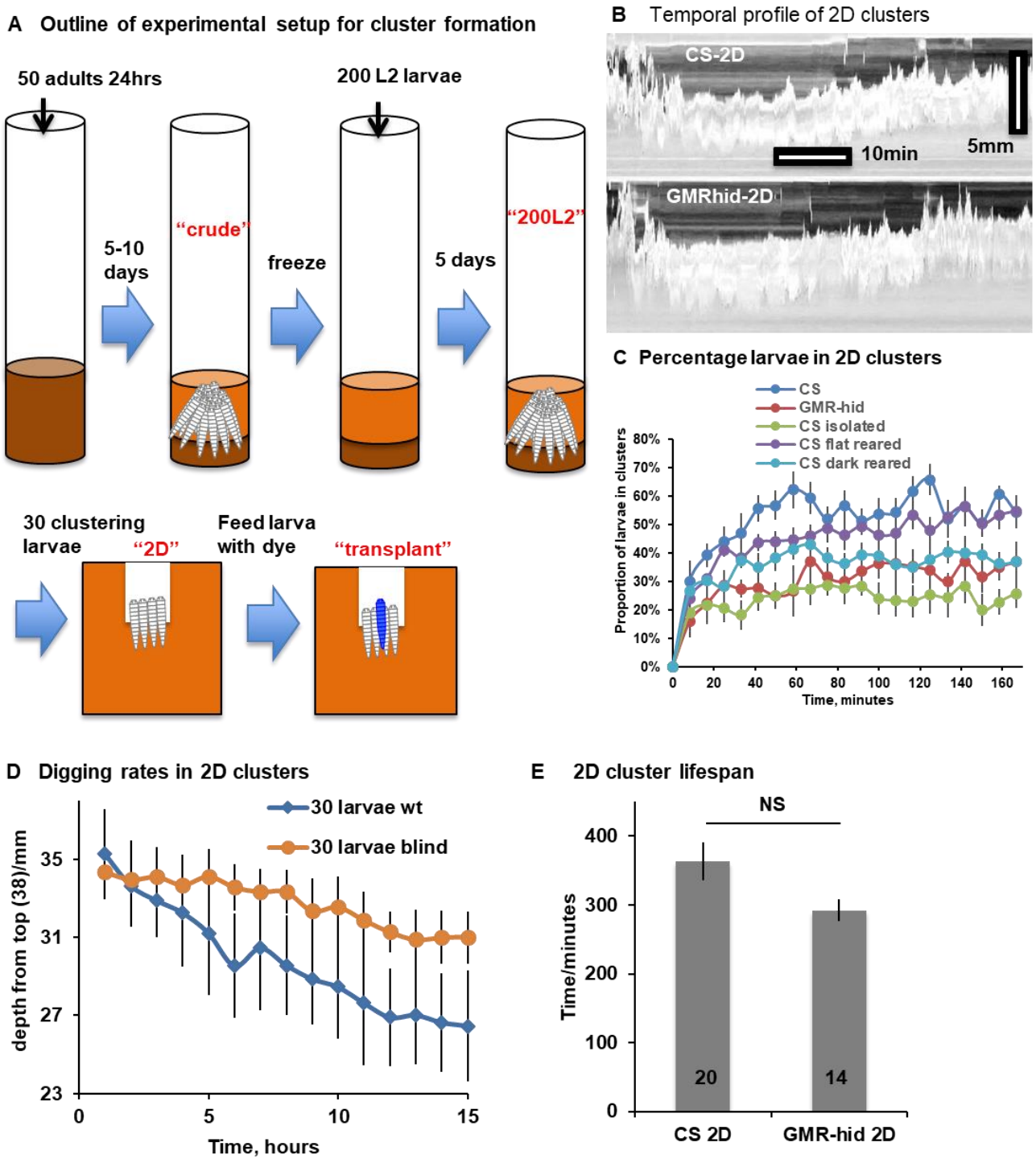
A Outline of experimental setup for cluster formation
50 adults 24hrs
5-10 days
"crude"
freeze
200 L2 larvae
5 days
"200L2"
30 clustering larvae
"2D"
Feed larva with dye
"transplant"
B Temporal profile of 2D clusters
CS-2D
10min
5mm
GMRhid-2D
C Percentage larvae in 2D clusters
CS
GMR-hid
CS isolated
CS flat reared
CS dark reared
Proportion of larvae in clusters
80%
70%
60%
50%
40%
30%
20%
10%
0%
0
20
40
60
80
100
120
140
160
Time, minutes
D Digging rates in 2D clusters
30 larvae wt
30 larvae blind
depth from top (38)/mm
35
31
27
23
0
5
10
15
Time, hours
E 2D cluster lifespan
NS
Time/minutes
400
300
200
100
0
20
14
CS 2D
GMR-hid 2D

Figure S2. Related to Figure 2

S2A: Outline of experimental setup for cluster formation: “crude” vials with egg-laying adults, “pre-processed” vials where 200 L2 larvae are placed in a pre-liquefied vial, 2D configuration and single larva transplantation experiments (Figure 2C).

S2B: Kymogram of 2D cluster at low resolution displaying temporal profile of cluster movements for wild type and blind (GMR-hid1) larvae. 2D clusters display movements similar to those seen in vials.

S2C: Number of larvae in clusters (expressed as percentage of the total number of larvae added to the 2D apparatus). Every larva was scored for cluster membership or not every 8 minutes. Blind (GMR-hid1) and wild type larvae reared in the darkness and in isolation display reduced cluster membership. Wild type larvae reared in a thin layer of food display an intermediate phenotype. Indicated are the averages and error bars represent the SEM.

S2D: Digging rates of wild type and blind (GMR-hid1) larvae in 2D clusters (digging depth is expressed as the distance from the top for all 30 larvae measured every 8 minutes and then averaged). Blind larvae show reduced digging rates compared to wild type larvae. The data points are the averages with error bars representing standard deviations.

S2E: Summary of 2D cluster life spans, measured for wild type and blind (GMR-hid1) larvae. Cluster life span time and error were derived from average clustering frequency. Indicated are the averages and error bars represent the SEM. Number of observations is shown in bold numbers. Statistical significance was calculated between each paired condition using the T-test.

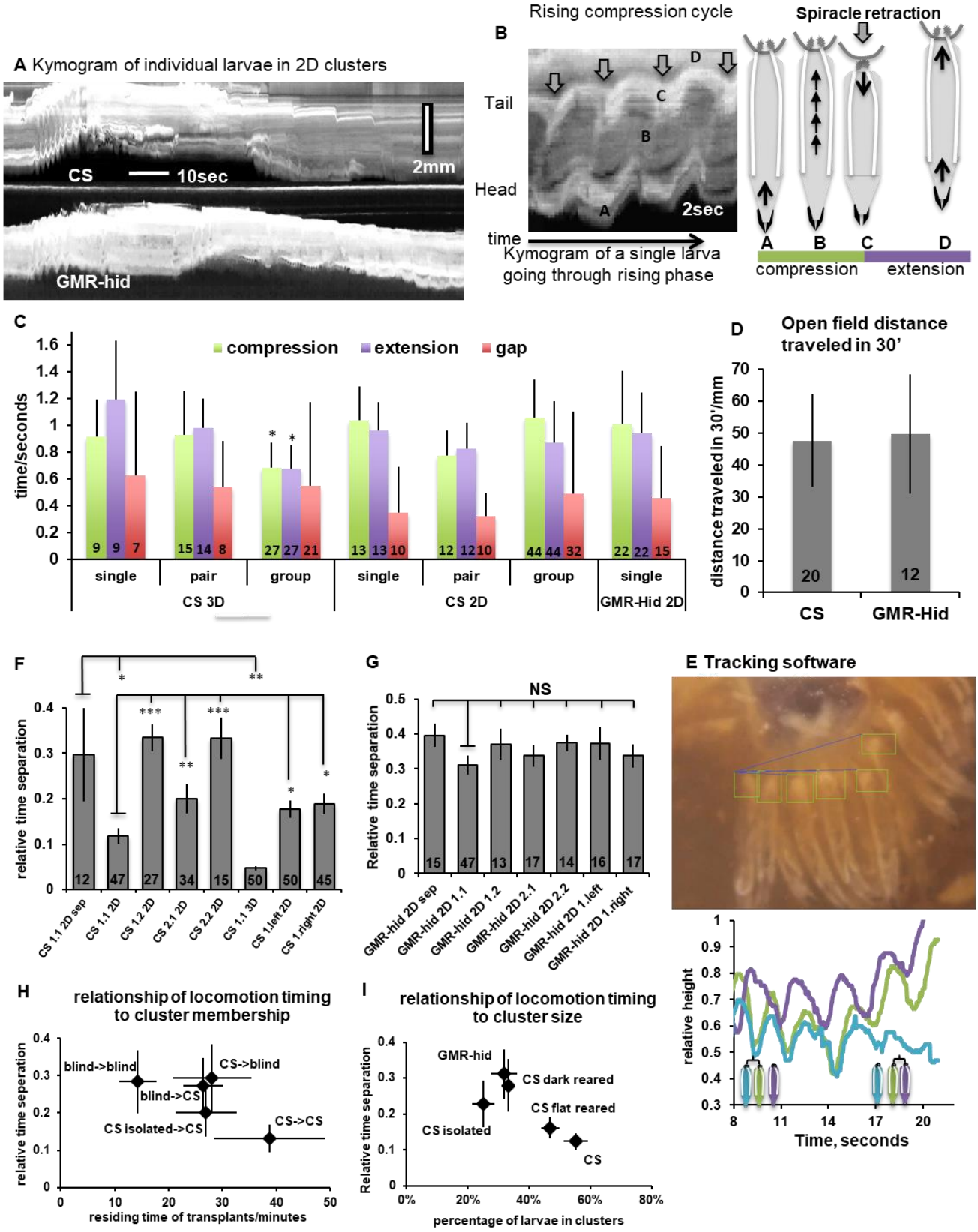
A Kymogram of individual larvae in 2D clusters
CS
10sec
2mm
GMR-hid
B
Rising compression cycle
Spiracle retraction
Tail
Head
time
A
B
C
D
2sec
Kymogram of a single larva going through rising phase
compression
extension
C
compression
extension
gap
time/seconds
single
pair
group
CS 3D
CS 2D
GMR-Hid 2D
D
Open field distance traveled in 30'
distance traveled in 30'/mm
CS
GMR-Hid
E Tracking software
relative height
Time, seconds
F
relative time separation
CS 1.1 2D sep
CS 1.1 2D
CS 1.2 2D
CS 2.1 2D
CS 2.2 2D
CS 1.1 3D
CS 1.left 2D
CS 1.right 2D
G
NS
Relative time separation
GMR-hid 2D sep
GMR-hid 2D 1.1
GMR-hid 2D 1.2
GMR-hid 2D 2.1
GMR-hid 2D 2.2
GMR-hid 2D 1.left
GMR-hid 2D 1.right
H
relationship of locomotion timing to cluster membership
relative time seperation
blind->blind
CS->blind
blind->CS
CS isolated->CS
CS->CS
residing time of transplants/minutes
I
relationship of locomotion timing to cluster size
Relative time separation
GMR-hid
CS dark reared
CS flat reared
CS isolated
CS
percentage of larvae in clusters

Figure S3. Related to Figure 3

S3A: A kymogram of a single larva in a 2D cluster with the distance from the top on the Y-axis and time on the X-axis. A wild type larva (top panel) is rapidly ascending for the first phase and then more slowly descending in the second phase. Blind larva (GMR-hid1, bottom panel) moves in a similar way.

S3B: A schematic overview of larval backward movements. Contractions begin with a head retraction (A) followed by a backward-propagating compression wave (B) that ends with a spiracle contraction (C) and then an upward movement of the whole larvae (D). The first three steps can be grouped as the compression phase, followed by an extension phase and then separated by a gap before the start of the next cycle. Each upward contraction cycle lasts for about 2 seconds followed by a variable delay before the next cycle.

S3C: The effect of vision and cluster configuration on backward locomotion parameters. In general, the timing of the compression events does not depend on cluster configuration (3D or 2D), number of neighbors (single, pair, group) or vision (no significant differences between wild type and GMR-hid1 larvae). Backward contraction cycles are about the same total length in different configurations and grouping states for CS as well as for blind larvae. However, the 3D grouped compression and extension phases are faster than other configurations. The "compression" phase is from head extension to spiracle retraction, the "extension" phase from spiracle retraction to maximum upward extension and the "gap" is the time between the end of extension and the start of the next contraction cycle. The contraction cycle was measured as the time between successive spiracle-withdrawals. Indicated are the averages and standard deviations. Statistical significance was calculated by ANOVA using Tukey's method: *P<0.05; **P<0.01; ***P<0.001.

S3D: Vision does not affect larval open field forward locomotion. Total distance traveled in 30 minutes was measured for CS and a blind larva (GMR-hid1). Indicated are the averages and standard deviations. Number of observations for each experiment is shown in bold.

S3E: Larval tracking software. Upper panel represents a screenshot of a Python-based tool developed to track individual larvae in a cluster and measure time disparities between neighbors' movements. Segmented larvae are boxed. The resultant data from three larvae are shown in the lower panel where height is plotted against time.

S3F: Temporal linking between wild type larval movements in a cluster. The differences in timing of spiracle contraction were compared between the middle larva and its left and right neighbor. For each triplet, the closest in time is indicated as "1.1" and the next closest as "1.2". For quintets, the next order neighbors are shown as "2.1" and "2.2". "Left" is only following a left neighbor, and "right" is only following a right neighbor. "Sep" represents a negative control where no temporal linking is expected, the timing differences between three single larvae, spaced out and undergoing backward locomotion, were measured. Our data suggest that for

any larval contraction, only one other larva, either to the left or to the right, will be closely following in time with its own contraction. Indicated are the averages and error bars represent SEM. Statistical significance was calculated by ANOVA using Tukey's method: *P<0.05; **P<0.01; ***P<0.001.

S3G: Temporal linking between blind (GMR-hid1) larval movements in a cluster. All measures were done as described for figure S3F. Our data indicate that blind larvae are not following the same rules as wild type larvae for movement coordination between neighbors. Indicated are the averages and error bars represent SEM. Statistical significance was calculated by ANOVA using Tukey's method: *P<0.05; **P<0.01; ***P<0.001.

S3H: Relationship between cluster membership and timing of movements between larval pairs. Plotted are the data from figures 3C and 2D. Cluster membership time, is inversely related to the time differences between larval movements. The closer in time larvae move together, the longer the time that larva will spend in a cluster. Indicated are the averages and error bars represent 99% confidence intervals.

S3I: Relationship between % of larvae in clusters and timing of movements between larval pairs. Plotted are the data from figures 2B and 3C. Percentage of larvae in clusters is inversely related to the time differences between larval movements. The closer in time larvae move together, the bigger and more stable clusters can be formed. Indicated are the averages and error bars represent 99% confidence intervals.

Chapter 3

A plastic visual pathway regulates cooperative behavior in *Drosophila* larvae

Authors:

Mark Dombrovski[1], Anna Kim[4], Leanne Poussard[1], Andrea Vaccari[3], Scott Acton[2], Emma Spillman[4], Barry Condron[1,5,*] and Quan Yuan[4*]

Author affiliations:

[1]Department of Biology, University of Virginia, 90 Geldard Dr., Charlottesville, VA 22901, USA

[2]Department of Electrical and Computer Engineering, University of Virginia, 351 McCormick Rd., Charlottesville, VA 22901, USA

[3]Department of Computer Science, Middlebury College, Bicentennial Way, Middlebury, VT 05753, USA

[4]National Institute of Neurological Disorders and Stroke, National Institutes of Health, 31 Center Dr., Bethesda, MD, 20892, USA

[5]Lead Contact

*Correspondence: bc4f@virginia.edu (B.C.), quan.yuan@nih.gov (Q.Y.)

Highlights

-Rh6-PR/lOLP pathway in the visual system controls fruit fly larvae social behavior

-Rh6-PR/lOLP pathway represents a movement-detecting module

-Proper development of Rh6-PR/lOLP pathway requires exposure to light and other larvae

-Experience-dependent changes occur pre- and postsynaptically in Rh6-PR/lOLP pathway

Keywords: cooperative behavior, vision, movement detection, circuit connectivity, plasticity, social experience, synchronized behavior

Dombrovski *et al.* report that a pathway in the visual system comprising Rh6 photoreceptors and downstream lOLP interneurons acts as a movement-detecting module regulating visually-guided cooperative behavior in *Drosophila* larvae. It also represents a cellular substrate for experience-dependent pre- and postsynaptic plasticity in the visual system

Published as a research paper:

Dombrovski, M., Kim, A., Poussard, L., E., Vaccari, A., Acton, S., Spillman, E.,

Condron, B., and Yuan, Q., 2019. Plastic visual pathway regulating cooperative behaviorin Drosophila larvae. Current Biology, 29(11), pp1866-1876.E5, June 03, 2019

https://doi.org/10.1016/j.cub.2019.04.060

Summary

Cooperative behavior emerges in biological systems through coordinated actions amongst individuals [125,203]. Although widely observed across animal species, the cellular and molecular mechanisms underlying the establishment and maintenance of cooperative behaviors remain largely unknown [166]. To characterize the circuit mechanisms serving the needs of independent individuals and social groups, we investigated cooperative digging behavior in *Drosophila* larvae [31,60,126]. While chemical and mechanical sensations are important for larval aggregation at specific sites [149,169,242], an individual larva's ability to participate in a cooperative burrowing cluster relies on direct visual input as well as visual and social experience during development. In addition, vision modulates cluster dynamics by promoting coordinated movements between pairs of larvae [60]. To determine the specific pathways within the larval visual circuit underlying cooperative social clustering, we examined larval photoreceptors (PRs) and the downstream local interneurons (lOLPs) using anatomical and functional studies [109,136]. Our results indicate that Rhodopsin 6-expressing-PRs (Rh6-PRs) and lOLPs are required for both cooperative clustering and movement detection. Remarkably, visual deprivation and social isolation strongly impact the structural and functional connectivity between Rh6-PRs and lOLPs, while at the same time having no effect on the adjacent Rhodopsin 5-expressing PRs (Rh5-PRs). Together, our findings demonstrate that a specific larval visual pathway involved in social interactions undergoes experience-dependent modifications during development, suggesting that plasticity in sensory circuits could act as the cellular substrate for social learning, a possible mechanism allowing an animal to integrate into a malleable social environment and engage in complex social behaviors.

Results and Discussion

Rh6-PRs and lOLP neurons are required for cooperative social clustering

The simple larval visual system [205] is an effective model to dissect the cellular pathways underlying visually guided behaviors. Compared to the complexity of adult *Drosophila* compound eyes [185], the larva has only twelve photoreceptors (PRs) on each side, which reside in the Bolwig's organ and project to a small compartment in the larval brain called the larval optic neuropil (LON) (Figure 1A) [123,124,136,205,206]. Four of these PRs express Rhodopsin-5 (Rh5-PRs), and eight express Rhodopsin-6 (Rh6-PRs). PRs exhibit different spectral sensitivity with distinct functions and connectivity patterns to the downstream visual interneurons. Recent connectome studies revealed that Rh5-PRs synapse directly onto visual projection neurons (VPNs) that relay information into the higher-order brain regions. In contrast, the majority of Rh6-PR axonal terminals first project to two reciprocally connected visual local interneurons named optic lobe pioneer neurons (lOLPs) (Figure 1B), one cholinergic (cha-lOLP) and another glutamatergic (glu-lOLP), which in turn converge onto the VPNs (Figure 1A) [21,136,206]. Importantly, the latest studies have shed more light on the possible correlation between structure and function of the Rh5-PR and Rh6-PR/lOLP pathways in larval visual system. While Rh5-PRs implement general visual processes such as light/dark discrimination, circadian entrainment and visual associative learning [79,123,124,150,205], Rh6-PRs have a specific role in processing temporal cues [109]. The focus of our study was a deeper investigation of the properties of visual pathways in the context of complex larval behavior.

Given the essential role of vision and visual experience in the emergence of larval cooperative clustering behavior [60], we aimed to elucidate the functions of PR subtypes via two assays that provide quantitative measurements of larval engagement into social groups and intra-cluster visually guided cooperation, respectively [60]. In the 2D clustering assay, the percentage of larvae participating digging clusters (Figures 1C, top and S1B) serves as an indicator of their ability to form cooperative groups, while the temporal delays between digging movements of neighboring larvae within a cluster (Figure 1C, bottom and Figure S1C) measure the ability of larvae to follow each other and maintain the cluster's integrity. The minimal temporal delay between neighboring larvae indicates their synchronized movements that are important for maintaining the cluster integrity. Therefore, we used these two parameters to assess the role of vision in larval cooperative behavior [60].

Consistent with the essential role of Rh5-PRs in general vision [109,120,123,124,136,205] both genetic mutants of Rh5 and larvae with genetically silenced Rh5-PRs displayed a significant reduction in their engagement in clusters (Figure 1C, top), coupled with increased time delays between neighbors (Figure 1C, bottom). Surprisingly, Rh6 mutants and larvae with silenced Rh6-PRs showed similar behavioral deficits (Figures 1C, S1B and S1C), suggesting that both Rh6- and Rh5-PRs are important for social clustering. Because Rh5 and Rh6 are also expressed outside of the larval PRs and are involved in regulating larval thermal preference [202], to demonstrate the clustering functions of Rh5/6 specifically in PRs, we genetically ablated the PRs using a GMR-hid transgene.

This manipulation largely eliminated larval PRs through the expression of a cell death gene *hid* driven by an eye-specific enhancer [90] and produced phenotypes similar to Rh5/6-PR mutant animals and larvae with silenced PRs (Figure 1C).

Next, we tested whether lOLPs, the downstream targets of Rh6-PRs, are required for clustering. Specific enhancer GAL4 lines were used to label and genetically silence both lOLPs (R84E12-Gal4), the glu-lOLP (R72E03-Gal4) or the cha-lOLP (R84E12-Gal4, VGluT-Gal80) (Figure 1B) [21]. Silencing the cha-lOLP, glu-lOLP or both resulted in a significantly reduced percentage of larvae forming clusters (Figure 1D, top), accompanied by increased time delays between neighbors (Figure 1D, bottom). These results strongly suggest that the Rh6-PR/lOLP circuit is required for visually-guided social clustering.

Social clustering and movement detection share a common visual pathway that is sensitive to visual experience

To determine whether social clustering engages visual processing beyond the simple perception of light, we compared the percentages of larvae that exhibit light avoidance [147] or form clusters using population assays [60]**.** Consistent with the results obtained from the 2D clustering analysis (Figure 1C, D), a significant reduction of the clustering frequency was observed in larvae with compromised Rh6-PRs and either or both lOLPs, which are phenotypically indistinguishable from blind animals (GMR-hid) and larvae with altered Rh5-PR function (Figure 2A). In contrast, interfering with the function of either Rh6-PRs or any of the lOLPs had no

effect on light preference in larvae (Figure 2B), confirming their dispensable role in general vision [108,109,150].

Previous studies indicate that the larval visual system is capable of sensing the movements of other larvae [119]. As visually guided clustering behavior likely requires identifying movement patterns of neighboring larvae, we next tested movement detection using larval visual attraction assays [119,200]. This behavioral test examines the degree of larval attraction to a tethered moving larva as compared to a large stationary object (Figure S1D). In accordance with the assumption that attraction to a fixed target reflects the detection of the differences in light intensity or contrast (i.e. serving as a measure of general vision), we observed that impaired function of Rh5-PRs significantly reduced the time spent near both fixed as well as moving targets (Figure 2C). On the other hand, larvae with only compromised Rh6-PR cells displayed altered attraction to a moving target but maintained normal levels of attraction to a fixed target (Figure 2C). In addition, genetic silencing of both lOLPs was sufficient to reduce moving target attraction without affecting fixed target detection, mimicking the phenotype of animals with compromised Rh6-PRs (Figure 2C). Importantly, compared to the wild-type controls, none of the manipulations generated significant changes in the larvae's locomotor activity, suggesting that the altered attraction levels to either moving or fixed target are not due to locomotion deficits (Figure S1E).

Taken together, our behavioral studies revealed a correlation between the results of cooperative clustering experiments and moving target attraction assays, both of which requires normal function of Rh6-PRs and lOLPs. These findings

support the notion that in order to perform cooperative social digging behavior, larvae utilize the Rh6-PRs/lOLP pathway to detect movements and coordinate actions between neighbors. Due to the strong impact of temperature shifts on larval clustering behavior, we did not perform the conditional silencing experiments using either Gal80^{ts} or Shi^{ts}. Therefore, we cannot exclude the possibilities that potential developmental defects caused by silencing either Rh6-PR or lOLPs contribute to the phenotypes we observed. Future studies using other inducible neuronal silencing techniques could resolve this issue and reveal the specific developmental stages associated with the Rh6-PR/lOLP' functions in larval clustering.

Our previous findings indicate that social isolation affects the larval ability to detect moving, but not fixed, targets and that prior exposure to light and other larvae is necessary for the emergence of clustering behavior [60,119,200]. Given the close connection between these behaviors, we hypothesized that visual experience is also necessary for movement detection but not general vision (light-dark discrimination). To test this, we subjected larvae to either light or dark rearing conditions since egg laying, then analyzed their light avoidance and visual attraction to fixed and moving targets. We found that neither light preference nor levels of fixed target attraction were affected by light deprivation (Figure 2D). In contrast, dark-reared animals performed poorly on moving target attraction assays (Figure 2D), strengthening the argument that movement detection and social clustering behaviors share a common cellular pathway strongly influenced by visual experience during development.

Rh6-PRs, but not Rh5-PRs, are modified by visual and social experience during development

Next, we asked whether substantial structural and functional plasticity can be observed in Rh6-PRs or the lOLPs accompanying the acquisition of movement detection and clustering behavior during development. To study the morphological plasticity in the larval visual circuit, we started by investigating the effect of light on the development of PR presynaptic terminals.

Previous studies [205,206] indicate that PR axons form around four globular presynaptic terminal boutons per PR, starting from the first instar stage. We visualized these boutons by expressing fluorescent markers in Rh5- and Rh6-PRs (Figure S2A). Notably, while the size of Rh5-PR boutons remained largely unchanged between second (L2) to late third (L3F3) instar, a significant increase in size was observed in Rh6-PR boutons (Figure S2A). To assess bouton sizes with improved spatial resolution, we took advantage of the Brainbow Multicolor Flip-Out (MCFO) technique [163] to visualize single PRs and individual presynaptic boutons (Figures 3A, S2B, S2C). This was followed by reconstruction and quantification of the bouton size using 3D visualization and analysis software [215] (Figure S2C). Consistent with previous observations, the diameters of Rh5-PR boutons maintain a stable size throughout larval development (Figures 3A, 3C). In contrast, Rh6-PR boutons display a consistent growth that is especially notable between the L2 and L3F3 stages (Figures 3A, 3C, S2B), coinciding with the time when larvae acquire experience-dependent attraction to a moving target and clustering behavior [60,200].

To test whether the development of the Rh6-PR bouton is also affected by visual and social experience, we compared animals reared in light vs. dark since egg laying. Unlike Rh5-PR boutons, which did not change in size between the two conditions (Figures 3B and 3C), dark-rearing produced a strong effect in Rh6-PRs, where the size of presynaptic boutons showed a 2-fold difference at the L3F1 stage and almost a 3-fold difference at the L3F3 and L3Fc stages when compared to light-reared control animals (Figures 3B and 3C). We next reproduced the effect of light deprivation on Rh6-PR bouton size using genetic silencing experiments, in which a GFP-tagged potassium channel Kir2.1 was expressed in the PRs to reduce neuronal excitability while providing a fluorescent marker for measuring bouton size [124,246]. Compared to the control group expressing regular GFP, Rh5-PRs expressing Kir2.1::GFP showed no change in their bouton size, while Rh6-PRs with Kir2.1::GFP displayed a significant decrease in bouton size at all larval stages tested (Figure 3D). These findings strongly support the idea that, as a cellular substrate for social clustering, Rh6-PRs require visual input for proper morphological development.

The emergence of moving target detection likely underlies social clustering and, as we show, is provided by the Rh6-PR/lOLP pathway, relies on visual input within a specific time window during late L2-early L3F1 stages [200]. We wondered whether the effect of visual experience on Rh6-PR bouton development is also restricted to this specific developmental period. To address this question, we used two paradigms for time-specific light deprivation with subsequent assessments of presynaptic bouton size in Rh5- and Rh6-PRs. All larvae were tested in the mid

L3F3 stage (~132h after egg laying, AEL). ‘Dark-since’ larvae were first raised in light, then transferred into darkness beginning from a designated stage (L2, L3F1 or L3F2), while ‘light-since’ were first raised in the darkness, then transferred into light (beginning from L2, L3F1 or L3F2 stages) (Figure 3E). This allowed the larvae to experience controlled exposures to light. The results were compared to the all-light-reared positive control and the all-dark-reared negative control.

As expected, time-specific light deprivation using either paradigm produced no observable effect on the Rh5-PR bouton size (Figure S2D). In contrast, light deprivation starting from the L2 stage for various durations, including a short 36hr period of light deprivation right before testing, was sufficient to significantly reduce Rh6-PR bouton size to the level of the negative control (Figure 3E), suggesting a sustained requirement of light input after the L2 stage. Results obtained from the “light since” paradigm support this observation; boutons of animals deprived of light before entering the L2 stage (“light since L2”) were not different from the positive control (Figure 3E). On the other hand, although Rh6-PR boutons of larvae deprived from light until L3F1 and L3F2 were larger than the negative controls, they were also significantly smaller than light-reared positive controls. Combined results from these time specific visual deprivation experiments indicate that the light exposure during the L2-L3F1 stages is necessary but not sufficient for the normal expansion of Rh6-PR boutons, which appear to be regulated by the overall duration of light exposure during larval development.

Given the essential role of social conditioning in the acquisition of moving target attraction and clustering behavior [60,200], we tested whether social

interactions influence PR bouton morphology by comparing PR bouton sizes in larvae raised in groups (social) or in isolation (isolated) (Figures 3F and S2E). As expected, no differences were observed in Rh5-PR bouton size between social vs. isolated groups (Figure S2E). However, prolonged social isolation (since the L2 and since L3F1 stages) reduced bouton size in Rh6-PRs, while isolation later in development (since L3F2) did not produce a significant reduction (Figure 3F). This result is consistent with the late L2-early L3F1 stage being the critical period for development of movement detection underlying social clustering [60,200]. Importantly, the overall effect of social isolation on bouton morphology was notably less than the effect of light deprivation, suggesting that visual cues perceived from other larvae likely constitute only part of the general visual experience for the developing larvae.

Taken together, we demonstrate that presynaptic boutons in Rh6-PRs, but not in Rh5-PRs, are susceptible to experience-dependent structural plasticity and require exposure to light and social environment for proper development. Importantly, these observations are in line with our behavioral results and further strengthen the role for Rh6-PRs in social clustering.

Functional connectivity between Rh6-PRs and lOLPs is regulated by visual experience

To examine whether the Rh6-PR bouton size changes have physiological relevance, we next examined the number of Rh6-PR synaptic contacts as well as

their functional connectivity to downstream lOLPs. To identify putative synaptic sites generated by Rh6-PR axonal projections, we used an mCherry-tagged presynaptic active zone component Bruchpilot (Brp). The Brp::mCherry puncta label presynaptic release sites and provide quantitative assessments of the number of putative synapses [129,159,225].

Images obtained from the larval brain indicate that Rh6-Brp:mCherry puncta mark the Rh6-PR presynaptic terminals in close proximity with lOLP projections (Figure S3A). Using 3D reconstruction and quantification (Figure S3B), we measured the number and total volume of the Rh6-Brp:mCherry puncta in larvae subjected to light or dark-rearing since egg laying. We found that the effect of light deprivation on Rh6-Brp:mCherry puncta was similar to the one observed for Rh6-PR bouton morphology; starting from the L3F1 stage, both number and total volume of the puncta were significantly reduced in dark-reared animals compared to the light-reared controls (Figures 4A, 4B, S3C). In addition, the time-restricted light deprivation experiments also produced similar results to the ones obtained from the Rh6-PR bouton morphology analyses. Even a short 36hr period of darkness right before the testing is sufficient to generate a significant decrease in the number of Rh6-Brp:mCherry puncta, while early light deprivation with a long recovery period lead to only moderate changes (Figure S3D). Consistent with the findings for Rh6-PR bouton development, the presynaptic terminals of Rh6-PRs also displayed sensitivity to social conditions; both number and volume of Rh6-Brp:mCherry puncta were reduced in isolated animals as compared to the group-reared controls (Figures 4C, S3E).

Together, these experiments suggest that, besides regulating the growth of Rh6-PR boutons, light and social conditions during development also influence the number of presynaptic sites generated by Rh6-PR axonal projections, which potentially leads to changes in circuit properties and corresponding behaviors. To test whether light or social deprivation leads to deficits in functional connectivity between Rh6-PRs and downstream lOLPs, we examined light-elicited physiological responses in lOLPs using calcium imaging [36,208]. This approach allowed us to observe light-induced activation of cha-lOLP, corresponding to a large and immediate calcium rise, as well as light-induced inhibition in glu-lOLP, corresponding to an initial dip followed by a small and delayed calcium transient (Figure 4D) [21]. Compared to the light-reared control animals, dark-reared larvae showed significant reductions in the amplitude of lOLPs' calcium responses, suggesting that light deprivation dampens light-elicited activity in both cha- and glu-lOLPs (Figure 4E).

On the other hand, social isolation, which produced a mild reduction of the number of Rh6-PR presynaptic terminals (Figures 4C, S3E), did not generate significant reductions in light-elicited calcium responses in either lOLPs (Figures 4F and 4G). Although it is likely that our calcium imaging approach is not sensitive enough to detect subtle changes in the lOLP physiology, it is also possible that behavior deficits induced by social isolation are due to its profound impacts on the larval nervous system, beyond morphological and/or physiological alterations in the Rh6-PR/lOLP pathway. More sensitive recording methods with improved spatial and temporal resolutions are likely needed to discern those possibilities.

Visual function in larval social interactions

Drosophila larvae perform cooperative digging to facilitate food digestion and to avoid desiccation and predators [32,91]. It is therefore not surprising that multiple sensory inputs are utilized to ensure the establishment and maintenance of this ethologically important behavior. Previous studies indicate the involvement of pheromone detection, olfaction, nutrient sensing and mechanosensation in larval aggregation, which initiates social interactions [149,169,242]. However, to form coordinated actions within the social clusters and maintain these dynamic structures over time, visual recognition of other larvae's movements is also required [60,119,200]. Visual regulation of larval social clustering elevates the complexity of the behavior and incorporates the possibility of experience-dependent modification through sensory experience and social learning.

Although there is a strong correlation between the Rh6-PR bouton size and the larva's ability to efficiently engage in social clusters, due to the complex effect of visual activity on Rh6-PR bouton development, lOLP light responses and clustering behavior, the causal relationship among these events are yet to be determined. Genetic manipulations targeting specific molecular pathways will be essential to illustrate the functional role of the plasticity we observed.

A plastic movement-detecting pathway in the larval visual circuit

The most striking finding of this study is the distinction between Rh5- and Rh6-PRs. Behavioral studies indicate that Rh5-PRs are essential for most vision-

related behaviors in larvae. Rh6-PRs, on the other hand, appear to be generally dispensable for light-induced behaviors, with the exception of being required for the perception of temporal light information during larval navigation [79,108,109,120,123,124,136,150]. The data presented here illustrate functions of the Rh6-PRs in movement detection and social clustering, thus clearly demonstrating a specific requirement of Rh6-PR/lOLP pathway in complex visual processing. These observations also raise important questions about how larvae compute motion using a primitive visual circuit. Although direct physiological evidence is still missing, connectome studies indicate that, besides the inputs from Rh5-PRs, larval VPNs also receive inputs from both cha- and glu-lOLPs, which, as shown by our recent physiological studies, are ON and OFF detectors, respectively [21]. Therefore, similar to the direction-selective movement detectors in adult fly visual systems and mammalian retinas [24,185,217], larval VPNs possess the intrinsic ability to integrate spatial and temporal information of the visual scene and compute motion [21,109,136]. The specificity of larval visual processing likely emerges at the level of these VPNs, the majority of which have not yet been characterized. Future investigations on individual VPNs will identify the downstream target of Rh6-PR/lOLP in regulating social clustering.

Remarkably, although both PRs are required for social clustering and movement detection, only Rh6-PRs exhibit susceptibility to alterations of the visual and social environment. The increases in Rh6-PR bouton size and synapse number occur after the L2 stage, temporally correlating with the emergence of clustering behavior as well as the critical period required for the development of

movement detection. Taken together, these differences between the Rh5- and Rh6-PR pathways suggest that the restricted cellular resources in the larval nervous system demands effective use of a simple circuit, which is compartmentalized into a hardwired light sensing apparatus and plastic movement detectors.

In conclusion, our studies suggest that plasticity in a specific visual pathway could potentially support the social learning required for the emergence of larval cooperative behavior and thus provide an example of how the “social brain” is established in the nervous system that serves the needs of both independent individuals and cooperative social groups. In addition, the striking differences in Rh5- and Rh6-PRs’ susceptibility to visual deprivation also opens up new avenues for molecular studies on experience-dependent structural plasticity. Although decades of investigations have established *Drosophila* larvae as an effective model system for behavioral analyses on functional plasticity, including learning memory, addiction and sleep regulation [2,65,121,193,216], there are only limited examples of structural plasticity in Drosophila CNS [183,246]. Molecular understanding of the phenomenon we observed in larval visual circuit will not only help us identify the common components involved in social learning and associative learning, but also provide a comprehensive view on how structural and functional plasticity is cooperatively regulated during development for the acquisition of complex behaviors.

Acknowledgements

We thank the Bloomington Stock Center (NSF DBI0,841,154) for providing fly stocks. We thank Jay Hirsh, Sarah Siegrist, Chris Deppmann, Ali Guler, T. Angel, Simon Sprecher and members of the Condron lab (Nitesh Alluri, Grace Kaupas, Tiffany Tran, Hunter Shelton and Rives Kuhar) for providing advice and comments. This work was supported by NSF Grant ABI1062433 (SA and BC), the Hobby Foundation (SA and BC) and the Jefferson Scholars Foundation (MD), Owens Foundation (BC), 3Cavaliers Fund (BC & SA), and the intramural research program of National Institute of Neurological Disorders and Stroke (NINDS), Project number 1ZIANS003137 (QY). Mouse monoclonal anti-chaoptin (developed by S. Benzer and N. Colley) and anti-LacZ (developed by J.R. Sanes) antibodies, were obtained from the Developmental Studies Hybridoma Bank, created by the NICHD of the NIH and maintained at The University of Iowa, Department of Biology, Iowa City, IA 52242.

Author contributions

Conceptualization & Methodology: B.C., M.D., Q.Y.; Investigation & Data collection: M.D., A.K., L.P., E.S., Q.Y; Data analysis: M.D., L.P, A.K.; Software development: A.V., S.A. Writing, reviewing and editing: M.D., B.C., A.K.; Q.Y. Funding acquisition: B.C., Q.Y.

Declaration of interests

The authors declare no competing interests.

Materials and Methods

Experimental model and subject details

All *Drosophila* strains were raised in vials containing standard media (cornmeal, yeast, molasses, and agar) at 25°C, 30% humidity under 12h light/12h dark cycle (unless further specified in "Light/Dark-rearing experiments" methods section) at ~1000 lux light intensity. Flies used for behavioral assays were backcrossed to wild type Canton-S background for 6 generations. For egg production, ~50 adult flies 3-4 days old were transferred into egg cups and kept in the same conditions. Eggs were collected on 35mm petri dishes containing standard agar-molasses food and yeast every 6 hours for experimental procedures and eggs/larvae were kept (unless specified) in the same light/temperature/humidity conditions.

Preparation of "pre-processed" vials and cluster frequency assays.

Techniques for "pre-processed" vial production and transplantation of 200 L2 larvae were adapted from our previous study [60]. To produce L3Fc larvae (Figures 3A, 3C, 3D, 4B, S1A, S2C, S3C), animals were transferred into pre-processed vials at L2 stage and reared until day 5 of 3rd instar (180h AEL). For cluster frequency measurements (Figure 2A), 5 to 7 "pre-processed" vials with previously transferred 200 L2 larvae of a designated genotype raised in normal conditions were recorded for 3 consecutive days (24hrs non-stop) starting from L3F3 stage (120h AEL).

2D cluster preparation and assays (% in clusters and time delays measurements)

Techniques for 2D cluster preparation and assays were adapted from our previous study [60]. Video recording began as soon as 30 larvae were transplanted in a 2D apparatus and lasted for 5 hours. In order to derive clear data on the percentage

of larvae engaged in clustering, the first 2 hours of recording were not analyzed to give larvae time to adjust to the new environment and start forming clusters (Figure S1B). After a 5-hour time period, a clearly visible cluster in each 2D apparatus was zoomed in and recorded in high-resolution to produce 10-minute videos for time delays measurements (Figure S1C).

Light avoidance assay

In order to determine if larvae maintained normal light avoidance (used as a measure of general vision), a modified version of a standard light preference assay developed for *Drosophila* larvae [147] was used. 30 middle 3rd instar larvae raised in normal light/dark conditions were collected from food plates, briefly washed in tap water and transferred onto a 100mm petri dish split into 4 quadrants of equal area, 2 of which are exposed to light coming from an LED light box located below and 2 of which were left in the darkness using underlaid pieces of black cardboard paper and aluminum foil forming an X-mask (Figure 2B). The bottom of the dish was covered with a thin layer of 2% agarose. An assay was performed in a completely dark room with the only source of light coming from the LED light box (~1500 lux light intensity). The camera was located directly above the petri dish. Larvae originally placed in the center of the dish were recorded for 5 minutes, after which the plate was discarded and replaced with a fresh plate with new larvae.

Visual attraction assays

The methodology was adapted from Justice et al. [119] with minor changes. Individual larvae staged middle L3F3 (132h AEL) were assayed on 100mm petri dishes covered with 2% agarose. For fixed target assays, a 10x5mm piece of black plastic was attached to the lid with superglue, 10mm away from the edge. For moving target assays, 5 larvae were tethered to the outer side of the bottom of the petri dish with superglue, 10mm away from the edge, in a way that enabled rotational movements during the course of the assay (Figure S1D). Assays were

performed in closed behavioral chambers with internal LED light sources (~1000 lux light intensity). The camera was located directly above the petri dish. After each assay, the agarose and tethered larvae were discarded.

Light/Dark-rearing experiments

For experiments involving light deprivation, dark-reared larvae were kept in a dark room for the designated time period in a food plate/vial covered with aluminum foil. For light-reared controls, animals were raised in constant light conditions during designated time periods. For light avoidance, moving or fixed target attraction assays, Brp puncta measurements and calcium imaging in light-deprived animals (Figures 2D, 4A, 4B and 4E), larvae were reared in darkness since egg laying, then tested in light at the middle of the L3F3 stage (132h AEL) for behavioral assays and calcium imaging or at the designated stage for Brp puncta measurements. For clustering assays in light-deprived animals (Figure 2D), 200 larvae were reared in the darkness until the L2 stage, then transferred into a vial with pre-processed food under infrared light until being transferred onto the 2D apparatus in light for percentage in clusters and time delay measurements in the middle L3F3 stage. All assays were performed as described in the corresponding methods section. For morphological measurements (Figure 3) all larvae were tested in the middle L3F3 stage after being reared in the designated light/dark conditions. For the “dark since” paradigm, larvae were reared in constant light until the designated stage (L2, L3F1 or L3F2), then transferred into darkness until dissection at the middle L3F3 stage. For “light since” paradigm, larvae were kept in the darkness since egg laying until the designated stage (L2, L3F1 or L3F2), then transferred to constant light conditions until dissection at the middle L3F3 stage.

Social isolation experiments

The technique of social isolation was generally adapted from our previous study [200]. Animals were raised under normal social conditions until the L2 stage (48h AEL) for Brp puncta measurements (Figure 4C) and calcium imaging (Figure 4F) or until the designated stage (L2, L3F1 or L3F2) for bouton measurements (Figures 3F and S2E), then individually transferred into separate food plates and reared in isolation under otherwise normal conditions until the middle L3F3 stage with subsequent dissections.

Stochastic Multicolor Flip-Out (Brainbow) technique

For visualization of presynaptic boutons in individual PR cells, *Rh5-GAL4* and *Rh6-GAL4* lines were used to drive the expression of UAS-Brainbow in PR cells [163]. To ensure stochastic labeling of about 15-20% cells (Figures 3A, 3B, S2B, S2C), larvae were heat shocked at 38ºC for 30min during the middle L1 stage (36h AEL), transferred back to normal temperature and dissected at the designated stage.

Video recordings

For behavioral assays, videos were recorded on an iPhone 5 at full resolution and 1 frame/2 sec (for visual attraction assays), 1 frame/10 sec (for percentage larvae in 2D clusters) or 1 frame/60 sec (for cluster frequency in vials and light avoidance assay) using “Lapseit” software. For time delays in 2D clusters measurements, a Nikon D3100 CMOS camera with 50mm lens and fitted with a Raynox Macroscopic 4x lens was used. Videos were recorded at 24fps at 1920x1080 resolution. Video analysis was further performed in iMovie followed by ImageJ and customized Python-based software (see Segmentation and Tracking for more details).

Immunohistochemistry and confocal imaging

Unless specified, brains were collected from middle L3F3 larvae (132h AEL) and placed in the fixative solution (4% paraformaldehyde (PFA) in PBS at pH 7.4) for 1 hr, then washed in PBS for 10 min and transferred into permeabilizing solution (0.2% Triton X-100 in PBS (PBST)) and incubated overnight in primary antibodies at 4ºC. The brains were then washed with PBST (3x10 min at room temperature) and incubated with the appropriate secondary antibodies overnight at 4ºC. The stained brains were washed in PBST (3x10 min at room temperature) and in PBS (1x10 min at room temperature), then mounted on slides using antifade solution. Images were captured with Nikon eclipse E800 microscope (100x, oil-immersion lens, NA=1.3) equipped with a Hamamatsu ORCA-ER camera and a Perkin-Elmer spinning disc confocal unit using Perkin Elmer v5.5 acquisition software. The microscope and camera were calibrated using calibration beads, Fluorescent Microspheres Kit (6 µm, Molecular Probes, F-24633). All images were acquired using 2x2 binning and 0.14 µm-thick sections at 80x60µm resolution. Exposure times varied from 150 to 700 ms, depending on the intensity of the immunofluorescence. The following primary antibodies were used: anti-GFP (chicken, 1:1000, AB_300798), anti-serotonin (rat, 1:1000, AB_11199213), anti-chaoptin (mouse, 1:100, RRID:AB_528161), anti-LacZ (mouse, 1:100, AB_2314509), anti-DsRed (1:1000, rabbit, AB_912560), anti-V5 (1:500, mouse, AB_322378), anti-HA (1:1000, rabbit, AB_1549585). The secondary antibodies (Thermo Fisher Scientific) used were: goat anti-chicken (1:200, AB_142924), goat anti-rabbit (1:200, AB_143157) and goat anti-mouse (1:200, AB_141693).

Visual stimulation and two-photon calcium Imaging

Late third instar larvae (L3F3 stage) expressing R84E12-Gal4 driving UAS-GCaMP6f were used for calcium imaging experiments that were performed during the subjective day between ZT1-ZT8 (ZT: zeitgeber time in a 12:12h light/dark cycle; lights-on at ZT0, lights-off at ZT12). Procedures for dissection and preparation of larval brain explants were as described [29]. The eye-brain explant

containing the Bolwig's organ, the Bolwig's nerve, eye discs and the larval brain were dissected in PBS and then transferred into an external saline solution (120 mM NaCl, 4 mM MgCl2, 3 mM KCl, 10 mM NaHCO3, 10 mM Glucose, 10 mM Sucrose, 5 mM TES, 10 mM HEPES, 2 mM Ca2+, PH 7.2) and maintained in a chamber between the slide and cover-glass during the recording sessions.

Two photon imaging of GCaMP6f was performed on a Zeiss LSM 780 confocal microscope equipped with a Coherent Vision II multiphoton laser. Time-lapse live imaging series were acquired at 100 ms per frame for 1000 frames using a 40x water objective with the 2photon laser tuned to 920 nm. Typical resolution for a single optical section is 256 µm x 96 µm with 3x optical zoom. The preparation was stimulated by 100 ms light pulses generated by the 561 nm confocal laser and delivered using the photobleaching program in the Zen software.

Quantification and statistical analysis

Segmentation and tracking

a. Visual attraction assays

A Python-based tool (see link below) was developed to track larval movements on a Petri dish. The input for the analysis is a video containing a single 100 mm Petri dish in which a single larva is allowed to move. Before the analysis begins, the user is required to select 5 points along the perimeter of the Petri dish (arena) and 5 points around a region of interest (target) within the arena. These points are used to generate two ellipses. The arena ellipse is used to correct for perspective deformation, the target ellipse is used to evaluate when the larva is within the target region, and the barycenter of the two ellipses is used to align the heat maps (see below) from different assays allowing for direct comparison. The video processing begins with background removal. The background is continuously estimated from the frames of the video using an exponentially weighted moving average (exponential smoothing): $B_t = (1 - \alpha)B_{t-1} + \alpha F_t$. In this equation F_t is the current frame, B_t is the current estimate of the background, B_{t-1} is the previous estimate

of the background, and α is known as the *smoothing factor*. In our work we used $\alpha = 0.02$ and considered the exponential smoothing to be fully initialized after 50 frames. After the exponential smoothing is fully initialized, the background is subtracted from each frame and a Canny edge detector [29] is applied to the resulting image after contrast stretching. If a close contour is detected within the arena, it is associated with the larva. This approach allows us not only to track the larva frame by frame, but also record the exact shape of the larva. The latter is used to generate normalized heat maps, stored as PNG images that represent the probability of observing the larva at a certain location within the arena. Furthermore, as the larva moves freely within the arena, its distance (normalized with respect to the size of the Petri dish) from both the arena's and the target area's center are computed. At the end of each video, the probability of observing a larva at a certain distance from either centers is computed using the kernel density estimator [198] provided by the *statsmodel* library [194] (Figure S1D). The location of the barycenter of the larval detected shape is used not only to evaluate location but also velocity and travelled distance at each frame (Figure S1E), controlling for the potential for altered locomotive patterns affecting the observed values of larval attraction to a target. These values were stored within an Excel spreadsheet used for further analysis. The Excel file also contains all the metadata relative to the assay as well as a standardized version of the oriented heat map evaluated by using a 1 cm square grid co-centered with the arena ellipse. These data were used to synthesize and compare the behavior of different larvae across visual attraction assays. We used the percentage of the total number of frames in which a larva was observed within 15 mm from the center of the target as a representation of visual attraction (Figures 2C, 2D). If the percentage of frames in which a larva was observed within 20 mm from the center of the petri dish exceeded 50%, the video was discarded due to concerns indicating mechanistic locomotion problems not involving vision, considering that larvae were originally placed in the center.

b. Clustering assays (measuring time delays between larvae)

Another customized Python-based software tool (available upon request) was developed to track larval movements and measure time delays in a 2D cluster [60]. The application allowed the user to identify regions of interest (larva tails) to be tracked simultaneously within hi-resolution video recordings (24fps at 1920x1080). For each region identified by the user, the software generates a template based on a running weighted average of the last 30 frames (with higher weight associated the most recent frames). This template is used to detect and track the larvae's tails from frame to frame. Using this approach, the absolute position of the larvae's tails as well as their position relative to each other are tracked over time. These displacements are plotted as they are measured and stored in a CSV format for further analysis. We used these datasheets to quantify the delays between upward compression movements between each pair of larvae within a triplet. For each genotype, 10-15 10-minute high-resolution recordings were acquired derived from different 2D cluster assays. Normalized time delays (Figures 1C, 1D, 2D) were expressed as time differences between contractions of adjacent larvae within a triplet divided by the length of larval contraction cycle (measured individually for each genotype). Data points represent time delay values derived from single contractions of a larval pair.

ImageJ video analysis

Videos from recordings of 2D cluster assays (percentage larvae in clusters measurements), vials (cluster frequency measurements) and light avoidance assays were imported into ImageJ (32-bit version) as QuickTime movies and manually analyzed frame-by-frame. For cluster frequency measurements, the number of frames with a clearly visible cluster was expressed as a fraction of the total number of frames recorded per day (1440 frames during a 24-hour period (see Video recordings for more details). Every data point (Figure 2A) represents the percentage of time a cluster was seen during a 24h recording of a single vial of a given genotype. Therefore, 15-21 data points were acquired for all strains. For

light avoidance assays, the light preference index (Figures 2B, 2D) was calculated as the ratio of larvae in light 5 min after the start of the experiment to the total number of larvae originally placed in the dish. Data points represent the results of individual 5 min assays. For the percentage of larvae in 2D clusters measurements (Figures 1C, 1D, 2D), 15 videos were analyzed for each genotype. The fraction of larvae engaged in clusters was calculated as the ratio of larvae observed within all visible clusters to the total number of larvae seen at a given time point. This value was assessed every 108 frames (18 min) for 3 hours (see 2D cluster preparation), producing 10 values that were subsequently averaged and expressed as a single resulting data point representing one 5-hour recording from a single 2D apparatus per designated strain (resulting in n=15 for all genotypes).

Volocity reconstructions and measurements

For the measurements of PR presynaptic bouton sizes and Rh6-Brp::mCherry puncta number evaluation, corresponding confocal Z-stacks were imported into Volocity, auto leveled and reconstructed in 3D for further analysis. Images were segmented and quantified using the Volocity Classifier [215]. Customized settings were used to identify and separate objects of a designated shape and size corresponding to a single Rh6-Brp::mCherry punctum (representing an individual T-bar) or a single Rh5 or Rh6-PR presynaptic bouton. For classification, the intensity distribution minimums and maximums were bounded, with additional noise reduction and touching object separation. The lower object size threshold was set at 0.1 (sphere) and 1 μm^3 (short ovoid) for Brp puncta and presynaptic boutons, respectively. For quantitative assessment of presynaptic bouton size in PRs, only images with clearly visible distinct presynaptic boutons were chosen (Figures 3A, 3B, S2C). Every data point represents a single bouton measurement. In most cases, 2-4 boutons (representing 1-2 cells) were measured per brain, and only 1 brain lobe was used for measurements. Therefore, every data set is represented by ~15-50 animals per genotype/light condition. For Rh6-Brp::mCherry puncta, total number (Figures 4B, 4C, S3B, S3D) and total volume

(Figures S3C, S3E) of puncta were evaluated. Each data point represents a number of Rh6-Brp::mCherry puncta in a single brain lobe (only one side of the brain was measured for all animals).

Calcium imaging analysis

The quantification and graphing of the calcium imaging data were performed using a custom written MATLAB script. Specifically, the average fluorescence intensity of the 20 frames prior to the stimulation was computed as F0. The change of fluorescence intensity after the stimulation was computed as (Ft-F0)/F0 (ΔF/F). For each sample, the peak amplitude, defined as the highest value of ΔF/F within the 80 frames after the stimulation, was computed and used for statistical analyses. Traces in Figures were generated by plotting the average ΔF/F of individual samples +/- standard error of the mean for each frame for the duration of 20 sec or 200 frames using a customized MATLAB script. Sample number n represents the numbers of animals used in the recording.

Statistical analysis

Unless otherwise stated, all data are presented as the mean and error bars represent the SEM for behavioral and calcium imaging experiments (Figures 1, 2 and 4) and 95% confidence intervals for boutons and Brp puncta morphological measurements (Figures 3 and 4). Statistical significance was calculated by one-way ANOVA using Tukey's method. When comparing two groups of normally distributed data, Student's two-tailed unpaired T-test was used. *$p<0.05$; **$p<0.01$; ***$p<0.001$. Statistical analysis is also reported within the Results section and Figure Legends. Analysis was conducted using the GraphPad Prism 7 statistical software for Windows.

Data and software availability

Sample confocal image stacks are available on Medeley Data: https://doi.org/10.17632/z6pfm23dcr.1. Other primary data (including video recordings, calcium imaging recordings and more image stacks) are available upon request. Information about and requests for data can be directed to and will be fulfilled by the Lead Contact, Barry Condron (bc4f@virginia.edu).

Python code for larval tracking software is available at the following links:

https://github.com/avaccari/DrosophilaAttraction (tracking software used for visual attraction assays)

https://github.com/avaccari/DrosophilaCooperative (tracking software used for clustering assays)

KEY RESOURCES TABLE

REAGENT or RESOURCE	SOURCE	IDENTIFIER
Antibodies		
Mouse monoclonal anti-chaoptin	DSHB	Cat#24B10 RRID:AB_528161
Chicken polyclonal anti-GFP	Abcam	Cat#ab13970 RRID:AB_300798
Mouse monoclonal anti-LacZ	DSHB	Cat#40-1a RRID:AB_2314509
Rabbit polyclonal anti-DsRed	BioVision	Cat#3993-100 RRID:AB_912560
Goat polyclonal anti-rabbit IgG (H+L) Alexa Fluor 568 conjugated	Thermo Fisher Scientific	**Cat#**A-11011 RRID:AB_143157
Goat polyclonal anti-chicken IgG (H+L) Alexa Fluor 488 conjugated	Thermo Fisher Scientific	**Cat#**A-11039 RRID:AB_142924
Goat polyclonal anti-mouse IgG (H+L) Alexa Fluor 647 conjugated	Thermo Fisher Scientific	**Cat#**A-21235 RRID:AB_141693

Mouse monoclonal anti-V5-TAG Clone SV5-Pk1	Bio-Rad	Cat#MCA1360 RRID:AB_322378
Rabbit polyclonal anti-HA	Cell Signaling Technology	Cat#3724, RRID:AB_1549585
Phalloidin (Invitrogen™ Alexa Fluor™ 633)	Thermo Fisher Scientific	Cat#A22284
Experimental Models: Fly strains		
Canton S	Ed Lewis, Caltech	N/A
GMR-hid^{G1}	Bloomington stock center	Cat#5771
R72E03-GAL4	Bloomington stock center	Cat#47445
R84E12-GAL4	Janelia Farm Flylight	N/A
vGluT-GAL80	Bloomington stock center	Cat#60316
UAS-GCaMP6f	Bloomington stock center	Cat#42747
rh5^{2} (loss-of-function null allele)	Chi-Hon Lee, NIH	N/A
rh6^{1} (loss-of-function null allele)	Chi-Hon Lee, NIH	N/A
rh5^{2}/rh6^{1}	Chi-Hon Lee, NIH	N/A
Rh6-Brp:mCherry	Chi-Hon Lee, NIH	N/A
UAS-Brainbow	Bloomington stock center	Cat#64085
UAS-Kir2.1::EGFP	Bloomington stock center	Cat#6595
UAS-mCD8::GFP	Bloomington stock center	Cat#5137
Rh5-GAL4	Bloomington stock center	Cat#7458
Rh6-GAL4	Bloomington stock center	Cat#66672
UAS-LacZ	Bloomington stock center	Cat#3955
Software and Algorithms		
Software (Python) for larval tracking (clustering and visual attraction assays)	This paper	https://github.com/avaccari/DrosophilaAttraction

		https://github.com/avaccari/DrosophilaCooperative
ImageJ for Windows 32-bit	NIH	https://imagej.nih.gov/ij/
Volocity 6.5.1 Windows 32-bit	Quorum Technologies	https://www.quorumtechnologies.com/index.php/2014-06-19-13-10-00/2014-06-19-13-14-30/image-analysis/2-uncategorised/110-volocity-downloads
Prism 7	GraphPad Software	https://www.graphpad.com/scientific-software/prism/
Perkin Elmer image acquisition software v5.5	N/A	http://www.perkinelmer.com/lab-products-and-services/resources/in-vivo-imaging-software-downloads.html
Primary data		
-sample confocal image stacks (Rh5/Rh6 presynaptic boutons and Rh6-Brp::mCherry puncta)	This paper	https://doi.org/10.17632/z6pfm23dcr.1
-Video recordings and primary output files of behavioral assays -More confocal image stacks -Calcium imaging recordings	This paper	Available upon request

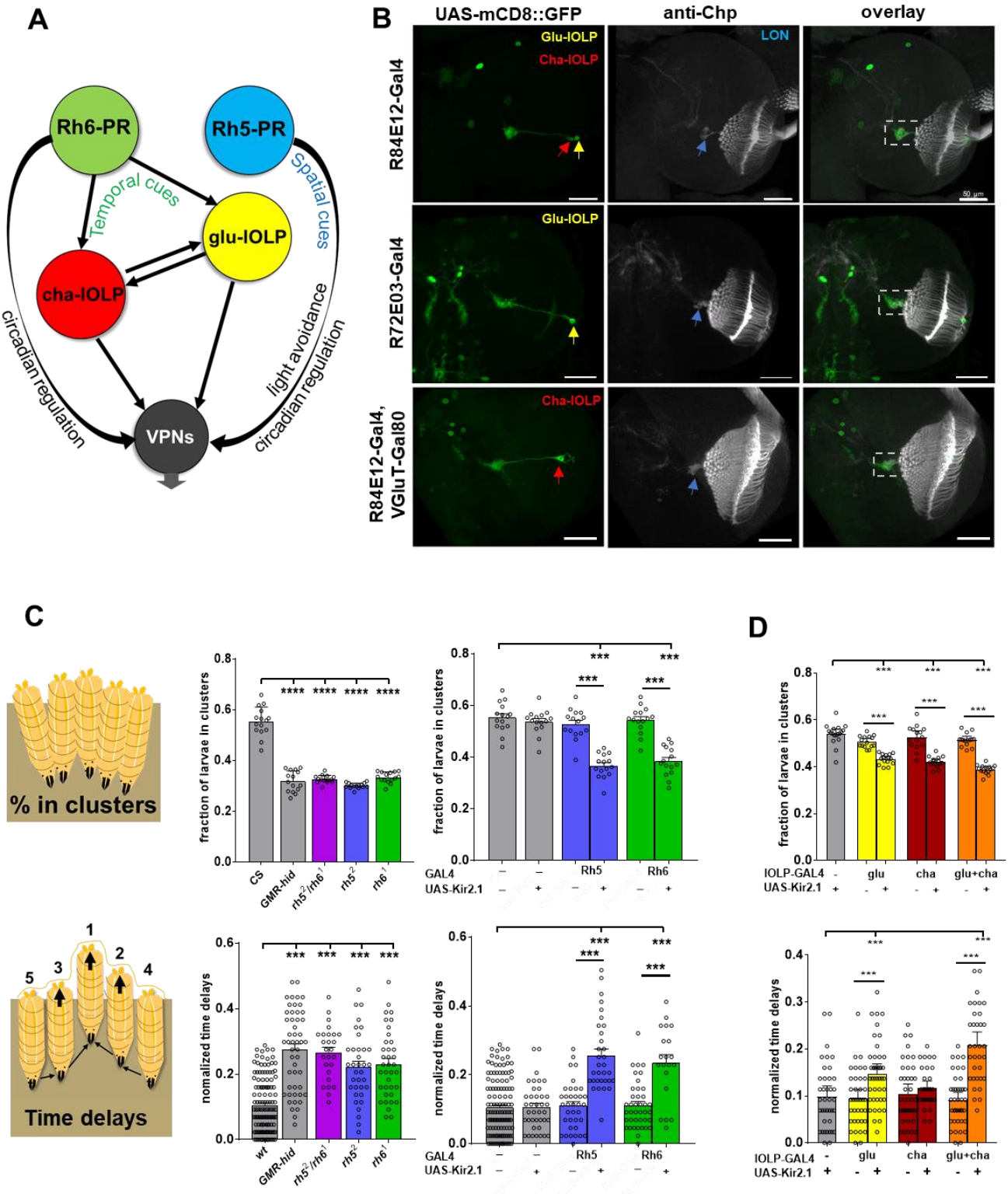
A
Rh6-PR
Rh5-PR
Temporal cues
Spatial cues
glu-lOLP
cha-lOLP
circadian regulation
light avoidance
circadian regulation
VPNs
B
UAS-mCD8::GFP
anti-Chp
overlay
R84E12-Gal4
R72E03-Gal4
R84E12-Gal4, VGluT-Gal80
Glu-lOLP
Cha-lOLP
LON
50 µm
C
% in clusters
fraction of larvae in clusters
CS
GMR-hid
rh5²/rh6¹
rh5²
rh6¹
GAL4
UAS-Kir2.1
Rh5
Rh6
Time delays
normalized time delays
wt
D
lOLP-GAL4
glu
cha
glu+cha

Figure 1. Rh6-PRs and lOLP neurons are required for social clustering behavior

(A) Schematic diagram of the *Drosophila* larval visual circuit with two pathways. Rh6-PRs and Rh5-PRs project onto different primary postsynaptic targets in the larval optic neuropil (LON). Rh5-PRs connect directly with visual projection neurons (VPNs), while the majority of Rh6-PRs axon terminals connect to two local interneurons (lOLPs) that subsequently converge onto the VPNs. Either PR type is sufficient for circadian entrainment, but only Rh5-PRs are necessary for light avoidance behavior. Perception of temporal light cues is implemented by the Rh6-PR/lOLP pathway, while Rh5-PRs perceive spatial light cues [109].

(B) PR axonal terminals form connections with lOLPs in the LON. R84E12-Gal4 (labels both lOLPs), R72E03-GAL4 (labels glu-lOLP) and R84E12-GAL4; VGluT-GAL80 (labels cha-lOLP) were used to drive the expression of UAS-mCD8::GFP. Left panel: yellow arrow indicates the cell body of glu-lOLP. Red arrow indicates the cell body of cha-lOLP. Middle panel: PR axonal projections were visualized by anti-chaoptin staining (anti-Chp, grey). Blue arrow indicates presynaptic terminals of Rh5-PRs and Rh6-PRs. Right panel: dashed rectangles indicate the overlapping areas between PR axonal projections and lOLP terminals in the LON. Images represent maximum intensity projections of confocal image stacks obtained from third instar larval brains. Scale bars represent 50 μm.

(C and D) Clustering assays in animals with compromised function of PRs and lOLPs indicate an essential role of the Rh6-PR/lOLP pathway for visually-guided cooperative digging behavior. $rh5^{2}$, $rh6^{1}$ and double $rh5^{2}/rh6^{1}$ mutants were examined along with the blind control GMR-hid (C, middle panel). Rh5-GAL4, Rh6-GAL4 (C, right panel), R84E12-Gal4, R72E03-GAL4 and R84E12-Gal4; VGlut-GAL80 lines were used to silence subgroups of PRs and lOLPs by driving expression of UAS-Kir2.1 in Rh5-PRs, Rh6-PRs, both lOLPs, glu-lOLP and cha-lOLP, respectively (D). Manipulations with Rh6-PRs and either or both lOLPs significantly reduce the percentage of larvae forming clusters (C and D, top) and increase intra-cluster time delays between larvae (C and D, bottom).

See also Figure S1

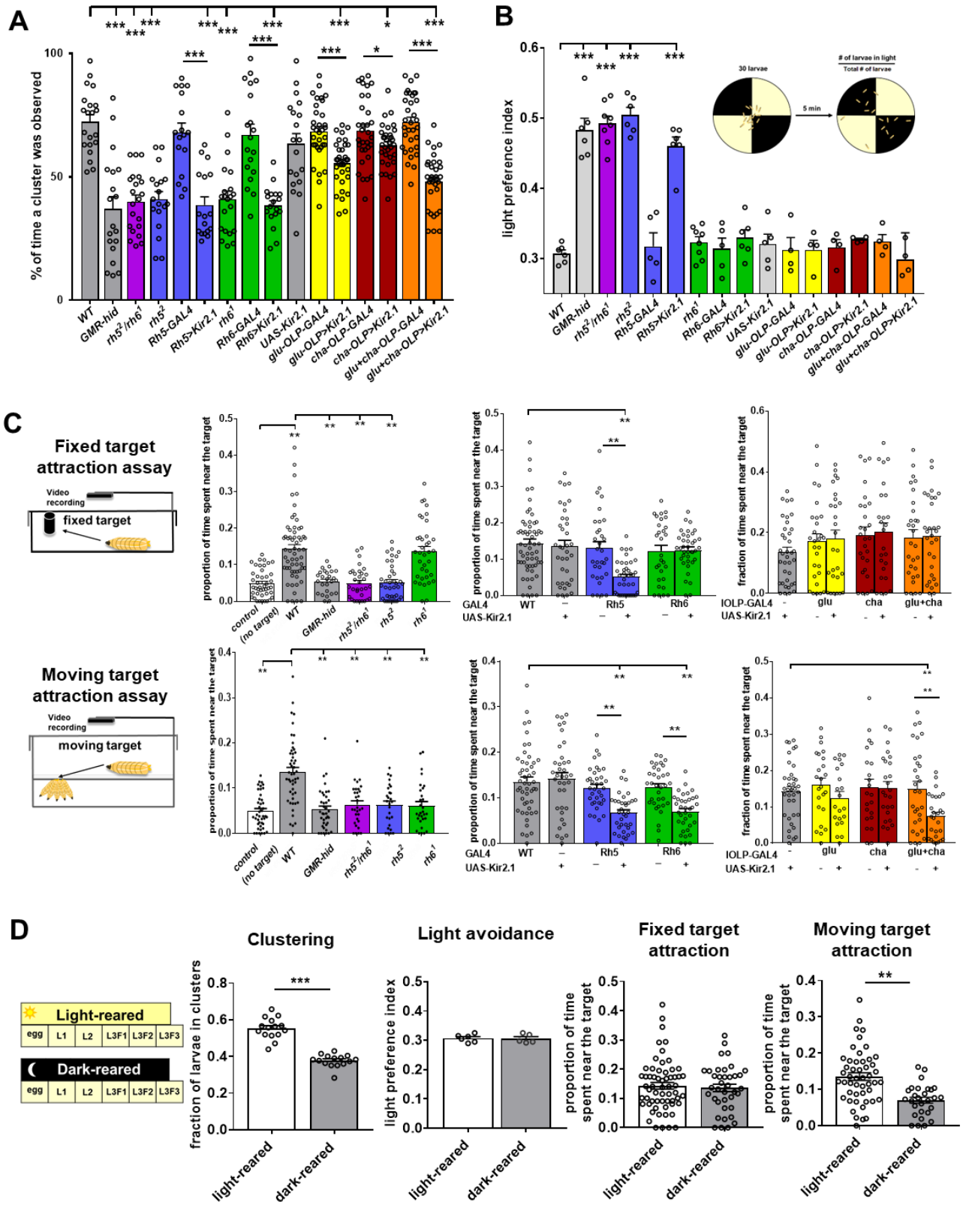
A
% of time a cluster was observed
WT
GMR-hid
rh5²/rh6¹
rh5²
Rh5-GAL4
Rh5>Kir2.1
rh6¹
Rh6-GAL4
Rh6>Kir2.1
UAS-Kir2.1
glu-OLP-GAL4
glu-OLP>Kir2.1
cha-OLP-GAL4
cha-OLP>Kir2.1
glu+cha-OLP-GAL4
glu+cha-OLP>Kir2.1
B
light preference index
30 larvae
5 min
# of larvae in light
Total # of larvae
C
Fixed target attraction assay
Video recording
fixed target
proportion of time spent near the target
control (no target)
GAL4
UAS-Kir2.1
fraction of time spent near the target
IOLP-GAL4
glu
cha
glu+cha
Moving target attraction assay
moving target
D
Light-reared
Dark-reared
egg
L1
L2
L3F1
L3F2
L3F3
Clustering
fraction of larvae in clusters
Light avoidance
light preference index
Fixed target attraction
Moving target attraction
proportion of time spent near the target
light-reared
dark-reared

Figure 2: Social clustering and movement detection share a common visual pathway that is sensitive to visual experience

(A and B) Social clustering represents a distinct visually-guided behavior unrelated to simple light-dark discrimination and is implemented by the Rh6-PR/lOLP pathway. Cluster frequency measures in vials (A) confirms the requirement of the Rh6-PR/lOLP pathway for cooperative digging behavior. At the same time, light avoidance assays (B) indicate the dispensability of the Rh6-PR/lOLP pathway for general visual functions.

(C) Visual attraction assays indicate that the Rh6-PR/lOLP pathway is required specifically for movement detection. Attraction to a fixed or moving target was measured in larvae with compromised PRs or lOLPs. Mutants carrying loss-of-function null alleles of *Rh6* (left panels) display reduced attraction to a moving but not fixed target. Similar effects were observed in animals expressing Kir2.1 in the Rh6-PRs but not their genetic controls (*Rh6-GAL4* and *UAS-Kir2.1*) (middle panels). Silencing both lOLPs also (right panels) reduces attraction to a moving but not fixed target.

(D) Light deprivation since egg-laying does not affect light avoidance and attraction to a fixed target, but generates deficits in social clustering and visual attraction to a moving target, both of which involve the function of the Rh6-PR/lOLP pathway.

See also Figure S1

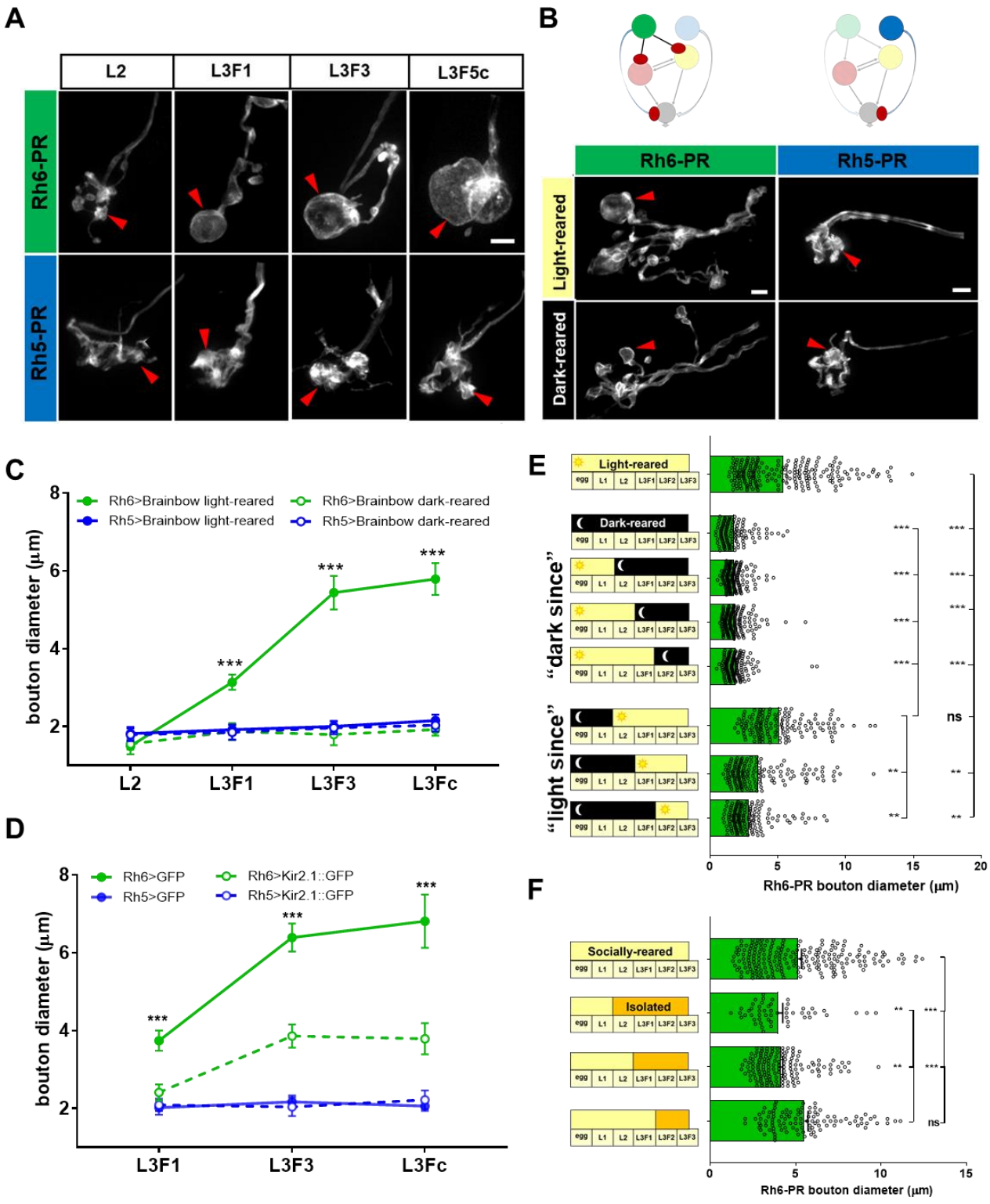

Figure 3. Rh6-PRs, but not Rh5-PRs, are modified by visual and social experience during development

(A and B) Presynaptic boutons of Rh6-PRs (A, top), but not Rh5-PRs (A, bottom), display a gradual increase in size throughout larval development in light-reared animals. Light deprivation since egg-laying leads to a reduction of presynaptic bouton size in Rh6-PRs (B, left), but not in Rh5-PRs (B, right). Images represent maximum intensity projections of confocal image stacks. In most images, 1-2 PR terminals can be seen with 1-3 presynaptic boutons (red arrows). Scale bars represent 5 µm.

(C) Dark-rearing specifically affects Rh6-PR bouton development. Quantification of Rh5-PR and Rh6-PR bouton size in animals reared in light vs. darkness since egg laying is shown. No difference was observed in Rh5-PR bouton size between light- and dark-reared animals. Dark-rearing eliminates the developmental increases in Rh6-PR bouton sizes and generates significant differences between light-reared and dark-reared animals starting from the L3 stage. n=42, 98, 126, 69 for *Rh5-GAL4>UAS-Brainbow* light-reared; n=68, 99, 76, 78 for *Rh5-GAL4>UAS-Brainbow* dark-reared; n=79, 198, 204, 204 for *Rh6-GAL4>UAS*-Brainbow light-reared; n=70, 46, 110, 80 for *Rh6-GAL4>UAS-Brainbow* dark-reared (L2, L3F1, L3F3 and L3Fc stages, respectively).

(D) Activity-dependent presynaptic bouton growth in Rh6-PRs. Quantification of the Rh6-PR bouton sizes is shown. Expression of GFP-tagged Kir2.1 in PRs hindered Rh6-PR bouton growth, but had no effect on Rh5-PR boutons. The control groups express regular GFP. n=57, 61, 66 for *Rh5-GAL4>UAS-GFP*; n=67, 71, 66 for *Rh5-GAL4>UAS-Kir2.1::GFP*; n=59, 63, 54 for *Rh6-GAL4>UAS-GFP*; n=97, 146, 58 for *Rh6-GAL4>UAS-Kir2.1::GFP* (L3F1, L3F3 and L3Fc stages, respectively).

(E) The development of Rh6-PR presynaptic boutons relies on light input, starting from the L2 stage. Quantification of the Rh6-PR bouton sizes collected from the time-restricted dark-rearing experiments is shown. Compared to the light-reared control group, dark rearing since either egg laying or the L2, L3F1 and L3F2 stages all led to significant reductions of Rh6-PR bouton sizes. Similar effects were observed in animals dark-reared until the L3F1 and L3F2 stages. Dark-rearing until the L2 stage did not produce a significant effect compared to the light-reared control group.

(F) Social interactions during the L2 to L3F1 stages contribute to the visual input that supports Rh6-PR bouton development. Compared to the group-reared controls, social deprivation starting from either the L2 or L3F1 stages generated significant differences in presynaptic bouton size in Rh6-PRs. No difference was seen in animals isolated since the L3F2 stage.

See also Figure S2

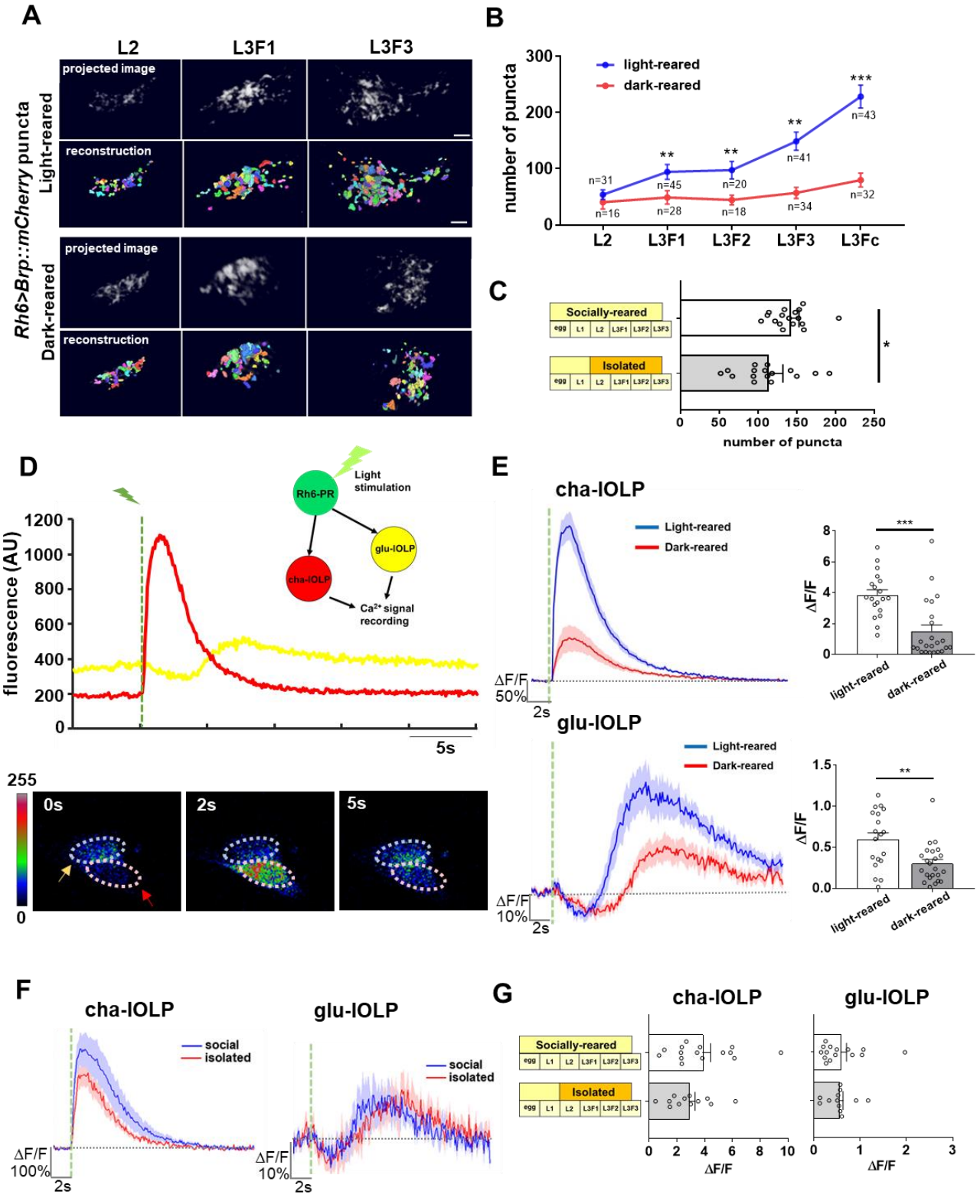
A
L2
L3F1
L3F3
projected image
reconstruction
Light-reared
Dark-reared
Rh6>Brp::mCherry puncta
B
light-reared
dark-reared
number of puncta
300
200
100
0
**
**
**
***
n=31
n=45
n=20
n=41
n=43
n=16
n=28
n=18
n=34
n=32
L2
L3F1
L3F2
L3F3
L3Fc
C
Socially-reared
Isolated
egg
L1
L2
L3F1
L3F2
L3F3
*
0
50
100
150
200
250
number of puncta
D
Light stimulation
Rh6-PR
glu-lOLP
cha-lOLP
Ca2+ signal recording
fluorescence (AU)
1200
1000
800
600
400
200
0
5s
255
0
0s
2s
5s
E
cha-lOLP
Light-reared
Dark-reared
ΔF/F
50%
2s
***
ΔF/F
light-reared
dark-reared
glu-lOLP
Light-reared
Dark-reared
ΔF/F
10%
2s
**
ΔF/F
light-reared
dark-reared
F
cha-lOLP
glu-lOLP
social
isolated
ΔF/F
100%
2s
social
isolated
ΔF/F
10%
2s
G
cha-lOLP
glu-lOLP
Socially-reared
Isolated
egg
L1
L2
L3F1
L3F2
L3F3
0
2
4
6
8
10
ΔF/F
0
1
2
3
ΔF/F

Figure 4. Functional connectivity between Rh6-PRs and lOLPs is modified by visual experience

(A and B) Light deprivation by dark-rearing reduces the number of presynaptic terminals in Rh6-PRs. An Rh6 enhancer-driven mCherry-tagged Brp protein (Rh6>Brp::mCherry) was used to label Rh6-PR presynaptic terminals. Raw images (A, top) represent maximum intensity projections of confocal image stacks (stained against mCherry) that were subsequently reconstructed in 3D (A, bottom) and quantified (B). Control animals display higher numbers of Rh6>Brp::mCherry puncta compared to larvae dark-reared since egg laying (B). No difference in Rh6>Brp::mCherry puncta number was found between light- and dark-reared animals at the L2 stage.

(C) Social deprivation since the L2 stage reduces the number of presynaptic terminals in Rh6-PRs. Quantification of the number of Rh6>Brp::mCherry puncta is shown. Comparing to the group-reared controls, single-reared larvae have fewer Rh6>Brp::mCherry puncta.

(D) Light-elicited physiological responses in lOLPs are affected by visual experience. Schematic diagram illustrating the setup of the calcium imaging experiment, in which light activates Rh6-PRs and induces calcium transients in downstream lOLPs as detected by GCaMP6f expression driven by R84E12-GAL4. Representative raw traces (top) and frames from a GCaMP6f recording (bottom) are shown. Dashed green line indicates the delivery of a 100ms light pulse. The yellow arrow indicates the glu-lOLP and the red arrow indicates the cha-lOLP.

(E) Light deprivation since egg-laying significantly dampened light-induced calcium responses in both lOLPs. The average traces (left) and the quantification of the response (right) are shown.

(F and G) Social deprivation since the L2 stage did not generate significant changes in the light-elicited calcium responses in lOLPs. The average traces (F) and the quantification of the response (G) are shown.

See also Figure S3

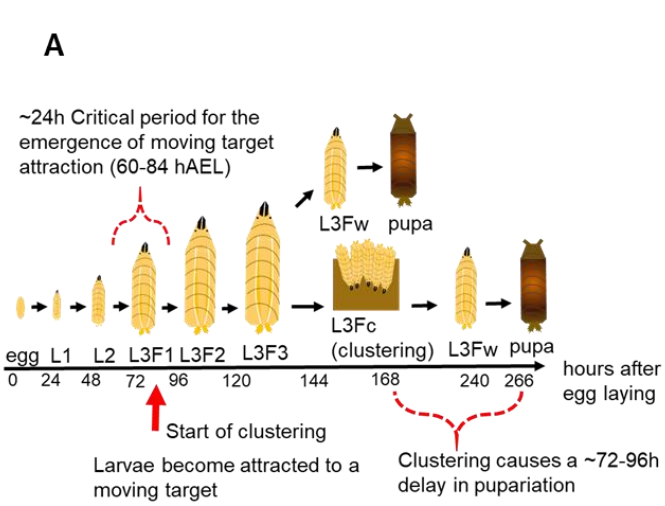
A
~24h Critical period for the emergence of moving target attraction (60-84 hAEL)
L3Fw
pupa
L3Fc
(clustering)
L3Fw
pupa
egg L1 L2 L3F1 L3F2 L3F3
0 24 48 72 96 120 144 168 240 266
hours after egg laying
Start of clustering
Larvae become attracted to a moving target
Clustering causes a ~72-96h delay in pupariation

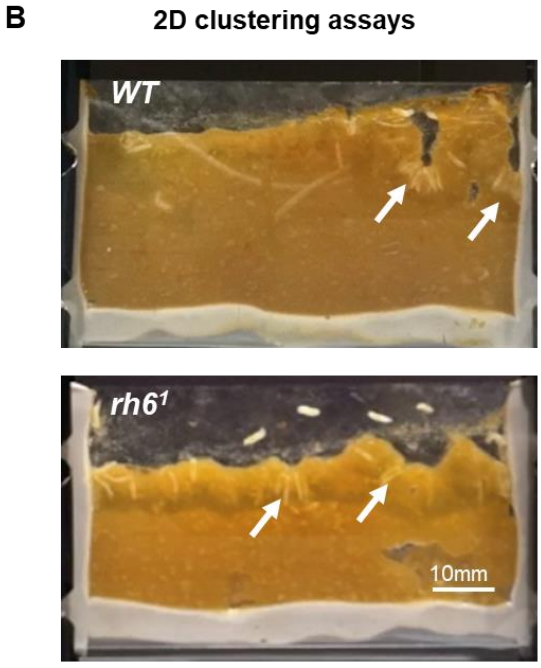
B
2D clustering assays
WT
rh6¹
10mm

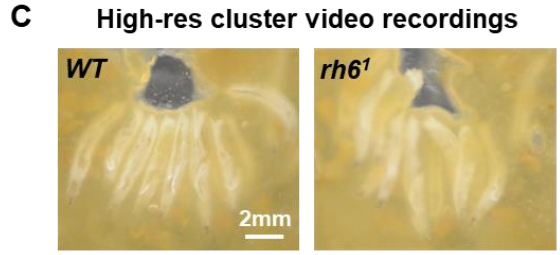
C
High-res cluster video recordings
WT
rh6¹
2mm

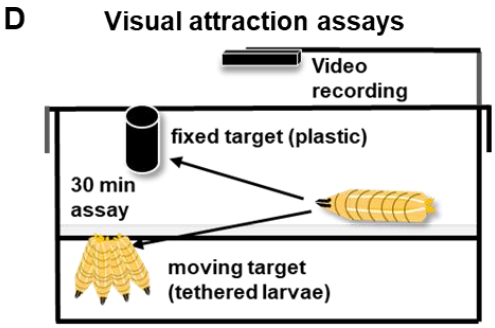
D
Visual attraction assays
Video recording
fixed target (plastic)
30 min assay
moving target (tethered larvae)

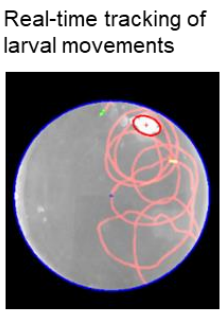
Real-time tracking of larval movements

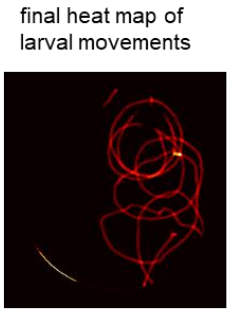
final heat map of larval movements

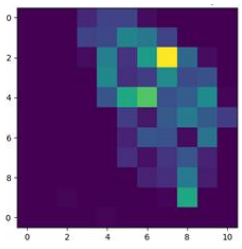
Rasterized and standardized heat map

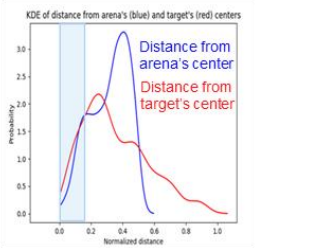
Output probability of finding a larva at a certain distance from target and arena centers
KDE of distance from arena's (blue) and target's (red) centers
Distance from arena's center
Distance from target's center
Probability
Normalized distance

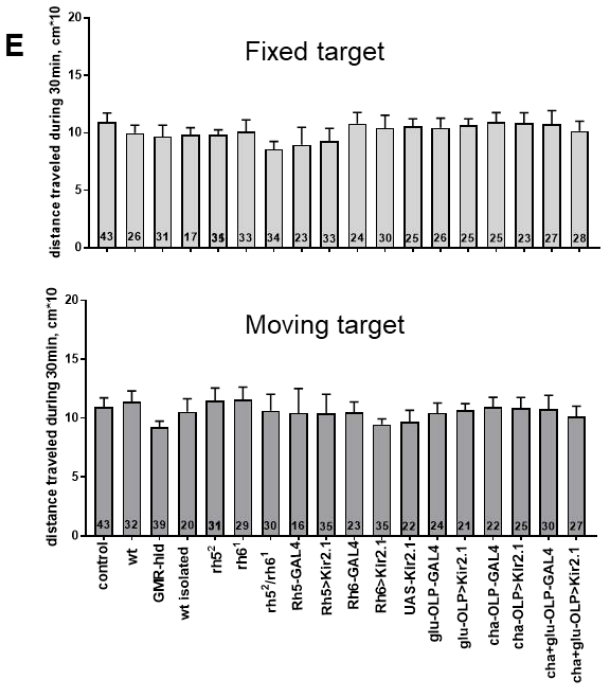
E
Fixed target
distance traveled during 30min, cm*10
43 26 31 17 35 33 34 23 33 24 30 25 26 25 25 23 27 28
Moving target
distance traveled during 30min, cm*10
43 32 39 20 31 29 30 16 35 23 35 22 24 21 22 25 30 27
control-
wt
GMR-hid
wt isolated
rh5²
rh6¹
rh5²/rh6¹
Rh5-GAL4
Rh5>Kir2.1
Rh6-GAL4
Rh6>Kir2.1
UAS-Kir2.1
glu-OLP-GAL4
glu-OLP>Kir2.1
cha-OLP-GAL4
cha-OLP>Kir2.1
cha+glu-OLP-GAL4
cha+glu-OLP>Kir2.1

Figure S1. Related to Figures 1 and 2

(A) Schematic representation of larval developmental stages. While solitary animals and larvae raised on a food plate pupariate at 168h AEL, clustering animals raised in vials display a 72-96h delay in pupariation. Clustering usually begins at middle L3F1 stage (~84h AEL), which coincides with the closure of the ~24h critical period for the emergence of moving target detection.

(B and C) Comparison of clusters formed by wild type larvae and animals with compromised function of Rh6-PRs. Rh6 mutants display a reduced engagement in clusters in 2D assays resulting in decreased digging efficiency (B). This originates from inability to visually cooperate and maintain the integrity of a cluster, as observed in high resolution recordings of 2D clusters (C).

(D) Description of visual attraction assays. Schematic representation of fixed and moving target 30min attraction assays performed with single animals on Petri dishes (top). Example of real-time user interface displayed while analyzing the larval movements (middle left). The blue ellipse (selectable by the user) represents the arena where the larva motion will be tracked. The red ellipse (selectable by the user) represent the area where the target is located. The green shape represents the outline of the larva being tracked. The light red traces show the heat map of the tracked motion of the larva in real time. Example of a final heat map generated by the analysis software (middle right). To allow comparison with previously manually acquired data, the standardized heat map is sampled (rasterized) over a grid (bottom left) where each square identifies a 1cm x 1cm area within the Petri dish. Once the data is collected, the probability of observing a larva at a certain distance from the centers of target and arena is computed using the kernel density estimator provided by the python *statsmodel* library (bottom right, blue rectangle indicates 0.15 cm distance threshold).

(E) Locomotion controls for visual attraction assays. Distance travelled by individual animals during 30min assays was measured using a python-based attraction tool (see Methods). No locomotion deficits were found in larvae with compromised PRs and lOLPs, suggesting that all phenotypes (Figure 2C) originate from altered vision specifically. Data are presented as means + SEM.

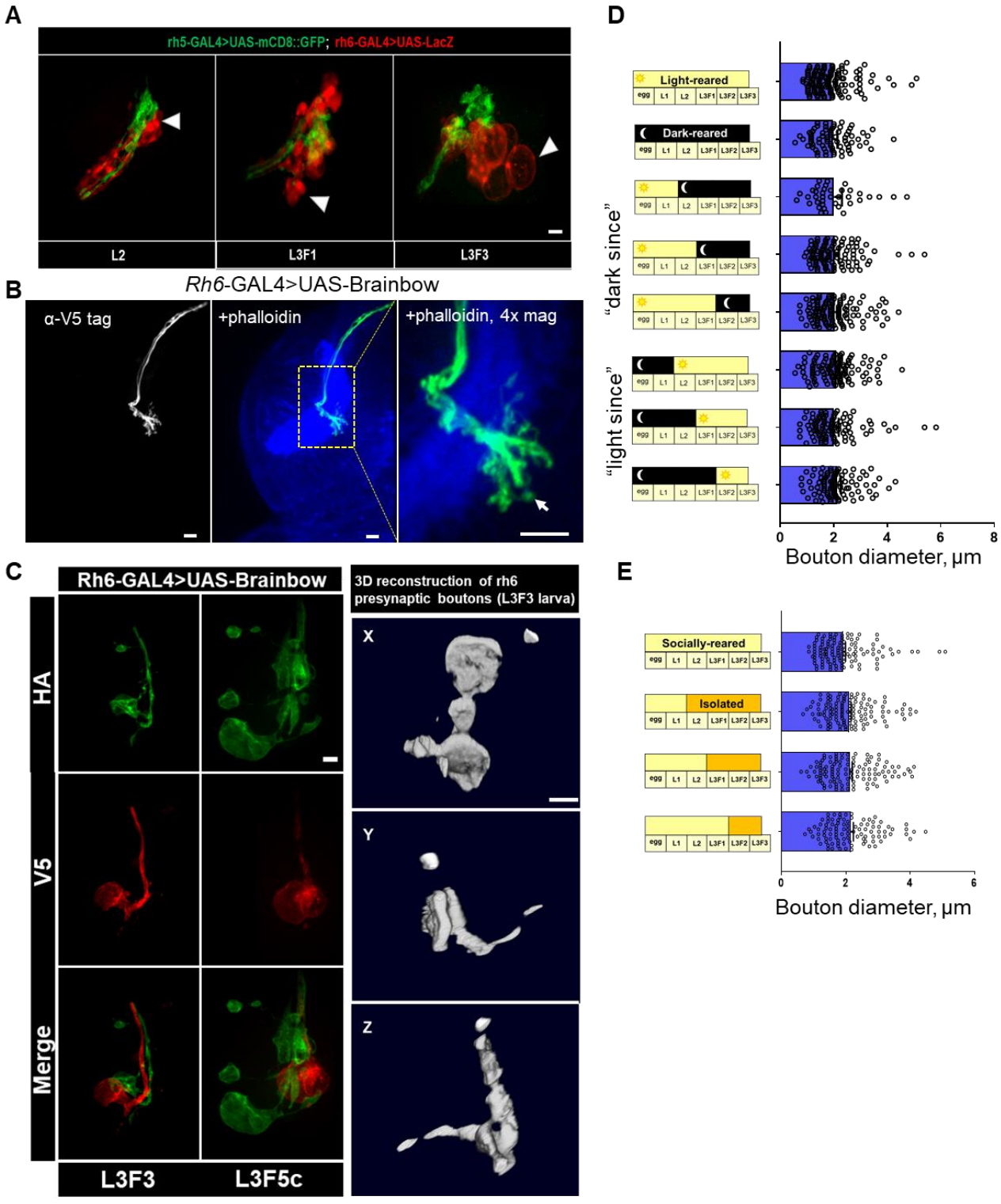
A
rh5-GAL4>UAS-mCD8::GFP; rh6-GAL4>UAS-LacZ
L2
L3F1
L3F3
B
Rh6-GAL4>UAS-Brainbow
α-V5 tag
+phalloidin
+phalloidin, 4x mag
C
Rh6-GAL4>UAS-Brainbow
3D reconstruction of rh6 presynaptic boutons (L3F3 larva)
HA
V5
Merge
L3F3
L3F5c
X
Y
Z
D
Light-reared
Dark-reared
"dark since"
"light since"
egg L1 L2 L3F1 L3F2 L3F3
0 2 4 6 8
Bouton diameter, μm
E
Socially-reared
Isolated
0 2 4 6
Bouton diameter, μm

Figure S2. Related to Figure 3

(A) Visualization of PR presynaptic terminals using fluorescent marker expression. Images represent maximum intensity projections of confocal image stacks. White arrows indicate Rh6-PR presynaptic boutons. Notable growth of Rh6- but not Rh5-PR boutons is observed throughout larval development. Genotypes: Rh5-GAL4>UAS-GPF; Rh6-GAL4>UAS-LacZ. Scale bar represents 5µm.

(B) Localization of Rh6-PR axonal projections in the larval brain (L3F1 larval stage). A subset of Rh6-PR cells is visualized using multicolor stochastic flipout (Brainbow) technique and stained against V5 tag (with fluorescent phalloidin for background staining). Presynaptic boutons are indicated with a white arrow. Approximate boundaries of the LON are delineated with a yellow dashed rectangle. Scale bars represent 10 µm

(C) Visualization of individual Rh6-PR presynaptic boutons in late 3rd instar larvae with increased spatial resolution using Brainbow technique (left) followed by 3D reconstruction using Volocity (right). Genotype: Rh6-GAL4>UAS-Brainbow. Stained against HA and V5 tags. Scale bar represents 5µm.

(D and E) Presynaptic morphology of Rh5-PRs in not affected by visual experience. Quantifications of the Rh6-PR bouton sizes collected from the time-restricted dark-rearing experiments (C) and time-restricted social isolation experiments (D) are shown. Deprivation from neither light input (C), nor social interactions at any stage has any effect on Rh5-PR bouton size. Genotype: Rh5-GAL4>UAS-Brainbow. Data are presented as means + SEM.

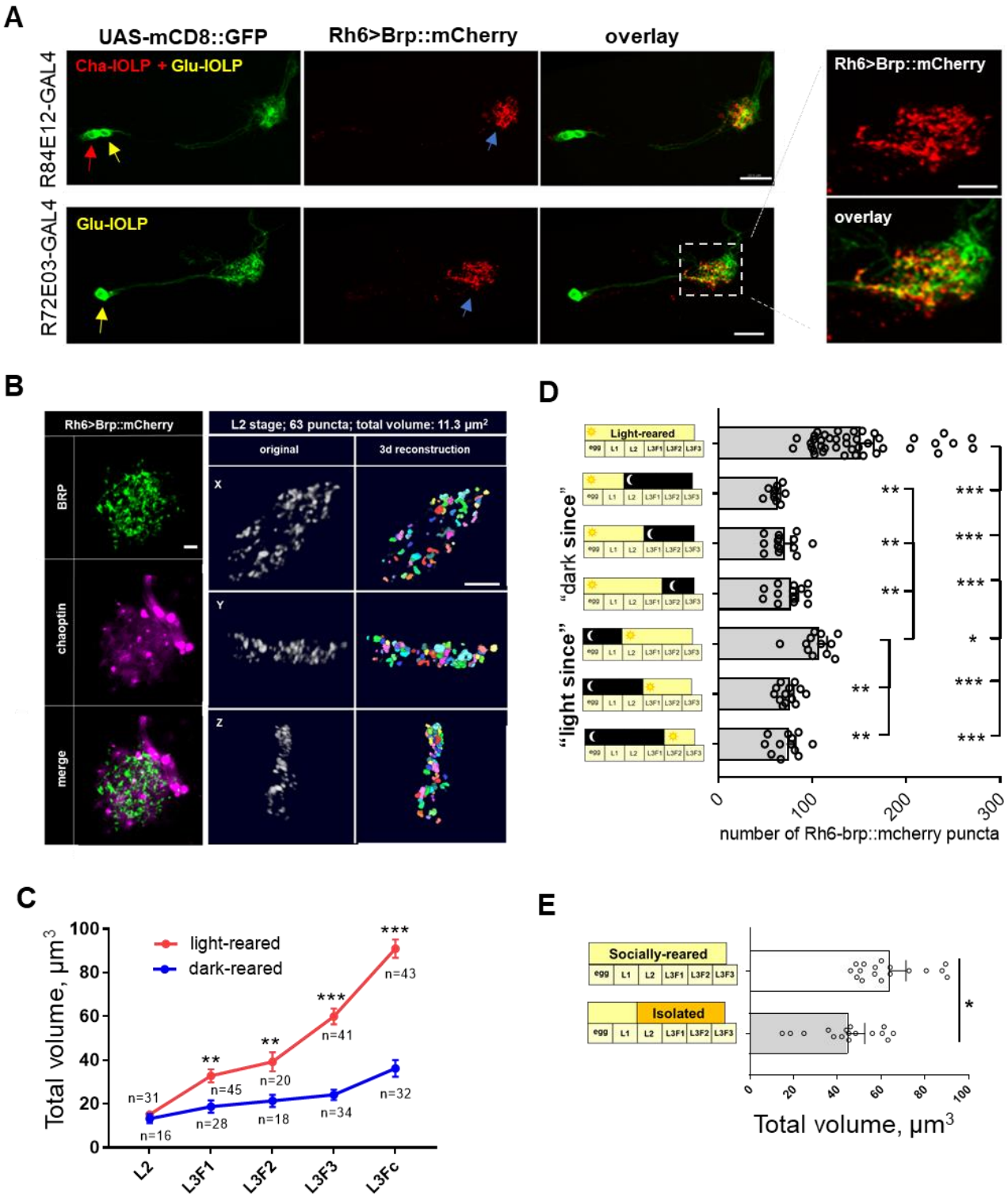
A
UAS-mCD8::GFP
Rh6>Brp::mCherry
overlay
R84E12-GAL4
Cha-IOLP + Glu-IOLP
R72E03-GAL4
Glu-IOLP
Rh6>Brp::mCherry
overlay
B
Rh6>Brp::mCherry
L2 stage; 63 puncta; total volume: 11.3 µm²
original
3d reconstruction
BRP
chaoptin
merge
X
Y
Z
D
Light-reared
"dark since"
"light since"
egg L1 L2 L3F1 L3F2 L3F3
number of Rh6-brp::mcherry puncta
C
light-reared
dark-reared
Total volume, µm³
n=31
n=16
n=45
n=28
n=20
n=18
n=41
n=34
n=43
n=32
L2
L3F1
L3F2
L3F3
L3Fc
E
Socially-reared
Isolated
Total volume, µm³

Figure S3. Related to Figure 4

(A) Rh6-Brp:mCherry puncta mark the Rh6-PR presynaptic terminals in close proximity with the lOLP projections. Arrows indicate cell bodies of glu-lOLP (yellow), cha-lOLP (red) and Rh6-PRs presynaptic active zones marked with Brp::mCherry puncta (blue). Dashed rectangle indicates an area of overlap between postsynaptic terminals of lOLPs and presynaptic sites of Rh6-PRs. Genotypes: R84E12-GAL4>UAS-CD8::GFP, R72E03-GAL4>UAS-CD8::GFP, Rh6>Brp::mCherry. Scale bars represent 20 µm (left) and 5µm (right).

(B) Rh6-Brp:mCherry puncta mark the PR presynaptic terminals visualized by anti-chaoptin staining (left). 3D reconstruction of Rh6-PR presynaptic active zones marked with Brp::mCherry using Volocity software (right). Scale bars represent 5µm.

(C) Light deprivation by dark-rearing reduces the total volume of Rh6>Brp::mcherry puncta. Control animals display a higher total volume of Rh6>Brp::mCherry puncta compared to larvae at L3F1-L3Fc stages dark-reared since egg laying. No difference in Rh6>Brp::mCherry puncta total volume was found between light- and dark-reared animals at L2 stage. Data are presented as means + SEM.

(D) The number of Rh6-PR presynaptic active zones continually relies on the light input, Quantifications of the Rh6>Brp::mCherry puncta from animals exposed to the time-restricted dark-rearing experiments are shown. Compared to the light-reared control groups, dark rearing since egg laying or L2, L3F1 and L3F2 stages all led to significant reductions of Rh6>Brp::mcherry puncta number. Dark-rearing until the L2 stage produced the least notable effect compared to other light deprivation paradigms. Data are presented as means + SEM.

(E) Social isolation reduces the total volume of Rh6>Brp::mCherry puncta. A significant decrease of total volume of Rh6>Brp::mCherry puncta was observed in animals reared in social isolation since L2 stage compared to the group-reared controls. Data are presented as means + SEM.

Chapter 4

Cooperative foraging during larval stage affects fitness in *Drosophila*

Authors:

Mark Dombrovski[1], Rives Kuhar[1*], Alexandra Mitchell[1*], Hunter Shelton[1*] and Barry Condron[1,2,**]

Author affiliations:

[1]Department of Biology, University of Virginia, Charlottesville, VA 22901, USA

[2]Lead Contact

*Authors have contributed equally

**Correspondence: bc4f@virginia.edu (B.C.)

Prepared for submission as a research paper (Journal of Comparative Physiology B):

Highlights

-Processed food and high population density cause a developmental delay in *Drosophila* larvae that is associated with decreased adult fitness

-Participation in cooperative foraging groups further delays larval development

-Flies that were engaged in cooperative foraging during larval stage have fitness advantages over descendants of solitary feeding larvae

-Emergence of larval cooperative foraging may serve as an evolutionary tradeoff to compensate the negative fitness effects of malnutrition

Keywords: Drosophila, foraging, cooperation, social behavior, group membership fitness

Dombrovski *et al*. report that in conditions of high population density and limited food resources Drosophila larvae experience a developmental delay coupled with fitness deficits. However, similar environmental conditions promote formation of social foraging groups membership in which rescues negative effects on fitness

Summary

Cooperative behavior can confer advantages to animals. This is especially true for cooperative foraging that is thought to provide fitness benefits through more efficient acquisition and consumption of food resources. While examples of group foraging have been widely described, principles governing the formation of such aggregations as well as rules that determine cooperative group membership remain poorly understood. Here we take advantage of an experimental model system featuring cooperative foraging behavior in *Drosophila*. Under crowded conditions, fruit fly larvae form coordinated digging groups (clusters), in which individuals are linked together by sensory cues and stable group membership requires prior social experience. However, ecological benefits of *Drosophila* larval clustering remain to be determined. We demonstrate that when grown on food that has been previously processed by other larvae, animals experience a developmental delay presumably due to malnutrition associated with a decrease in adult fitness, as measured by wing size, when compared to larvae raised on fresh food. Intriguingly, similar conditions also promote the formation of cooperative foraging clusters which further extends larval stage compared to non-clustering animals. Remarkably, this developmental retardation also results in a relative increase in wing size. Thus, we find that clustering-induced developmental delay is outweighed by trophic benefits, suggesting that foraging group membership provides advantages over solitary feeding in processed food. Therefore, cooperative behavior, while delaying development, may have evolved to give *Drosophila* larvae benefits when presented with severe competition for limited food resources.

Introduction

Group foraging is a major component of cooperative animal behavior [7]. It can be defined as inter- and intraspecific cooperation in search, acquisition, defense and consumption of a common food source and can provide benefits in survival and reproduction for a variety of animals [84,211]. Participation in a cooperative feeding group can provide a significant increase in average feeding efficiency for two reasons: (1) increased food processing efficiency resulting in less investment for higher nutritional return [33,174,227,231] and (2) the potential to sequester a common food source from competing species or different populations of the same species [62,75,221]. In addition, aggregation can also lead to a decreased risk of predation, serving a complementary advantage of forming cooperative groups [181,230]. All of these factors contribute to an increase in individual's chances of survival and reproductive success which serve as the main measures of fitness [41]. Importantly, benefits of cooperative foraging can often take effect in only certain conditions when availability and distribution of food resources determines the advantage of cooperation, [8,67,158,190]. This may serve as an example of Allee effect [48] in context of cooperative feeding, where individual's fitness gains correlate with group size and density only up to a certain limit, beyond which acquired benefits may get leveled and negatively outweighed by emerging complex non-trophic factors of group membership, such as intra-group competition [33,42,180].

Remarkably, cooperative foraging behavior has been observed among a broad range of animal taxa. Group hunting strategy was described in carnivorous mammals [40,78], birds [94] and fish [67], all of which predominantly utilize active coordinated search tactics when hunting prey. Herbivores also widely engage in cooperative feeding [75,158,174]. Invertebrates also provide examples of the effective use of cooperative foraging including elevated rates of food ingestion in grouped flatworms [33] and increased dietary diversity in gregariously feeding mollusks [229], while a great variety of cooperative behaviors including examples of interspecific aggregations comes from arthropods [25]. These include complex sensory communication facilitating localization of feeding sites in treehoppers [43]. Scavenger ants normally forage individually but easily employ cooperation when dealing with oversized prey [8]. Sand flies synchronize their efforts during blood meal initiation thereby minimizing time and resources spent by an individual animal [227]. Many studies focus on insect larvae in which food consumption becomes a top priority [72], implying that it is specifically at the larval stage when animals are most sensitive to trophic advantages of foraging group membership. Indeed, highly efficient foraging clusters feeding on pine foliage were described in sawfly larvae [80,144]. Various species of caterpillars were shown to dramatically increase feeding efficiency and developmental rates when engaged in cooperative groups [40]. Corpse-devouring necrophagous flies acquire significant fitness benefits through cooperative exodigestion strengthened by significant heat production resulting in decomposition of soft tissues [180,188]. Importantly, the same factors that provide trophic benefits can serve as tradeoffs in case of severe overcrowding

(e.g. overly elevated temperature and proteotoxic stress caused by excessive tissue digestion), implying a complex non-linear and very often case-specific pattern of relationship between group size, food source availability, degree of individuals' investment into cooperative efforts and their potential gained benefits [48,84,231]. In this regard, using a laboratory model system might provide the right tools and metrics to begin dissecting out various complex parameters governing collective foraging behavior that are yet to be understood.

This model makes use of a novel experimental model system featuring cooperative foraging behavior in larval *Drosophila melanogaster*. Interestingly, although behavioral and developmental aspects of larval solitary foraging behavior were addressed long time ago [86,87,127,204,242], mechanistic and neuroethological features of cooperative digging and foraging in larval *Drosophila* have only recently been characterized [60,61,63], while its ecological and evolutionary roles still remain elusive. Feeding clusters formed in semi-liquid food comprise 10-200 animals and share a unique set of characteristics that make it an attractive model for studying collective social behavior. In particular, clustering larvae engage in synchronous reciprocating digging, where each group member utilizes visual cues to coordinate its movements with immediate neighbors [60]. Intriguingly, cluster membership and ability to efficiently engage in visually guided cooperation requires prior visual and social experience during a distinct critical period in development [60,200]. In addition, emergence of clustering is associated with profound changes in larval visual circuit [61]. This raises the question as to the function of this behavior and its emergence in the evolution. Our study was

aimed at identifying specific ecological benefits associated with social clustering, whether it refers to more efficient burrowing [60], escape from predators [30] or more efficient utilization of food resources [91,188].

Our preliminary data indicate that clustering larvae experience a significant delay in pupariation and eclosion [60,61]. Such a delay has been previously reported as an indicator of adverse conditions including malnutrition and, in some cases, might lead to animal deterioration [155,156.224]. New experiments reveal that food quality is primary cause of developmental retardation: several hundred larvae process and liquefy media in food plates within 48 hours after hatching, which mimics a naturally occurring situation on a surface of a decaying piece of fruit. Not surprisingly, such rapid and dramatic change in food source composition affects nutritional state of late L2 – early L3F1 larvae and results in a delayed metamorphosis, which is explained by pre-critical weight malnutrition [45,154-157]. In addition, animals raised on processed food displayed significant fitness deficits in adult stage measured by wing size. To further elucidate the role of cooperative foraging on larval growth and development, we used a set of simple tools to manipulate clustering efficiency at otherwise unchanged conditions. This allowed to clearly distinguish between the roles of clustering and processed food in pupariation and eclosion delays. Remarkably, we found that animals engaged in clustering display an additional developmental delay compared to their solitary digging counterparts in processed food. Most importantly, adult flies descending from clustering larvae showed significantly greater wing size compared to animals that never clustered as larvae. Therefore, we find a strong correlation between

time spent in clusters during larval stage and size in adult flies. Presumably, extended larval stage in clustering animals serves as compensatory mechanism that allows to maximize trophic benefits from cooperative digestion and consumption of low-quality food. This suggests an ecological and evolutionary significance for cooperative foraging among larval *Drosophila*.

Results

Processed food delays development and reduces size in *Drosophila*

Processed food and crowded conditions increase the duration of larval development [60]. Here we further investigated the separate contribution of each of these factors. Preparation of vials with processed food followed by larval transplantations was adapted from previous studies [60,61] (Fig. 1a). In our first experiment (Fig. 1b) we compared the effects of fresh versus processed food on larval pupariation and eclosion rates. To exclude the role of cooperative feeding, we used a low population density paradigm and transplanted 20 L2 wild type larvae (previously raised in normal conditions on fresh food) into plates and vials with processed food. We found that both pupariation (Fig. 1b) and eclosion (Fig. 1c) were significantly delayed in animals raised on processed food, but no difference was observed between rearing in plates and vials. Importantly, no effect on survival was found (Fig. S1a, left) and blind GMR-hid larvae displayed a similar eclosion delay in processed food. (Fig. S1b). In summary, processed food yielded in a ~16h

delay in pupariation and in eclosion in which a sub-cooperative number (20) of larvae were transplanted at L2 stage.

It has been reported that insufficient nutrition during larval stage reduces size in adult flies [45,137,155]. Therefore, we next examined whether an observed developmental retardation was accompanied with size deficits. For this, we measured wing size in newly eclosed female flies, which serves a good estimate of general body size and weight [220,222]. As a control for experiments described in Figs. 2 and 3, we replicated the same conditions in the darkness. We found that, regardless of light regime and plates/vials animals reared on fresh food had significantly bigger wings (Fig. 1d), suggesting a negative impact of processed food on larval growth. In addition, we performed L3F2 larval stage transplantations into processed food vials and plates to see if decreased time spent in adverse nutritional environment would fully or partially rescue size deficits. We saw that, wing size in L3F2 transplants raised on processed food was significantly smaller compared to fresh food-reared larvae (Fig. 1d). However, the effect of processed food was less pronounced than in case of L2 transplants, indicating that time spent in processed food during larval stage negatively correlates with adult size. Alternatively, these results could also be explained by the fact that transplantation occurred after reaching critical weight [154-157]. Survival rates were unchanged among all experimental paradigms (Fig. S1a).

We next wondered how high population density changed the way processed food affects developmental timing especially with the potential appearance of cooperative foraging. For that, we used 200 L2 wild type larvae in vials and plates

with either fresh or processed food and compared their pupariation and eclosion rates (Fig. 1e). For control, GMR-hid larvae were exposed to similar experimental conditions (Fig. S1b). There was no difference in developmental rates between fresh and processed vials (Figs. 1e and S1c), which can be explained by very fast food processing by 200 animals. However, larvae reared in high-density in vials with processed food displayed dramatically delayed pupariation and eclosion compared not only to fresh food plates but even to processed food plates and processed food vials with low-density conditions (Figs. 1e and S1c). This is likely due to the formation of cooperative clusters and so was further examined.

Cooperative foraging further delays larval development in processed food at high population density

In order to examine the role of cooperative foraging in larval development, we took advantage of approaches shown in Fig. 2a, all of which were intended to use clustering rates in wild type animals

In particular, we previously showed that wild type animals display dramatically reduced clustering when either deprived from light for a long time [61] or even immediately after being placed in the darkness [60] (Fig. 2a). Here we compared developmental rates in wild type larvae reared in normal conditions and in the darkness and found that a clear delay in pupariation and eclosion times (Figs. 2b and S1d) was observed in normally reared animals. However, this effect was notable only in case of high population density that promotes clustering and

no difference was found in case of 20 animals transplanted (Figs. 2b and S1d). Moreover, no difference in developmental timing was observed between normal- and dark reared GMR-hid larvae that cannot form clusters (Figs. 2b and S1b). Animal survival rates were not affected by dark rearing (Figs. S1b, S1d).

Our previous study also indicates that introduction of “disruptors” into wild type clusters decreases cluster lifetime [60], which we used as another tool to manipulate clustering efficiency (Fig. 2a). For this experiment, we looked at developmental timing in all-wild type 200L2 larval groups, as well as mixed groups (Fig. 2c) containing 25 and 50% GMR-hid or Tubby larvae (both negatively interfering with clustering through their inability to either integrate into or efficiently cooperate within a cooperative group, as shown by Dombrovski et al. [60]. Vials were constantly recorded and cluster frequency in each vial was further assessed (Fig. 2c, right). The same experimental conditions were reproduced in dark reared larvae. We saw that the length of a delay in eclosion highly correlated with clustering frequency: it was most notable in all-wild type group and significantly decreased in a stepwise manner in 25% and 50% GMR-hid/Tubby groups, similarly to a decrease in clustering frequencies observed among the corresponding groups (Fig. 2c). Most importantly, no effect of group composition on developmental timing was seen in animals reared in the darkness (Fig. S2e, left), suggesting that clustering was a decisive factor. Survival rates were unchanged between light/dark conditions and group compositions (Fig. S2e, right).

Earlier studies also indicate that in order to cluster, larvae must pass through a visual critical period early in the third instar [60,61] and animals

transplanted into vials of processed food after this critical period show greatly reduced clustering. Therefore, we tested the effects of reducing clustering behavior by this post-visual critical period transplantation. In addition, we reproduced the same experiment in the darkness, with 20 larvae and with a mixed group containing 50% GMR-hid larvae. We found that in standard high-density conditions in light L3F2-transplanted larvae displayed no visible delay in eclosion compared to L2 transplants (Figs. 2d and S2a). Interestingly, neither dark rearing, nor adding blind larvae and using 20 animals yielded a significant change in eclosion rates in L3F2 transplants. At the same time, these conditions had a strong impact on L2 transplants and shortened their developmental delay (Figs. 2d and S2a). Importantly, clustering frequency was significantly reduced in L3F2 transplants (Fig. 2d, right). These results implied that, since cooperative foraging was eventually absent in late-transplanted animals, none of the factors reducing clustering efficiency was affecting their development, as opposed to L2-transplanted larvae being very sensitive to each of those factors (Fig. 2d). However, other interpretations of results seen in L3F2 transplants are possible. Increased survival rates compared to L2-transplanted larvae (Fig. S2b) and the fact that L3F2-transplanted blind GMR-hid larvae also showed a reduced developmental delay compared to L2 transplants (Fig. S2b) strongly suggested that the observed phenotype could also result from post-critical weight transplantation. In this case nutritional environment could have had no effect on L3F2 transplants' developmental timing, thus making the effect of reduced clustering negligible. Therefore, this question required further clarification. .

Cooperative foraging during larval stage rescues size deficits caused by processed food in adult *Drosophila*

The experiments described above show that clustering behavior further extends developmental time. Therefore, we next examined how this extra delay affected animal size as measured by wing size. We first compared wing size in 200L2 transplanted wild type larvae raised on processed food and reared in normal light conditions and in the darkness (Fig. 3a), considering that light deprivation prevented animals from clustering. We found that wings of dark-reared animals were significantly smaller compared to the control group (Fig. 3a). Interestingly, a similar magnitude of difference in wing size was previously observed between 20L2 transplanted wild type animals raised on fresh and processed food (Fig. 3a, dashed green and red lines, respectively). Thus, wing size was almost indistinguishable between animals raised on fresh food and animals derived from processed food, but only in conditions that promoted clustering (high population density and normal light regime). This suggests that cooperative foraging rescued the deficit in animal size caused by processed food. To further elucidate this phenomenon, we looked at how other factors interfering with clustering (Fig. 2a) affected wing size. Results from late post-critical period transplantation experiments of L3F2 larvae were intermediate between the two sizes in that wings were significantly smaller compared to positive control 200L2 transplants in light, they were also notably bigger than the negative control (200L2 in the darkness). However, they were almost identical to 20L3F2 transplants and not affected by light regime (Fig. 3a). This was in line with the data on L3F2 eclosion rates (Figs.

2d and S2a), implying that additional factors, such as post-critical weight effects play a role here.

In order to find more reliable correlation between changes in clustering and its effect on animal size, we compared wing size in wild type animals reared in clustering conditions but with cooperative behavior reduced in a regulated manner by the addition of blind and tubby cluster disruptors. (Figs. 2c and S1e). We added 12.5%-50% of either GMR-hid or Tubby larvae to wild type animals transplanted at L2 stage. Clustering frequency in each group was assessed and compared to the same conditions in darkness (Figs. 3b and S2d). We found no differences in wing size between groups reared in the darkness (Figs. 3b, right and 3c), where the absolute values were not different from the negative control. At the same time, a clear relationship was seen between group composition and wing size in light-reared animals (Figs. 3b, left and 3c): wing size decreased as clustering behavior was suppressed (Fig. S2d). Overall, we were able to trace the relationship between the time wild type animals spent in clusters and their resulting size. A strong positive correlation was observed between cluster frequency and wing size in wild type animals (Fig. 3d). In contrast no relationship between clustering conditions and wing size was seen in GMR-hid larvae (Fig. S2e), while the overall negative impact of processed food on wing size was present, consistent with the notion that blind animals are unable to use the benefits of cooperative foraging through their intrinsic inability to form cooperative foraging groups.

Discussion

Our study tests the idea that cooperative feeding among fruit fly larvae has a fitness benefit that is measured as body size and developmental time. Overall, we find mixed results in that larval stage is extended but animal size deficits is rescued despite the crowding and processed food compared to solitary feeding larvae in similar conditions. Therefore, our study indicates that cooperative foraging in fruit fly larvae will be beneficial in some but not all-natural conditions.

Processed food, which is predigested by larvae, slows developmental rates. It is likely that it has a lower nutritional value or at least an altered ratio of key macronutrients. According to a conventional notion, growth, larval developmental time and final size determination in insects including *Drosophila* are governed by of insulin-like hormones and TOR signaling in prothoracic gland (that is highly sensitive to nutritional status), as well as antagonistic actions and complex interplay of ecdysone and juvenile hormone [45,46,137]. In this context, malnutrition can have different impact on larval fate depending on whether it affects an animal before or after reaching critical weight, a key parameter that determines the readiness of the larvae to undergo metamorphosis and triggers the corresponding hormonal signals. If occurring before that checkpoint in the middle of L3F1 stage, malnutrition only delays metamorphosis, but doesn't affect adult fly body size. Conversely, post-critical period starvation later in development has no influence on developmental rates, but dramatically reduces body weight and size [155,156]. Interestingly, we observe both effects in solitary feeding animals, suggesting that processed food does provide less nutrients, but not to an extent

that would prevent larvae from reaching a minimum viable weight [155]. In contrast, flies derived from clustering larvae lack size deficits, but display an even longer developmental delay. It implies that once animals engage in cooperative foraging groups, the efficiency of their feeding increases dramatically leading to a rescue in body size deficits. This idea is strengthened by our results showing that larvae transplanted into vials at L3F2 stage do not delay metamorphosis (explained by post-critical weight transplantation), but still have reduced body size, because they cannot cluster to feed more efficiently (transplantation occurs after critical period to start clustering [60]). Thus, cooperative foraging can be regarded as an evolutionary adaptation that outweighs malnutrition at the cost of developmental retardation. At the same time, specific mechanisms responsible for an additional delay in metamorphosis observed among clustering larvae remain unclear and are subject for future investigation.

In addition to the above, the influence of more complex and integrative factors on larval development in processed food is also worth consideration. As an example, it has been shown that host microbiome is able to not only affect nutritional choices and feeding behavior in fruit fly larvae [141.177,234], but also directly control larval growth and developmental rates by influencing insulin signaling pathway [197], suggesting that the overall impact of symbiotic microbiota on fruit fly physiology and behavior might have been heavily underestimated. This may be especially relevant in our model system, where food processing by the larvae most likely leads to profound changes in its microbial composition.

Therefore, future studies aimed to reveal connections between microbiome and social foraging behavior are required to shed more light on this problem.

A question arising from previous observations is how clustering enhances the efficiency of food consumption. First, clustering larvae can take advantage of more efficient burrowing and reach fresher layers of food compared to solitary digging larvae and non-clustering blind or socially naive counterparts [60]. This should also increase chances to avoid predation and infection by parasitoid wasps [31]. In addition, clustering was shown to speed up the process of media liquefaction in vials [60] that could in turn facilitate food ingestion by foraging animals. A more complex explanation features a phenomenon of communal exodigestion mostly observed among maggots feeding on flesh and other high-protein substrates [188], but also documented in *Drosophila* [91]. Larvae are able to secrete a variety of enzymes digesting external polymers (amylose, cellulose and even chitin), therefore reducing energy expenditure per individual animal required to process and ingest a food source. Future metabolic studies are required to test this hypothesis.

Lastly, our model system makes it possible to reveal the applications of game theory in cooperative behaviors [83]. In order to dynamically balance between receiving benefits and paying costs for cooperative group membership, both of which can result from the same set of factors [12,33], individuals need to assess potential values and risks and make rational decisions on how much resources to invest into cooperation [41,83], which should lead to the emergence of cheaters and scroungers [175,235]. This is likely be a feature of *Drosophila*

clusters, where socially foraging larvae might need to generate a protective mechanism to prevent a cheater from joining the group. Intriguingly, some insights to that might have been provided by our previous studies. Slepian et al [200] and Dombrovski et al. [60] demonstrate that *Drosophila* larvae have a distinct critical period for the emergence of “social” vision, which later enables animals to cluster, while “naïve” larvae that did not interact with their peers during that time window, irreversibly lose an ability to cooperate with other cluster members. Interestingly, this notion was strengthened by our recent study [61] suggesting a circuit mechanism underlying plasticity in the visual system that occurs during critical period and likely leads to a generation of some key or password (probably encoded in perception of stereotyped visual patterns and movement frequencies). This might be an elegant and efficient way to segregate individuals of the same species not belonging to a current group and preventing them from free use of common resources. How exactly this process takes place and whether such approach can be used against other species is still poorly understood and will be examined in the future.

Author contributions

Conceptualization & Methodology: BC, MD; Data collection: MD, R.K, AM, HS; Data analysis: MD, RK; Writing, reviewing and editing: MD, BC; funding acquisition: BC, MD

Materials and Methods

Fly stock maintenance and egg collection

Wild type Canton S (CS) flies were donated by Ed Lewis (Caltech), blind GMR-hid^{G1} strain was obtained from Bloomington Stock Center (#5771), w^-;Sco/CyO;TM6B/TM3 flies were kindly provided by Sarah Siegrist. All *Drosophila melanogaster* strains were raised in food vials (unless further specified in experimental details) containing standard Caltech food mixture (1000ml molasses, 14000ml H_2O, 148g agar, 1000ml corn meal, 412g Baker's Yeast, 225ml Tegosept, 80ml propionic acid) at 22°C, 30% humidity under standard 12/12h light-dark cycle (unless further specified in experiments involving dark-rearing) at ~1000 lux light intensity. For egg production, ~50 adult flies 3-4 days old were transferred into egg cups and kept in the same conditions. Eggs were collected on 35mm petri dishes containing standard agar-molasses food and yeast every 6 hours for experimental procedures and eggs/larvae were kept (unless further specified) in the same light/temperature/humidity conditions.

Preparation of vials with "pre-processed" food and larval transplantations

Techniques of "pre-processed" vials production and transplantation of 200 L2 (60 hAEL) larvae were adapted from our previous studies [60,61] (Fig. 1a). ~50 adult flies 3-4 days old were kept in vials with fresh food for 24 hours and subsequently removed, vials were kept at standard conditions for 4-5 days allowing larvae to process food and pupariate. Vials were then frozen at -20ºC for 48 hours, defrosted and cleaned from pupae before new larvae were transplanted into processed food. This approach was developed to minimize variance of "pre-processed' food resources along with the absence of any unwanted animals and immediate exposure of transplanted larvae to designated food conditions

Cluster frequency measurements

For cluster frequency measurements, vials with previously transferred 200 L2/L3F2 larvae of a designated genotype/condition raised in normal conditions were recorded for 5 consecutive days (24hrs non-stop) starting immediately after transplantation. Recorded videos were subsequently analyzed using ImageJ (32-bit version for Windows). Percentage of frames with a clearly observed larval cluster (defined as a group of 5 or more larvae aligned and oriented vertically and buried into the food for more than ¾ of the body length) was calculated for each 12-hour light period during 3 consecutive days of recordings for each individual vial (days 3-5 after transplantation for L2 larvae and days 1-3 after transplantation for L3F2 larvae) of a designated genotype/condition (each of these measurements represents a single data point on the corresponding graphs). Values were subsequently averaged and represented and mean values for each genotype/condition.

Pupariation, eclosion and survival rates measurements

Newly formed pupae were counted on each food vial/plate of a designated genotype/condition twice a day (equal 12h periods and highlighted with a marker to avoid repeat counting. Eclosed flies were counted (for survival rates evaluation) and collected using CO2 anesthesia twice a day (equal 12h periods) and females were subsequently frozen at -20ºC in 1.5mL plastic tubes for subsequent wing size measurements. For pupariation and eclosion measurements, percentage of animals reached a designated developmental stage was calculated relative to the total number of pupariated/eclosed animals counted by the final day of observations (not the total number of originally transplanted larvae). Survival values were estimated as ratios of eclosed flies to the total number of originally transplanted larvae. In case of mixed populations, only wild type CS flies were counted (GMR-hid flies with no visible eyes and CyO;TM6B flies with curly wings were discarded).

Dark-rearing experiments

In all experiments involving light deprivation, dark-reared larvae were kept in a completely dark room for a designated time period in a food plate/vial additionally covered with a layer of aluminum foil. Dark rearing began immediately after larval transplantation at a designated stage and until the eclosion of all adult flies. Daily eclosion and pupariation rates measurements were performed in a room with dim red lights for each vial individually in order to minimize the time of possible light exposure.

Wing size measurements

Wing size (which serves as an estimate of a body size) of previously collected and frozen females was measured using technique adapted from [82] (distance from the base of the alula to the distal end of the third longitudinal vein, see Fig. 1a). A single wing from each animal was removed and mounted on a slide (with each slide representing 15-20 wings derived from animals from a single food plate/vial yielding in 4-6 slides per genotype/condition, where an individual wing measurement represented a single data point on the corresponding graphs). High-quality images of the slide were taken with a camera mounted on a tripod for subsequent wing size assessment using ImageJ (see below). Values were then averaged to give an estimate of the wing size for a designated genotype/condition.

Photography and Video recordings

For cluster frequency analysis, videos were recorded on an iPhone 5 at full resolution and 1 frame/60” using “Lapseit” software for IOS. For wing images, a Nikon D3100 CMOS camera with 50mm lens and fitted with a Raynox Macroscopic 4x lens was used. Video analysis was further performed in iMovie and ImageJ (32-bit version for Windows).

Statistical analysis

Unless otherwise stated, all data are presented as mean values and error bars represent 95% confidence intervals. Statistical significance was calculated by one-way ANOVA using Tukey's method. When comparing two groups of normally distributed data, Student's two-tailed unpaired T-test was used. *$p<0.05$; **$p<0.01$; ***$p<0.001$. Analysis was conducted using the GraphPad Prism 8 statistical software for Windows.

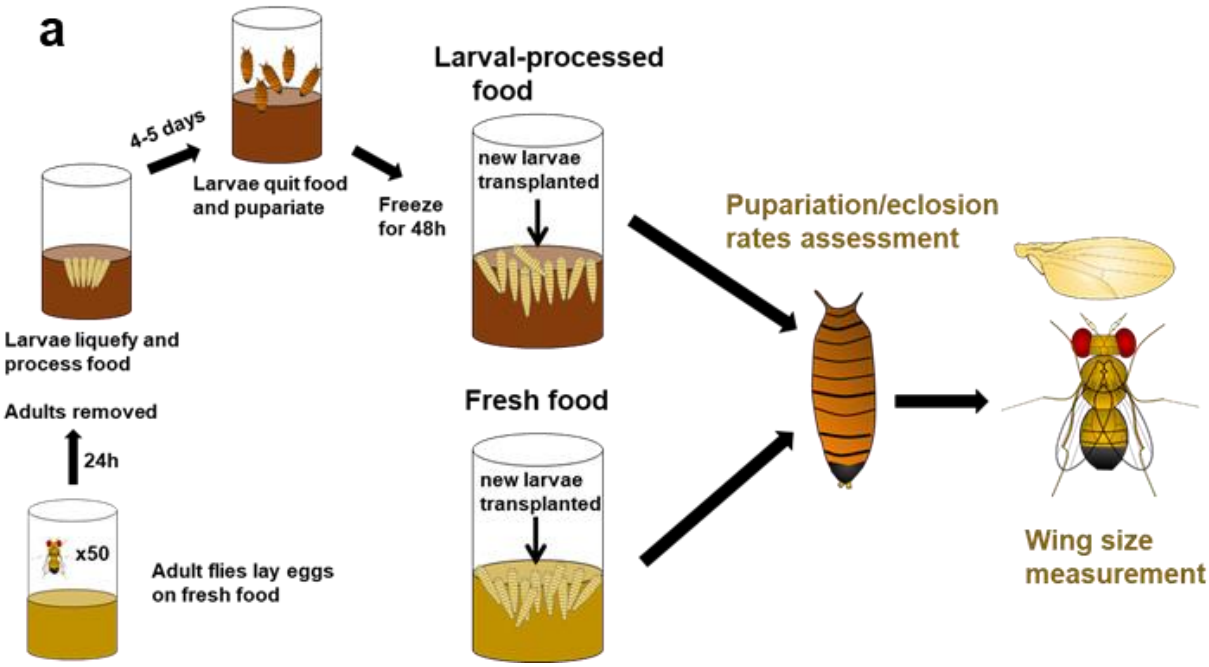
a
4-5 days
Larvae quit food and pupariate
Freeze for 48h
Larval-processed food
new larvae transplanted
Pupariation/eclosion rates assessment
Larvae liquefy and process food
Adults removed
24h
x50
Adult flies lay eggs on fresh food
Fresh food
new larvae transplanted
Wing size measurement

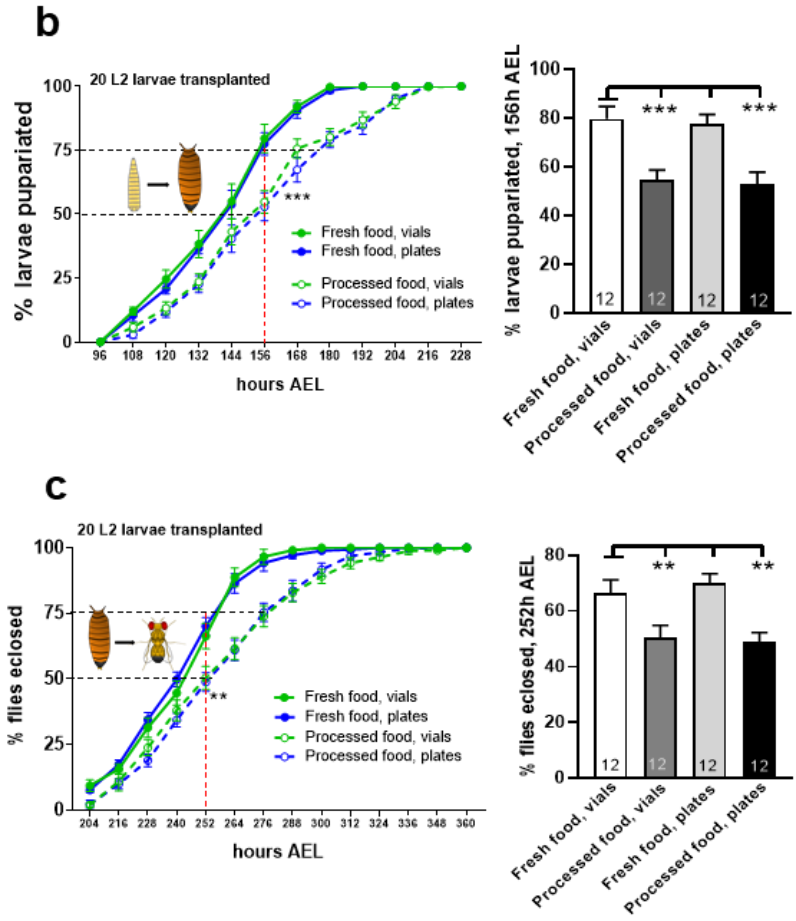
b
20 L2 larvae transplanted
% larvae pupariated
hours AEL
Fresh food, vials
Fresh food, plates
Processed food, vials
Processed food, plates
***
% larvae pupariated, 156h AEL
c
20 L2 larvae transplanted
% flies eclosed
hours AEL
**
% flies eclosed, 252h AEL

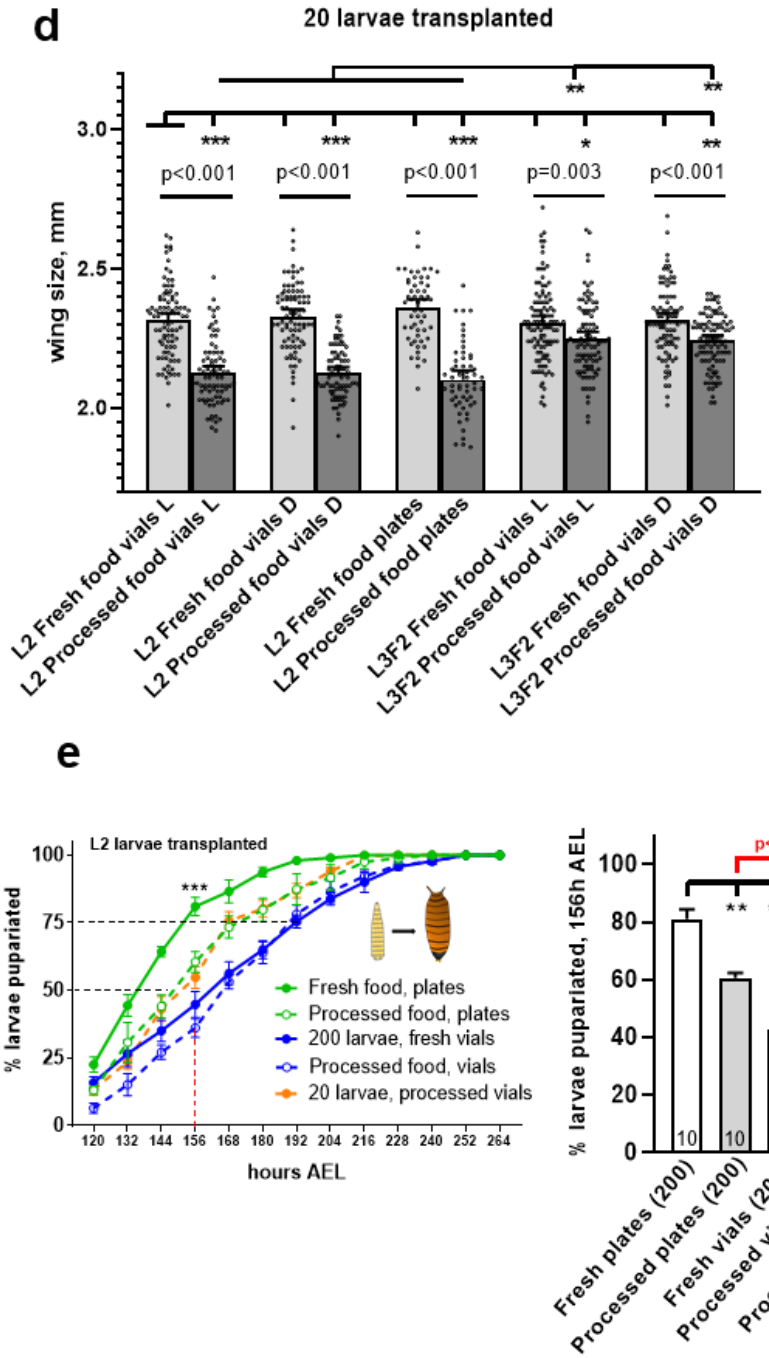
d
20 larvae transplanted
wing size, mm
3.0
2.5
2.0
p<0.001
p<0.001
p<0.001
p=0.003
p<0.001
L2 Fresh food vials L
L2 Processed food vials L
L2 Fresh food vials D
L2 Processed food vials D
L2 Fresh food plates
L2 Processed food plates
L3F2 Fresh food vials L
L3F2 Processed food vials L
L3F2 Fresh food vials D
L3F2 Processed food vials D
e
L2 larvae transplanted
% larvae pupariated
hours AEL
Fresh food, plates
Processed food, plates
200 larvae, fresh vials
Processed food, vials
20 larvae, processed vials
% larvae pupariated, 156h AEL
p<0.01
p=0.27
p<0.01
Fresh plates (200)
Processed plates (200)
Fresh vials (200)
Processed vials (200)
Processed vials (20)

Figure 1. Processed food delays larval development and decreases animal size

(A) Schematic view of experimental procedures. In order to produce processed food, ~50 adult flies were kept in fresh food vials for 24h and then removed, allowing a sufficient number of larvae to hatch and liquefy food within next 4-5 days. After all larvae pupariated, vials were frozen for 48h and cleaned. Newly collected larvae at a designated developmental stage were transplanted into defrosted vials with processed food in parallel with fresh food vials. Eclosion and pupariation rates were measured followed by assessment of adult female fly wing size to examine the effect of processed food on animal growth and development.

(B) and **(C)** Processed food causes a significant developmental retardation. 20L2 wild type larvae were transplanted in vials or plates with fresh and processed food and subsequently evaluated for developmental rates. Rearing in processed food results in a consistent ~16-20h delay in both pupariation **(B)** and eclosion **(C)**. No difference was seen between plates and vials. Percentage of larvae pupariated/eclosed was measured every 12h starting at 96 and 192h AEL, respectively. Here and further on, 156h AEL and 252h AEL checkpoints (indicated by dashed red lines) were compared for pupariation **(B)** and eclosion **(C),** respectively**,** with data represented in bar graphs.

(D) Processed food decreases wing size. 20 wild type larvae were transplanted into plates or vials with fresh or processed food with subsequent evaluation of adult fly wing size. In addition, effect of dark rearing or late transplantation (L3F2) was examined and compared between fresh and processed food vials. A significant ~8-9% decrease in wing size was observed in L2 transplants raised in processed food, regardless of being reared in plates or vials and in normal light conditions (L) or darkness (D). A smaller 3-4% reduction in wing size was seen in L3F2 transplants raised in processed food, with no difference between normal light-dark regime and darkness.

(E) Crowded conditions exacerbate developmental retardation. Pupariation rates were assessed in 20 and 200L2 wild type larvae transplanted into plates or vials with fresh or processed food. No difference was found between fresh and processed food vials. Importantly, 200 larvae raised in processed vials showed the biggest delay in pupariation, being significantly different from both 20 animals in processed food vials and 200 animals in processed food plates (highlighted in red).

See also Figure S1

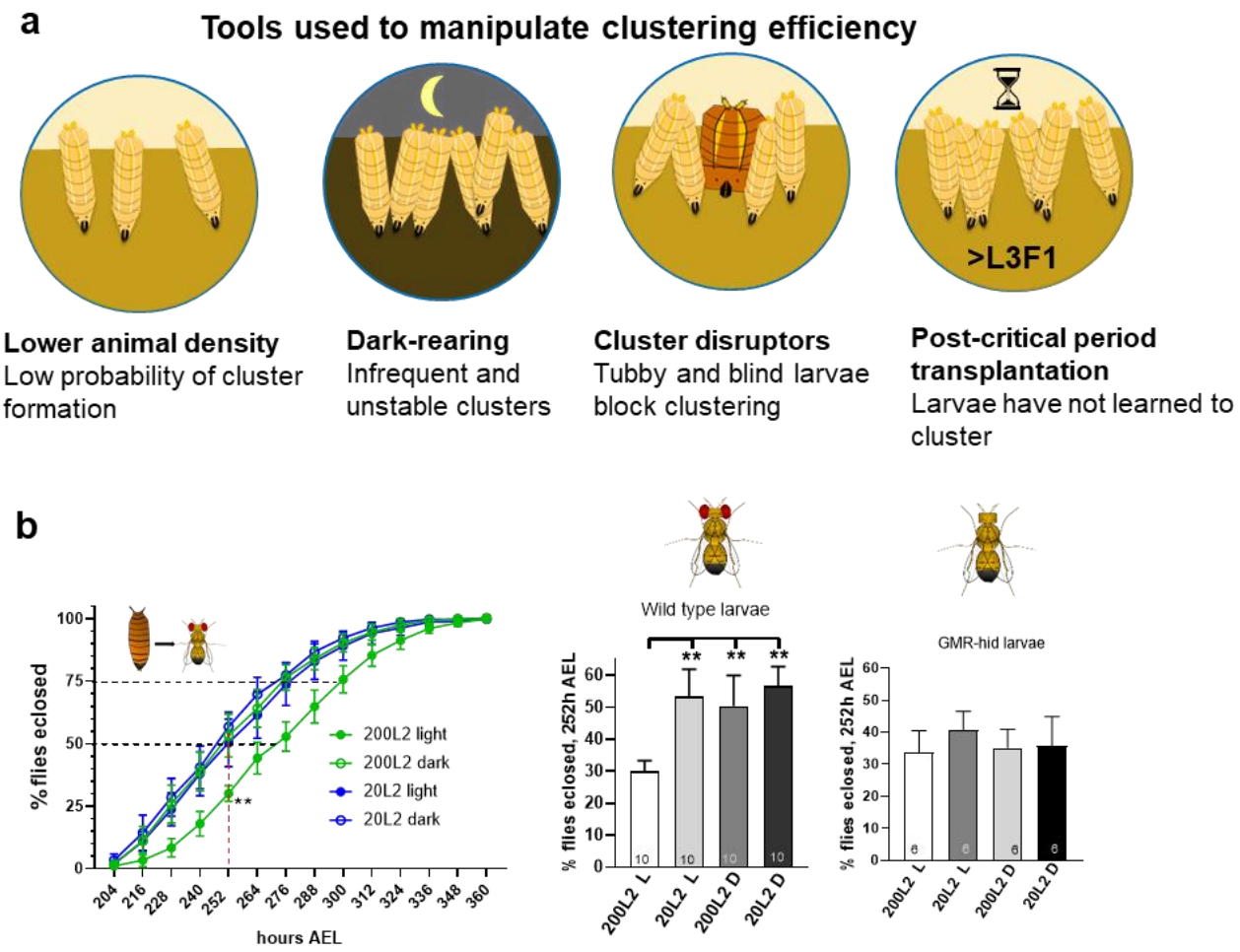

Figure 2. Cooperative foraging further delays larval development in processed food

(A) Schematic view of approaches further used (individually or in combination) to selectively reduce clustering efficiency in wild type animals.

(B) A difference in developmental rates is seen between light- and dark reared larvae, but only in conditions that otherwise promote clustering. Eclosion rates were compared between 20 and 200L2 transplanted wild type larvae reared in normal light conditions (L) and in the darkness (D). Eclosion delay was significantly reduced in dark reared 200L2 larvae compared to animals raised in normal conditions. However, no significant difference was found in case of 20L2 transplants. In addition, no difference in developmental timing was seen among blind GMR-hid larvae exposed to the same experimental conditions (right panel).

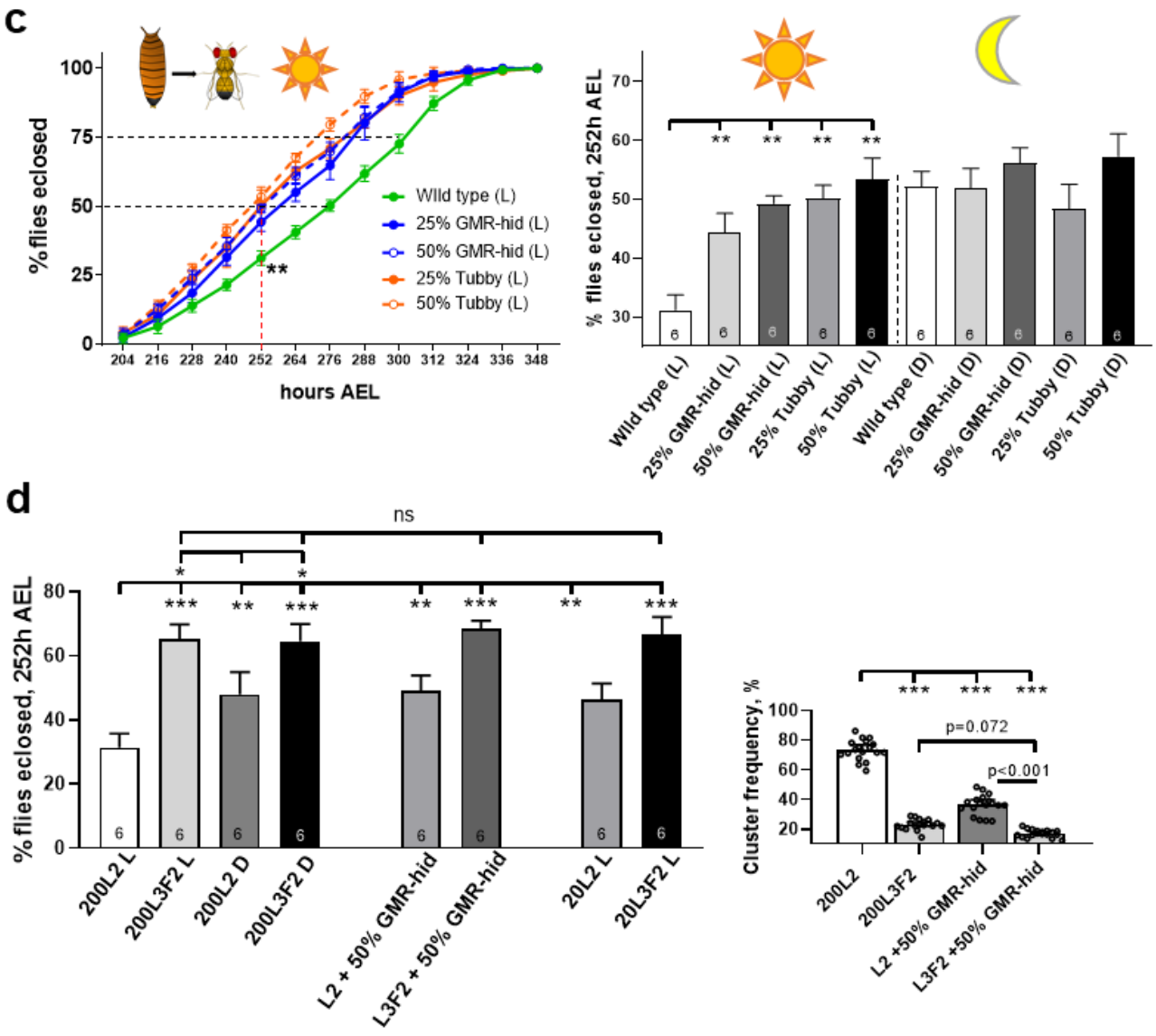

(C) Addition of cluster disruptors reduces larval developmental delay, but only in conditions that otherwise promote clustering. Eclosion rates were compared between 200L2 transplant groups containing 100% wild type larvae, 75% wild type + 25% GMR-hid or Tubby and 50% wild type + 50% GMR-hid or Tubby larvae. Same experiments were performed in the darkness. For animals reared in normal light conditions, cluster frequency was evaluated (right panel). For experiments performed in normal light conditions, addition of blind or tubby larvae resulted in a significantly decreased delay in eclosion compared to all-wild type groups. It was coupled with a corresponding decrease in clustering frequency. At the same time, no difference in eclosion rates was found between all-wild type and mixed groups for dark reared animals

(D) Transplantation after the critical period for clustering reduces larval developmental delay. Eclosion rates were compared between wild type larvae

transplanted at L2 and L3F2 stages, including comparison between 20 and 200 animals, normal light conditions (L) and dark rearing (D) and all-wild type populations and addition of 50% blind GMR-hid larvae. Regardless of any manipulations, L3F2 transplants displayed a significantly reduced delay in eclosion compared not only to 200L2 larvae in normal light conditions, but even 200L2s in the darkness and 20L2s as well as 200L2s in a mixed group (left panel). At the same time, L3F2 transplants showed significantly reduced clustering frequency compared to control wild type 200L2 and even mixed group 200L2 larvae (right panel).

See also Figures S1 and S2

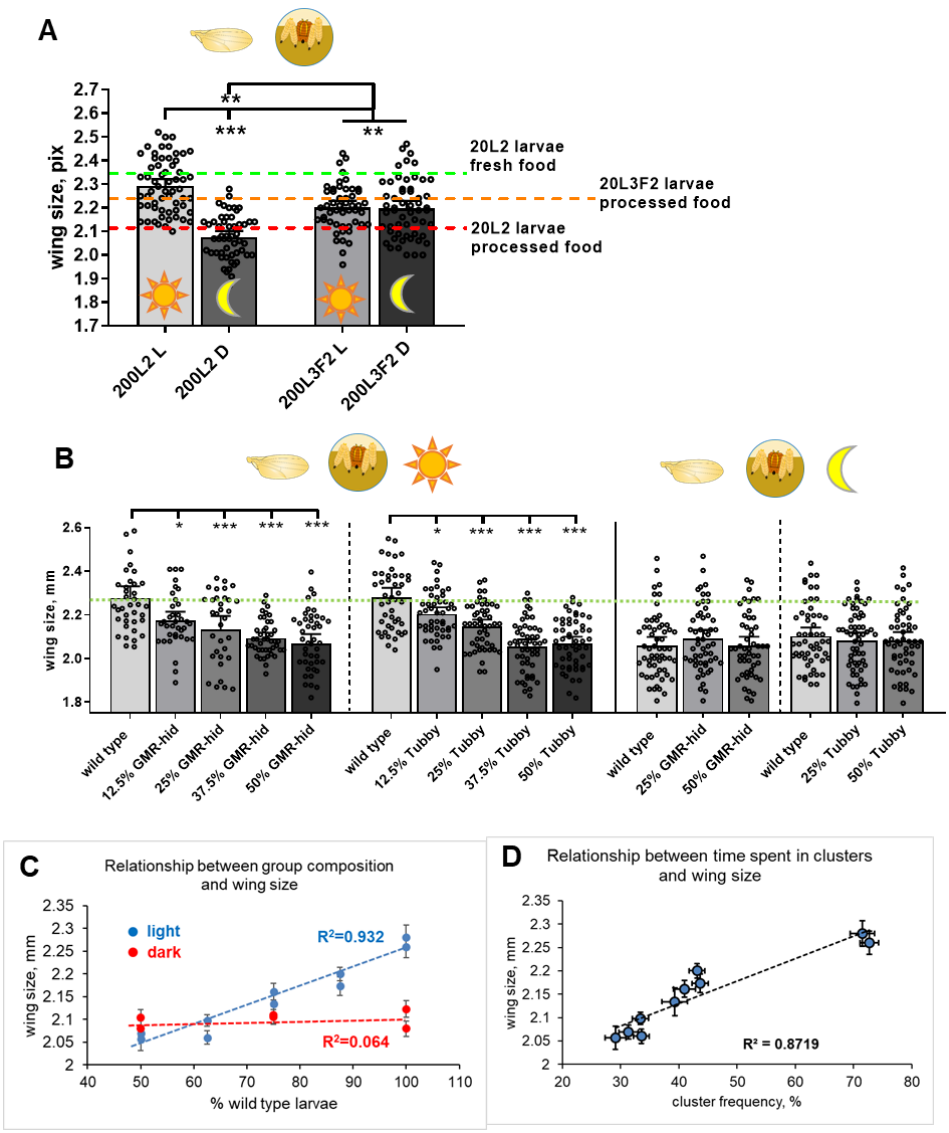

Figure 3. Clustering rescues fitness deficits caused by processed food

(A) Conditions that promote clustering also positively affect wing size. Wings size was compared between light- and dark reared L2 and L3F2 transplants (experiment shown in Figure 2D). 200L2 transplanted larvae reared in normal light conditions (L) have significantly bigger wings compared to their dark reared counterparts (D) and 20L2 larvae (indicated by a red dashed line, data from figure 1D) and only slightly smaller compared to 20L2 animals raised on fresh food serving as a positive control (indicated by a green dashed line, data from Figure 1D). In contrast, larvae transplanted at L3F2 stage display no difference in wing size between light- and dark reared animals, as well as 20L3F2 transplants in processed food (indicated by an orange dashed line, data from Figure 1D). Nevertheless, L3F2 larvae have smaller wings compared to 200L2 transplants reared in normal light conditions.

(B) Group composition affects wing size, but only in normal light conditions. Wing size was compared between 200L2 transplant groups containing 100%, 87.5%, 75%, 62.5% and 50% wild type larvae reared in normal light conditions with the rest of the group comprising either GMR-hid or Tubby larvae in corresponding percentages (left panel). For dark reared animals (right panel), 100%, 75% and 50% wild type groups were used. A significant difference in wing size was found between all wild type animals from mixed groups and control 100% wild type groups raised in normal conditions. On the contrary, no difference in wing size was seen between groups of different composition in dark-reared larvae (wild type larvae from all groups had reduced wings compared to normal light reared all-wild type control group).

(C) Relationship between group composition and wing size (data are related to Figure 3B). High positive correlation is seen between percentage of wild type larvae in a light reared group and wing size in flies derived from wild type larvae of the corresponding group. No correlation is observed in case of dark reared animals. Error bars represent SEM.

(D) Relationship between time spent in clusters and wing size. Data are taken from experiments involving 200L2 wild type larvae and 12.5-50% mixed groups involving GMR-hid and Tubby larvae (results presented in Figure 3B, left panel). Clustering frequency is represented on the X-axis (data shown in Figure S2C). A significant positive correlation is seen between percentage of time a cluster was observed in a group of a designated composition and wing size in flies derived from wild type larvae of the corresponding group. Error bars represent SEM.

A. Related to Figures 1B, 1C, 1D

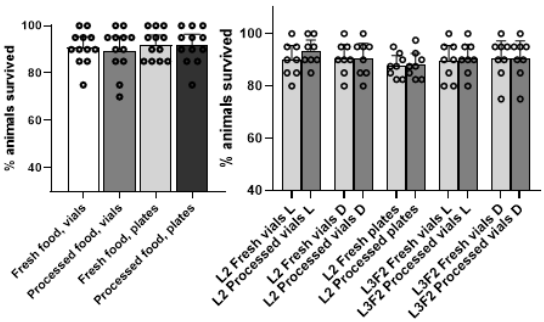

B. Related to Figures 1B, 1C, 1E, 2B

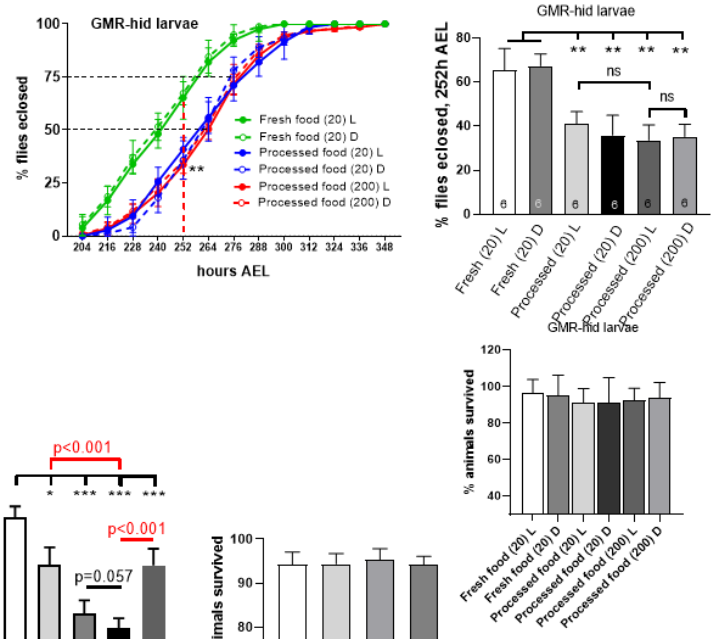

C. Related to Figure 1E

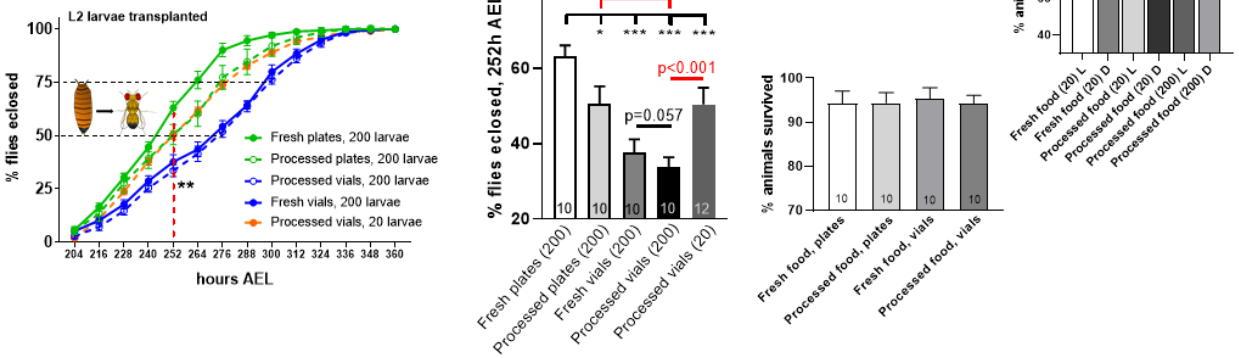

D. Related to Figure 2B

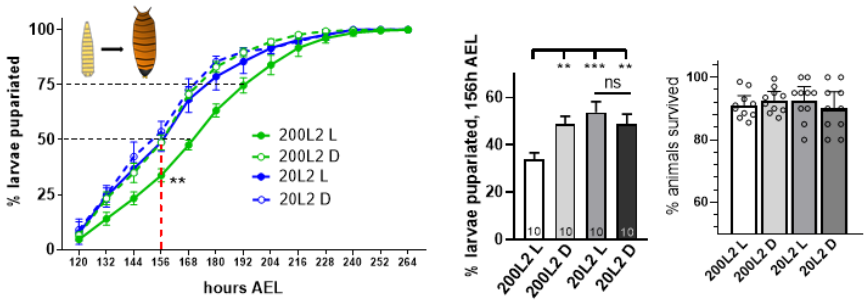

E. Related to Figure 2C

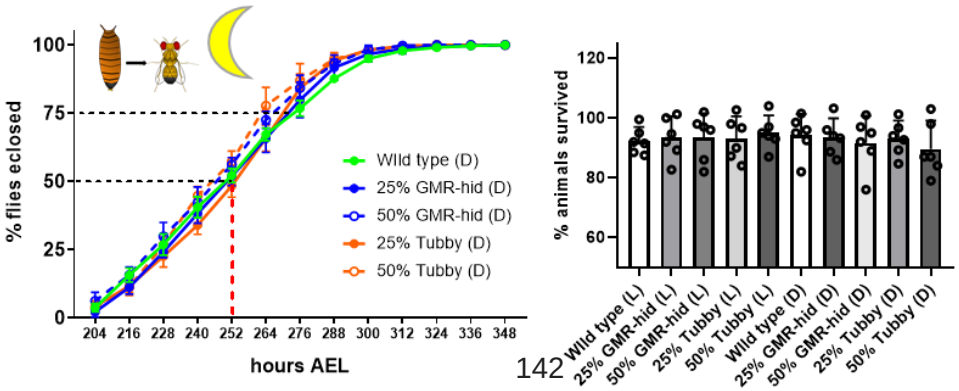

Figure S1. Related to Figures 1 and 2

(A) Survival rates are unaffected by food quality and rearing in plates/vials in case of 20L2 transplants (left panel, related to Figures 1B and 1C). No difference in survival rates was seen between normal and dark reared 20 L2 and 20 L3F2 transplants in fresh or processed food (right panel, related to Figure 1D).

(B) Processed food caused developmental retardation in GMR-hid larvae as well (left and middle panels, related to Figures 1B and 1C), but, unlike in case of wild type larvae, population size and light regime had no effect on developmental rates in processed food (left and middle panels, related to Figure 1E). Survival rates were not affected in any of those conditions (right panel).

(C) Eclosion rates in wild type larvae are also affected by crowded conditions (related to Figure 1E). Similarly to pupariation (Figure 1E), an increase in animal number and transition from plates to vials significantly delay eclosion in processed food (left and middle panels). No significant difference was found between animals raised in fresh and processed food vials. Animal survival rates were not affected by any of the conditions mentioned above (right panel).

(D) Pupariation rates compared between 20 and 200L2 transplanted wild type larvae reared in normal light conditions (L) and in the darkness (D). Pupariation delay was significantly reduced in dark reared 200L2 larvae compared to animals raised in normal conditions, but no difference was found between light- and dark reared 20L2 transplants (left and middle panels, related to Figure 2B). Survival rates were not affected by population size and light regime (right panel).

(E) Addition of cluster disruptors does not affect eclosion rates if animals are reared in the darkness (left panel, related to Figure 2C). Eclosion rates were compared between 200L2 transplant groups containing 100% wild type larvae, 75% wild type + 25% GMR-hid or Tubby and 50% wild type + 50% GMR-hid or Tubby larvae. No difference in survival rates was observed among all-wild type and mixed groups in normal light conditions and in the darkness (right panel).

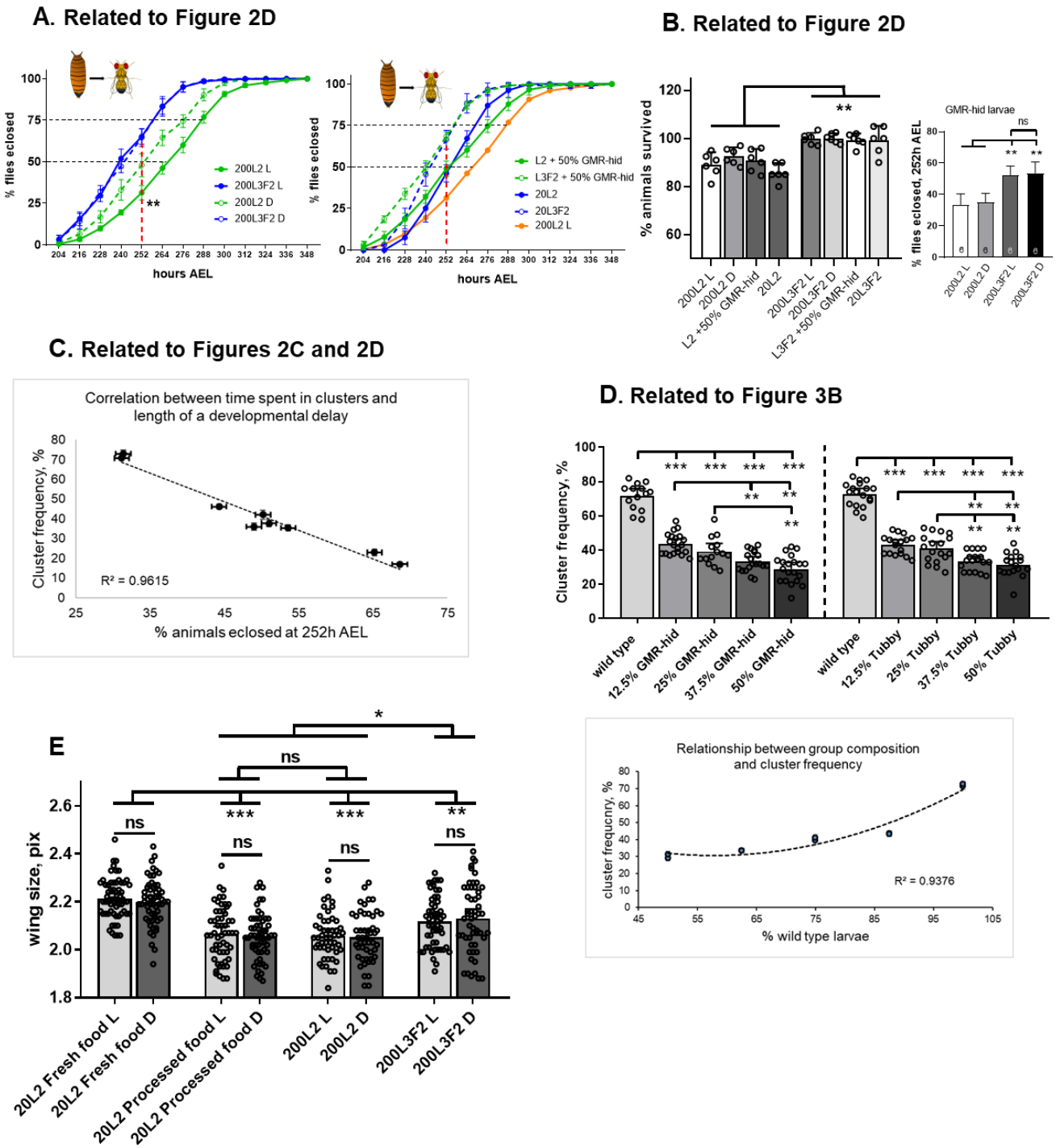
A. Related to Figure 2D
% flies eclosed
hours AEL
200L2 L
200L3F2 L
200L2 D
200L3F2 D
L2 + 50% GMR-hid
L3F2 + 50% GMR-hid
20L2
20L3F2
200L2 L
B. Related to Figure 2D
% animals survived
GMR-hid larvae
% flies eclosed, 252h AEL
C. Related to Figures 2C and 2D
Correlation between time spent in clusters and length of a developmental delay
Cluster frequency, %
% animals eclosed at 252h AEL
R² = 0.9615
D. Related to Figure 3B
Cluster frequency, %
wild type
12.5% GMR-hid
25% GMR-hid
37.5% GMR-hid
50% GMR-hid
12.5% Tubby
25% Tubby
37.5% Tubby
50% Tubby
E
wing size, pix
20L2 Fresh food L
20L2 Fresh food D
20L2 Processed food L
20L2 Processed food D
200L2 L
200L2 D
200L3F2 L
200L3F2 D
Relationship between group composition and cluster frequency
cluster frequency, %
% wild type larvae
R² = 0.9376

Figure S2. Related to Figures 2 and 3

(A) Post-critical period transplantation reduces eclosion delay in processed food (related to Figure 2D). Light regime does not affect eclosion rates in wild type L3F2 transplants compared to their L2 counterparts (left panel). Reduced animal density and addition of cluster disruptors has no effect on eclosion rates in L3F2 transplants compared to their L2 counterparts (right panel).

(B) Wild type L3F2 transplants show significantly higher survival rates compared to L2-transplnated larvae, regardless of animal density, light regime or addition of cluster disruptors (left panel, related to Figure 2D). GMR-hid L3F2 transplants similarly show increased survival rates compared to L2-transplanted blind larvae (right panel).

(C) Relationship between time spent in clusters and eclosion delay. A strong negative correlation is observed between cluster frequency and percentage of eclosed wild type animals at 252h AEL (data taken from experiments involving addition of cluster disruptors and L3F2 transplantations, related to Figures 2C and 2D).

(D) Cluster frequency is significantly reduced when cluster disruptors are added (related to Figure 3B). Sequential addition of 12%, 25%, 37.5% and 50% of GMR-hid or Tubby results in a gradual significant decrease in clustering frequency (top panel). A strong positive correlation is observed between percentage of wild type larvae in groups and clustering frequency (bottom panel).

(E) Controls for wing size in GMR-hid animals. Wing size is significantly reduced in animals reared in processed food compared to animals raised on fresh food. No effect of light regime was seen regardless of population size and transplantation stage. No effect of group size was observed. However, animals transplanted at L3F2 stage had slightly bigger wings compared to L2 transplants.

Chapter 5

Conclusions and Future Directions

Visual system in larval *Drosophila*: can we expect more complex functions from simple circuits?

Our research serves to expand the existing knowledge about the functions and application of the insect visual system. While olfaction, chemosensation and even mechanosensation have been well-described as tools for social communications in insects, only a few examples utilizing vision as a main sensory modality for interactions within a cooperative group have been documented. This is particularly noteworthy in the context of the relatively simple visual system of *Drosophila* larvae, whose more complex functions have only recently been examined. Up until recently the fruit fly larvae were only considered to possess a simple set of photobehaviors, such as light avoidance, circadian entrainment and barely efficient visual associative learning. However, the emerging evidence from our lab and other research groups has demonstrated not only the presence of complex functions that a simple larval visual circuit is capable of performing (recognition of complex images and detecting movements), but also a social relevance of these functions. Most importantly, cellular substrates underlying them have been identified and studied. To summarize, along with simple light-dark discrimination, an innate trait that is operated by a hard-wired Rh5 visual circuit, larvae are clearly capable of perceiving temporal light cues, which is

mechanistically related to movement detection. This is an acquired property that develops at a critical period during early 3rd instar stages and requires exposure to crowded conditions. We wondered whether the same visual function is required for clustering during inter-larval movement coordination, considering that its emergence is temporally correlated with the onset of clustering during early 3rd instar. Moreover, we suggested that these photobehaviors are operated by Rh6-lOLP pathway in larval visual system, the specific function of which was unknown at that time Using a set of behavioral tools and taking advantage of the accessible genetics of a fruit fly, we have shown that both recognition of moving targets and social clustering require the function of Rh6-lOLP pathway in a similar manner and therefore can be regarded as identical types of photobehavior. Further on we demonstrate a cellular basis for an experience-depending plasticity in Rh6-lOLP pathway underlying the emergence of clustering and movement detection. Our data suggest that it is associated with both morphological presynaptic changes in Rh6 photoreceptors and strengthening of postsynaptic physiological response in both lOLP interneurons. Taken together, our study was able to connect complex social behavior and underlying neuronal circuits, as well as provide evidence of structural plasticity in *Drosophila* CNS. At the same time, our results have led to the emergence of many new direct avenues of study to understand plasticity and social function of the brain.

In particular, precise developmental aspects of the observed behavioral plasticity have not been assessed. We were able to roughly correlate the emergence of behavior with changes in circuit morphology and physiology, but a

more accurate analysis of developmental stages associated with Rh6-lOLP function in larval photobehaviors will require the use of conditional neuronal silencing techniques, which were omitted in our study due to the strong impact of temperature shifts on larval locomotor activity and overall development. That will allow to see if changes in behavior are permanent and if not, whether they can be reversed similarly to presynaptic morphology of Rh6-PRs that we observed earlier.

Future experiments will need to identify specific circuit mechanisms underlying observed photobehaviors. So far, the notion is that Rh6-lOLP pathway acts a switch for an ON and OFF selectivity (depending on whether light intensity increases or decreases) through reciprocal inhibition of two lOLP neurons, and this could be the underlying mechanisms for movement detection. This hypothesis has physiological support based on calcium imaging recorded from lOLP neurons in response to artificial light stimulation, an approach that might not necessarily represent the naturally occurring conditions and lack temporal resolution. Therefore, further verification is required using a set of more sophisticated behavioral tools, presumably coupled with *in vivo* electrophysiological recordings not only from lOLPs, but also Rh6 photoreceptors. Another goal would be to determine how and where the perception of movements and complex images takes place in the larval visual system. It is not very likely that final computations are made as early as at the level of lOLPs. More realistically, temporal and spatial light signals get pre-processed by lOLPs and then undergo full processing at higher-order brain regions that are yet to be determined. Fortunately, availability of data from larval connectome reconstruction and access to a broad GAL4 library

highly facilitate the task to identify the downstream functional targets of Rh5- and Rh6-lOLP pathways.

An important next step will also be to identify and characterize molecular determinants underlying described experience-dependent plasticity in larval visual system that is restricted to a critical period. This would be a key step to complete the integrative model or a learned larval photobehavior and its development over time. Two major approaches include performing high-throughput forward genetic screens and (perhaps a more efficient one) RNA-seq aimed at identifying genes differentially expressed in lOLPs and Rh6-PRs before, during and after the critical period in L2-L3F1 larval stages. The former approach takes full advantage of fly genetics but lacks specificity, while the latter is complicated by the small numbers of the cells of interest. This will allow to generate the first invertebrate model of a critical period that integrates behavioral observations, circuit changes and underlying molecular components and might be of great value to developmental neurobiology.

Eventually, a more integrative look at experience-dependent plasticity in our model system is worth consideration. It would be interesting to see if light/social deprivations have any behavioral consequences in the adult fly, which is hard to predict based on structural changes that larval visual circuit undergoes during metamorphosis. In addition, it is intriguing to look at intersections of visual plasticity and clustering in general with other larval behaviors, such as associative learning and sleep, all of which contribute to create a complete neuroethological picture.

Clustering as a neuroethological model system of cooperative behavior

We have introduced an experimental model system that involves *Drosophila* larvae performing cooperative social foraging that requires sensory communications between individuals and is sensitive to prior visual and social experience that determines future group membership. The main advantage of our model is its relevance to naturally occurring behavior, but at the same time accessibility in laboratory conditions coupled with an array of tools in molecular genetics available for fruit flies. This allows to dissect out a variety of complex parameters governing the emergence of clustering behavior and rules it obeys, therefore making it possible to approach a single question from multiple angles. Having previously characterized the mechanistic and neurological basis of clustering behavior, as well as the contribution of individual animals to cooperative group formation and stability, we also addressed ecological and evolutionary aspects of clustering and aimed to elucidate how such robust behavior emerged in evolution and what benefits it provided. We were able to show that cluster membership provides a fitness advantage to social animals, as measured by adult female body size, which is known to highly correlate with survival probability and reproductive success. Interestingly, we also found that these benefits take effect in specific circumstances, when food quality and population density become rate limiting factors. Therefore, clustering can be regarded as an evolutionary behavioral solution which counteracts the negative influence of the environment and promotes the development of cooperative skills among individuals

Our findings also raise certain questions that will be addressed in the future. While we clearly show a correlation between the degree of animals' engagement in clusters and their fitness, the exact mechanisms underlying this effect are not understood. It is unlikely that there is an unequivocal answer to this question, due to the complexity of the possible interactions between individuals and the environment that occur under natural conditions. Multiple factors should be considered, including as simple as increased digging efficiency and as complex as possible cooperative exodigestion that involves an exchange in social stimuli resulting in deep behavioral changes. A question of great interest is whether the effect of these social stimuli on behavior can be carried out through neuronal circuit rearrangements. We have recently reported that social conditions can modify pathways in *Drosophila* visual system responsible for social recognition and visually guided cooperation in clusters. Therefore, it is possible that social environment and experience can induce structural and functional changes in circuits governing motor patterns of food intake that have recently been characterized as well as more complex control over attraction to food and associated cooperative burrowing. Moreover, the question of how exactly processed food implements its effect on individual animals remains unknown. Possible reasons could be diverse and include both reduced nutritional value as well as a complex change in bacterial composition that can affect larval physiology and behavior in a variety of ways. Complex metabolic and behavioral studies are required to further investigate this question.

Importantly, we describe a behavioral phenomenon that involves transition of individuals to group behavior and cooperation under specific conditions, which requires a better understanding of underlying rules and limitations. It is possible that applying approaches from game theory may be able to help understand how individual animals make conflicting decisions about joining a group, as well as how many resources to invest for the common good. In any case, the emergence of certain restrictions is not questioned, because our results suggest that animals have to undergo significant physiological and behavioral changes that consume time and resources in order to obtain cluster membership. This process is very likely to be accompanied by an emergence of a defense mechanism that protects a common group resource from being utilized by non-members. Further studies are required to shed more light on this interesting topic. Importantly, while we show that social learning can segregate members of the same population, it would be interesting to establish the role of clustering in interactions between different fly species that naturally coexist on the same food substrate. For that purpose, a series of studies on wild *Drosophila* populations may be required. Overall, any field observations and research highlighting the importance of larval cooperative behavior would be complementary to the results derived from the lab.

Last but not least, our model system provides an excellent opportunity to precisely look at critical developmental windows underlying development of complex behaviors. It is very likely that early 3rd larval instar that we focus on serves as a point of convergence for multiple critical periods including critical weight assessment, movement detection and clustering. Therefore, it may require

integrating approaches in ethology, neurobiology and evolutionary biology to answer questions of how external environment including social experience affects behaviors and shapes underlying circuits. Further use of the fly as a model system will take advantages of combining high-throughput behavioral analysis, easy genetic manipulations and accessible connectome data, which without a doubt opens huge prospects for better understanding the nature of experience-dependent plasticity in early postnatal life. This may be especially significant in context of dissecting cellular and molecular mechanisms underlying human neurological disorders linked to disruption of critical period circuit remodeling.

In summary, the results of our work took us a few steps closer to understanding how cooperative behavior is regulated on cellular, organismal, and even populational level. Using a simple model system, we demonstrated that a naturally occurring complex social behavior emerges in evolution to balance out negative environmental effects and ensure benefits in survival and reproduction for social individuals. A use of fruit fly as a genetically tractable and experimentally accessible organism allows us to correlate behavioral effects with corresponding changes in circuit physiology and suggest underlying molecular mechanisms. At the same time more and more emerging problems regarding evolution, neurobiology and genetics of social behaviors in animals including humans remain poorly elucidated and will be addressed in future. Therefore, a major contribution of this study is a framework it creates allowing to address profound neuroethological questions using an integrative and versatile approach.

References

1. Abbott, L.F. and Nelson, S.B., (2000). Synaptic plasticity: taming the beast. Nature neuroscience, 3(11s), p.1178.
2. Aceves-Piña, E. O., and Quinn, W. G. (1979). Learning in normal and mutant Drosophila larvae. Science 206, 93-96.
3. Ache, J.M., Polsky, J., Alghailani, S., Parekh, R., Breads, P., Peek, M.Y., Bock, D.D., von Reyn, C.R. and Card, G.M., (2019). Neural Basis for Looming Size and Velocity Encoding in the Drosophila Giant Fiber Escape Pathway. Current Biology.
4. Ainsley, J.A., Kim, M.J., Wegman, L.J., Pettus, J.M. and Johnson, W.A., (2008). Sensory mechanisms controlling the timing of larval developmental and behavioral transitions require the Drosophila DEG/ENaC subunit, Pickpocket1. Developmental biology, 322(1), pp.46-55.
5. Akin, O., Bajar, B.T., Keles, M.F., Frye, M.A. and Zipursky, S.L., (2019). Cell-Type-Specific Patterned Stimulus-Independent Neuronal Activity in the Drosophila Visual System during Synapse Formation. Neuron.
6. Alexander, R.D. (1974). The evolution of social behavior. Annu. Rev. Ecol. Syst. 5, 325-383.
7. Allee, W.C., (1927). Animal aggregations. The Quarterly Review of Biology, 2(3), pp.367-398.
8. Amor, F., Ortega, P., Cerdá, X. and Boulay, R., (2010). Cooperative prey-retrieving in the ant Cataglyphis floricola: an unusual short-distance recruitment. Insectes Sociaux, 57(1), pp.91-94.
9. Arthur Jr, B.I., Jallon, J.M., Caflisch, B., Choffat, Y. and Nöthiger, R., (1998). Sexual behaviour in Drosophila is irreversibly programmed during a critical period. Current biology, 8(21), pp.1187-1190.
10. Ashley, J., Cordy, B., Lucia, D., Fradkin, L.G., Budnik, V. and Thomson, T., (2018). Retrovirus-like Gag protein Arc1 binds RNA and traffics across synaptic boutons. Cell, 172(1-2), pp.262-274.
11. Aso, Y., Sitaraman, D., Ichinose, T., Kaun, K.R., Vogt, K., Belliart-Guérin, G., Plaçais, P.Y., Robie, A.A., Yamagata, N., Schnaitmann, C. and Rowell, W.J., (2014). Mushroom body output neurons encode valence and guide memory-based action selection in Drosophila. Elife, 3, p.e04580.
12. Aubernon, C., Hedouin, V. and Charabidze, D., (2019). The maggot, the ethologist and the forensic entomologist: Sociality and thermoregulation in necrophagous larvae. Journal of advanced research, 16, pp.67-73
13. Auer, T.O., Khallaf, M.A., Silbering, A.F., Zappia, G., Ellis, K., Hansson, B., Jefferis, G.S., Caron, S., Knaden, M. and Benton, R., (2019). The making of an olfactory specialist.
14. Barth, M. and Heisenberg, M., (1997). Vision affects mushroom bodies and central complex in Drosophila melanogaster. Learning & Memory, 4(2), pp.219-229.
15. Barth, M., Hirsch, H.V., Meinertzhagen, I.A. and Heisenberg, M., (1997). Experience-dependent developmental plasticity in the optic lobe of Drosophila melanogaster. Journal of Neuroscience, 17(4), pp.1493-1504.
16. Bateson, P., (1978). Sexual imprinting and optimal outbreeding. Nature, 273(5664), p.659.
17. Benton, R., Vannice, K.S., Gomez-Diaz, C. and Vosshall, L.B., (2009). Variant ionotropic glutamate receptors as chemosensory receptors in Drosophila. Cell, 136, 149-162.
18. Berardi, N., Pizzorusso, T. and Maffei, L., (2000). Critical periods during sensory development. Current opinion in neurobiology, 10(1), pp.138-145.
19. Berck, M.E., Khandelwal, A., Claus, L., Hernandez-Nunez, L., Si, G., Tabone, C.J., Li, F., Truman, J.W., Fetter, R.D., Louis, M. and Samuel, A.D., (2016). The wiring diagram of a glomerular olfactory system. Elife, 5, p.e14859.
20. Blakemore, S.J. and Mills, K.L., (2014). Is adolescence a sensitive period for sociocultural processing? Annual review of psychology, 65, pp.187-207.

21. Bo, Q., Humberg, T.H., Kim, A., Kim, H., Short, J., Diao, F., White, B.H., Sprecher, S.G. and Yuan, Q., (2019). Temporal control of inhibition via muscarinic acetylcholine receptor signaling generates ON and OFF selectivity in a simple visual circuit. bioRxiv, p.535427.
22. Boettiger, C.A. and Doupe, A.J., (2001). Developmentally restricted synaptic plasticity in a songbird nucleus required for song learning. Neuron, 31(5), pp.809-818.
23. Bolhuis, J.J., (1991). Mechanisms of avian imprinting: a review. Biological Reviews, 66(4), pp.303-345.
24. Borst, A., and Euler, T. (2011). Seeing things in motion: models, circuits, and mechanisms. Neuron 71, 974-994.
25. Boulay, J., Aubernon, C., Ruxton, G.D., Hédouin, V., Deneubourg, J.L. and Charabidzé, D., (2019). Mixed-species aggregations in arthropods. Insect science, 26(1), pp.2-19.
26. Bowtell, D.D., Simon, M.A. and Rubin, G.M., (1989). Ommatidia in the developing Drosophila eye require and can respond to sevenless for only a restricted period. Cell, 56(6), pp.931-936.
27. Burghardt, G.M. and Hess, E.H., (1966). Food imprinting in the snapping turtle, Chelydra serpentina. Science, 151(3706), pp.108-109.
28. Burghardt, G.M., (1992). Prior exposure to prey cues influences chemical prey preference and prey choice in neonatal garter snakes. Animal Behaviour.
29. Canny, J. (1987). A computational approach to edge detection. In Readings in computer vision, M.A. Fischler, ed. (San Francisco: Morgan Kaufmann Publishers Inc) pp. 184-203.
30. Carton, Y. and David, J.R., (1985). Relation between the genetic variability of digging behavior of Drosophila larvae and their susceptibility to a parasitic wasp. Behavior genetics, 15(2), pp.143-154.
31. Carton, Y., and David, J. R. (1985). Relation between the genetic variability of digging behavior of Drosophila larvae and their susceptibility to a parasitic wasp. Behav. Genet. 15, 143-154.
32. Carton, Y., and Sokolowski, M. B. (1992). Interactions between searching strategies of Drosophila parasitoids and the polymorphic behavior of their hosts. J. Insect Behav. 5, 161-175.
33. Cash, K.J., McKee, M.H. and Wrona, F.J., (1993). Short-and long-term consequences of grouping and group foraging in the free-living flatworm Dugesia tigrina. Journal of Animal Ecology, pp.529-535.
34. Certel, S.J., Savella, M.G., Schlegel, D.C. and Kravitz, E.A., (2007). Modulation of Drosophila male behavioral choice. Proceedings of the National Academy of Sciences, 104(11), pp.4706-4711.
35. Chang, E.F. and Merzenich, M.M., (2003). Environmental noise retards auditory cortical development. science, 300(5618), pp.498-502.
36. Chen, T.W., Wardill, T.J., Sun, Y., Pulver, S.R., Renninger, S.L., Baohan, A., Schreiter, E.R., Kerr, R.A., Orger, M.B., Jayaraman, V. and Looger, L.L. (2013). Ultrasensitive fluorescent proteins for imaging neuronal activity. Nature 499, 295.
37. Chen, Y., Akin, O., Nern, A., Tsui, C.K., Pecot, M.Y. and Zipursky, S.L., (2014). Cell-type-specific labeling of synapses in vivo through synaptic tagging with recombination. Neuron, 81(2), pp.280-293.
38. Chen, A.N. and Meliza, C.D., (2019). Experience-and sex-dependent intrinsic plasticity in the zebra finch auditory cortex during song memorization. bioRxiv, p.658104.
39. Cheng, K.Y., Colbath, R.A. and Frye, M.A., (2019). Olfactory and neuromodulatory signals reverse visual object avoidance to approach in Drosophila. Current Biology.
40. Clark, B.R. and Faeth, S.H., (1997). The consequences of larval aggregation in the butterfly Chlosyne lacinia. Ecological Entomology, 22(4), pp.408-415
41. Clark, C.W. and Mangel, M., (1986). The evolutionary advantages of group foraging. Theoretical population biology, 30(1), pp.45-75.
42. Clark, C.W., (1987). The lazy, adaptable lions: A Markovian model of group foraging. Animal Behaviour, 35(2), pp.361-368.
43. Cocroft, R.B., (2005). Vibrational communication facilitates cooperative foraging in a phloem-feeding insect. Proceedings of the Royal Society B: Biological Sciences, 272(1567), pp.1023-1029.

44. Cohn, R., Morantte, I. and Ruta, V., (2015). Coordinated and compartmentalized neuromodulation shapes sensory processing in Drosophila. Cell, 163(7), pp.1742-1755.
45. Colombani, J., Raisin, S., Pantalacci, S., Radimerski, T., Montagne, J. and Léopold, P., (2003). A nutrient sensor mechanism controls Drosophila growth. Cell, 114(6), pp.739-749.
46. Colombani, J., Bianchini, L., Layalle, S., Pondeville, E., Dauphin-Villemant, C., Antoniewski, C., Carré, C., Noselli, S. and Léopold, P., (2005). Antagonistic actions of ecdysone and insulins determine final size in Drosophila. Science, 310(5748), pp.667-670.
47. Colombani, J., Andersen, D.S. and Léopold, P., (2012). Secreted peptide Dilp8 coordinates Drosophila tissue growth with developmental timing. Science, 336(6081), pp.582-585.
48. Courchamp, F., Clutton-Brock, T. and Grenfell, B., (1999). Inverse density dependence and the Allee effect. Trends in ecology & evolution, 14(10), pp.405-410.
49. Couto, A., Alenius, M. and Dickson, B.J., (2005). Molecular, anatomical, and functional organization of the Drosophila olfactory system. Current Biology, 15(17), pp.1535-1547.
50. Crisp, S.J., Evers, J.F. and Bate, M., (2011). Endogenous patterns of activity are required for the maturation of a motor network. Journal of Neuroscience, 31(29), pp.10445-10450.
51. Cumberledge, S. and Krasnow, M.A., (1993). Intercellular signalling in Drosophila segment formation reconstructed in vitro. Nature, 363(6429), p.549.
52. Darmaillacq, A.S., Chichery, R. and Dickel, L., (2006). Food imprinting, new evidence from the cuttlefish Sepia officinalis. Biology letters, 2(3), pp.345-347.
53. Demir, E. and Dickson, B.J., (2005). fruitless splicing specifies male courtship behavior in Drosophila. Cell, 121(5), pp.785-794.
54. Devaud, J.M., Acebes, A., Ramaswami, M. and Ferrús, A., (2003). Structural and functional changes in the olfactory pathway of adult Drosophila take place at a critical age. Journal of neurobiology, 56(1), pp.13-23.
55. Devineni, A.V., Sun, B., Zhukovskaya, A. and Axel, R., (2019). Acetic acid activates distinct taste pathways in Drosophila to elicit opposing, state-dependent feeding responses. eLife, 8, p.e47677.
56. Di Cristo, G., Chattopadhyaya, B., Kuhlman, S.J., Fu, Y., Bélanger, M.C., Wu, C.Z., Rutishauser, U., Maffei, L. and Huang, Z.J., (2007). Activity-dependent PSA expression regulates inhibitory maturation and onset of critical period plasticity. Nature neuroscience, 10(12), p.1569.
57. Doll, C.A. and Broadie, K., (2014). Impaired activity-dependent neural circuit assembly and refinement in autism spectrum disorder genetic models. Frontiers in cellular neuroscience, 8, p.30.
58. Doll, C.A. and Broadie, K., (2015). Activity-dependent FMRP requirements in development of the neural circuitry of learning and memory. Development, 142(7), pp.1346-1356.
59. Doll, C.A., Vita, D.J. and Broadie, K., (2017). Fragile X mental retardation protein requirements in activity-dependent critical period neural circuit refinement. Current Biology, 27(15), pp.2318-2330.
60. Dombrovski, M., Poussard, L., Moalem, K., Kmecova, L., Hogan, N., Schott, E., Vaccari, A., Acton, S. and Condron, B., (2017). Cooperative behavior emerges among Drosophila larvae. Current Biology, 27(18), pp.2821-2826.
61. Dombrovski, M., Kim, A., Poussard, L., Vaccari, A., Acton, S., Spillman, E., Condron, B. and Yuan, Q., (2019). A Plastic Visual Pathway Regulates Cooperative Behavior in Drosophila Larvae. Current Biology. 29(11), pp 1866-1876.
62. Dubois, F., Giraldeau, L.A. and Grant, J.W., (2003). Resource defense in a group-foraging context. Behavioral Ecology, 14(1), pp.2-9. .
63. Durisko, Z., Kemp, R., Mubasher, R. and Dukas, R., (2014). Dynamics of social behavior in fruit fly larvae. PLoS One, 9(4), p.e95495.
64. Eberhard, M.J.W., (1975). The evolution of social behavior by kin selection. The Quarterly Review of Biology, 50(1), pp.1-33.
65. Eichler, K., Li, F., Litwin-Kumar, A., Park, Y., Andrade, I., Schneider-Mizell, C.M., Saumweber, T., Huser, A., Eschbach, C., Gerber, B. and Fetter, R.D., (2017). The complete connectome of a learning and memory centre in an insect brain. Nature, 548(7666), p.175.

66. Einon, D.F. and Morgan, M.J., (1977). A critical period for social isolation in the rat. Developmental Psychobiology: The Journal of the International Society for Developmental Psychobiology, 10(2), pp.123-132.
67. Eklöv, P., (1992). Group foraging versus solitary foraging efficiency in piscivorous predators: the perch, Perca fluviatilis, and pike, Esox lucius, patterns. Animal Behaviour, 44, pp.313-326.
68. Fagiolini, M., Pizzorusso, T., Berardi, N., Domenici, L. and Maffei, L., (1994). Functional postnatal development of the rat primary visual cortex and the role of visual experience: dark rearing and monocular deprivation. Vision research, 34(6), pp.709-720.
69. Feinberg, E.H., VanHoven, M.K., Bendesky, A., Wang, G., Fetter, R.D., Shen, K. and Bargmann, C.I., (2008). GFP Reconstitution Across Synaptic Partners (GRASP) defines cell contacts and synapses in living nervous systems. Neuron, 57(3), pp.353-363.
70. Ferveur, J.F., Savarit, F., O'kane, C.J., Sureau, G., Greenspan, R.J. and Jallon, J.M., (1997). Genetic feminization of pheromones and its behavioral consequences in Drosophila males. Science, 276(5318), pp.1555-1558.
71. Fischer, C., Trautman, E. P., Crawford, J. M., Stabb, E. V., Handelsman, J., and Broderick, N. A. (2017). Metabolite exchange between microbiome members produces compounds that influence Drosophila behavior. eLife 6, e18855.
72. Fitzgerald, T.D. and Peterson, S.C., (1988). Cooperative foraging and communication in caterpillars. BioScience, 38(1), pp.20-25.
73. Flege, J.E., (1987). A critical period for learning to pronounce foreign languages?Applied linguistics, 8(2), pp.162-177.
74. Fleury, F., Ris, N., Allemand, R., Fouillet, P., Carton, Y., and Boulétreau, M. (2004). Ecological and genetic interactions in Drosophila-parasitoids communities: a case study with D. melanogaster, D. simulans and their common Leptopilina parasitoids in southeastern France. In Drosophila melanogaster, Drosophila simulans: So Similar, So Different (Springer Netherlands), pp. 181-194.
75. Foster, S.A., (1985). Group foraging by a coral reef fish: a mechanism for gaining access to defended resources. Animal Behaviour, 33(3), pp.782-792.
76. Freedman, D.G., King, J.A. and Elliot, O., (1961). Critical period in the social development of dogs. Science, 133(3457), pp.1016-1017.
77. Fushiki, A., Kohsaka, H. and Nose, A., (2013). Role of sensory experience in functional development of Drosophila motor circuits. PLoS One, 8(4), p.e62199.
78. Gazda, S.K., Connor, R.C., Edgar, R.K. and Cox, F., (2005). A division of labour with role specialization in group–hunting bottlenose dolphins (Tursiops truncatus) off Cedar Key, Florida. Proceedings of the Royal Society B: Biological Sciences, 272(1559), pp.135-140.
79. Gerber, B., Scherer, S., Neuser, K., Michels, B., Hendel, T., Stocker, R. F., and Heisenberg, M. (2004). Visual learning in individually assayed Drosophila larvae. J. Exp. Biol. 207, 179-188.
80. Ghent, A.W., (1960). A study of the group-feeding behaviour of larvae of the jack pine sawfly, Neodiprion pratti banksianae Roh. Behaviour, pp.110-148.
81. Giachello, C.N. and Baines, R.A., (2015). Inappropriate neural activity during a sensitive period in embryogenesis results in persistent seizure-like behavior. Current Biology, 25(22), pp.2964-2968.
82. Gilchrist, A.S. and Partridge, L., (1999). A comparison of the genetic basis of wing size divergence in three parallel body size clines of Drosophila melanogaster. Genetics, 153(4), pp.1775-1787.
83. Giraldeau, L.A. and Livoreil, B., (1998). Game theory and social foraging. Game theory and animal behavior, pp.16-37.
84. Giraldeau, L.A. and Caraco, T., (2018). Social foraging theory. Princeton University Press.
85. Giuggioli, L., Potts, J. R., Rubenstein, D. I., and Levin, S. A. (2013). Stigmergy, collective actions, and animal social spacing. Proc. Natl. Acad. Sci. U.S.A. 110, 16904-16909.
86. Godoy-Herrera, R., (1977). Inter-and intrapopulational variation in digging in Drosophila melanogaster larvae. Behavior genetics, 7(6), pp.433-439.
87. Godoy-Herrera, R., (1986). The development and genetics of digging behaviour in Drosophila larvae. Heredity, 56(1), p.33.

88. Golovin, R.M., Vest, J., Vita, D.J. and Broadie, K., (2019). Activity-Dependent Remodeling of Drosophila Olfactory Sensory Neuron Brain Innervation During an Early-Life Critical Period. Journal of Neuroscience, 39(16), pp.2995-3012.
89. Gordon, J.A. and Stryker, M.P., (1996). Experience-dependent plasticity of binocular responses in the primary visual cortex of the mouse. Journal of Neuroscience, 16(10), pp.3274-3286.
90. Goyal, L., McCall, K., Agapite, J., Hartwieg, E., and Steller, H. (2000). Induction of apoptosis by Drosophila reaper, hid and grim through inhibition of IAP function. EMBO J. 19, 589-597.
91. Gregg, T. G., McCrate, A., Reveal, G., Hall, S., and Rypstra, A. L. (1990). Insectivory and social digestion in Drosophila. Biochem. Genet. 28, 197-207.
92. Groh, C. and Meinertzhagen, I.A., (2010). Brain plasticity in Diptera and Hymenoptera. Frontiers in bioscience (Scholar edition), 2, p.268.
93. Hakuta, K., Bialystok, E. and Wiley, E., (2003). Critical evidence: A test of the critical-period hypothesis for second-language acquisition. Psychological science, 14(1), pp.31-38.
94. Hector, D.P., (1986). Cooperative hunting and its relationship to foraging success and prey size in an avian predator. Ethology, 73(3), pp.247-257.
95. Heisenberg, M., Heusipp, M. and Wanke, C., (1995). Structural plasticity in the Drosophila brain. Journal of Neuroscience, 15(3), pp.1951-1960.
96. Hensch, T.K., (2004). Critical period regulation. Annu. Rev. Neurosci., 27, pp.549-579.
97. Hensch, T.K. and Bilimoria, P.M., (2012), July. Re-opening windows: manipulating critical periods for brain development. In Cerebrum: The Dana forum on brain science (Vol. 2012). Dana Foundation.
98. Hiesinger, P.R., Zhai, R.G., Zhou, Y., Koh, T.W., Mehta, S.Q., Schulze, K.L., Cao, Y., Verstreken, P., Clandinin, T.R., Fischbach, K.F. and Meinertzhagen, I.A., (2006). Activity-independent prespecification of synaptic partners in the visual map of Drosophila. Current biology, 16(18), pp.1835-1843.
99. Hiromi, Y., Mlodzik, M., West, S.R., Rubin, G.M. and Goodman, C.S., (1993). Ectopic expression of seven-up causes cell fate changes during ommatidial assembly. Development, 118(4), pp.1123-1135.
100. Hirsch, H.V., Potter, D., Zawierucha, D., Choudhri, T., Glasser, A., Murphey, R.K. and Byers, D., (1990). Rearing in darkness changes visually guided choice behavior in Drosophila. Visual neuroscience, 5(3), pp.281-289.
101. Holtmaat, A. and Svoboda, K., (2009). Experience-dependent structural synaptic plasticity in the mammalian brain. Nature Reviews Neuroscience, 10(9), p.647.
102. Hoopfer, E.D., Jung, Y., Inagaki, H.K., Rubin, G.M. and Anderson, D.J., (2015). P1 interneurons promote a persistent internal state that enhances inter-male aggression in Drosophila. Elife, 4, p.e11346.
103. Hourcade, B., Muenz, T.S., Sandoz, J.C., Rössler, W. and Devaud, J.M., (2010). Long-term memory leads to synaptic reorganization in the mushroom bodies: a memory trace in the insect brain? Journal of Neuroscience, 30(18), pp.6461-6465.
104. Huang, Z.J., Kirkwood, A., Pizzorusso, T., Porciatti, V., Morales, B., Bear, M.F., Maffei, L. and Tonegawa, S., (1999). BDNF regulates the maturation of inhibition and the critical period of plasticity in mouse visual cortex. Cell, 98(6), pp.739-755.
105. Hubel, D.H. and Wiesel, T.N., (1970). The period of susceptibility to the physiological effects of unilateral eye closure in kittens. The Journal of physiology, 206(2), pp.419-436.
106. Hübener, M. and Bonhoeffer, T., (2014). Neuronal plasticity: beyond the critical period. Cell, 159(4), pp.727-737.
107. Huckaby, A., Dombrovski, M., Maher, E., Naimi, W., Perez, M., Skyberg, R., Smolko, C., Barford, K., Winckler, B. and Deppmann, C., (2001). Signalling from Endosomes and Exosomes. eLS, pp.1-7
108. Humberg, T. H., and Sprecher, S. G. (2017). Age-and wavelength-dependency of Drosophila larval phototaxis and behavioral responses to natural lighting conditions. Front. Behav. Neurosci. 11, 66.

109. Humberg, T. H., Bruegger, P., Afonso, B., Zlatic, M., Truman, J. W., Gershow, M., Samuel, A. and Sprecher, S. G. (2018). Dedicated photoreceptor pathways in Drosophila larvae mediate navigation by processing either spatial or temporal cues. Nat. Commun. 9, 1260.
110. Hurford, J.R., (1991). The evolution of the critical period for language acquisition. Cognition, 40(3), pp.159-201.
111. Immelmann, K.,)1972). Sexual and other long-term aspects of imprinting in birds and other species. In Advances in the Study of Behavior (Vol. 4, pp. 147-174). Academic press.
112. Immelmann, K., (1975). Ecological significance of imprinting and early learning. Annual review of ecology and systematics, 6(1), pp.15-37.
113. Inagaki, H.K., Jung, Y., Hoopfer, E.D., Wong, A.M., Mishra, N., Lin, J.Y., Tsien, R.Y. and Anderson, D.J., (2014). Optogenetic control of Drosophila using a red-shifted channelrhodopsin reveals experience-dependent influences on courtship. Nature methods, 11(3), p.325.
114. Irwin, D.E. and Price, T., (1999). Sexual imprinting, learning and speciation. Heredity, 82(4), p.347.
115. Jarecki, J. and Keshishian, H., (1995). Role of neural activity during synaptogenesis in Drosophila. Journal of Neuroscience, 15(12), pp.8177-8190.
116. Jenett, A., Rubin, G.M., Ngo, T.T., Shepherd, D., Murphy, C., Dionne, H., Pfeiffer, B.D., Cavallaro, A., Hall, D., Jeter, J. and Iyer, N., (2012). A GAL4-driver line resource for Drosophila neurobiology. Cell reports, 2(4), pp.991-1001.
117. Johnson, W.A. and Carder, J.W., (2012). Drosophila nociceptors mediate larval aversion to dry surface environments utilizing both the painless TRP channel and the DEG/ENaC subunit, PPK1. PloS one, 7(3), p.e32878.
118. Joseph, R.M., Devineni, A.V., King, I.F. and Heberlein, U., (2009). Oviposition preference for and positional avoidance of acetic acid provide a model for competing behavioral drives in Drosophila. Proceedings of the National Academy of Sciences, 106(27), pp.11352-11357.
119. Justice, E. D., Macedonia, N. J., Hamilton, C., and Condron, B. (2012). The simple fly larval visual system can process complex images. Nat. Commun. 3, 1156.
120. Kane, E.A., Gershow, M., Afonso, B., Larderet, I., Klein, M., Carter, A.R., De Bivort, B.L., Sprecher, S.G. and Samuel, A.D. (2013). Sensorimotor structure of Drosophila larva phototaxis. Proc. Natl. Acad. Sci. 110, E3868-E3877.
121. Kaun, K. R., Devineni, A. V., and Heberlein, U. (2012). Drosophila melanogaster as a model to study drug addiction. Hum. Genet. 131, 959-975.
122. Kayser, M.S., Yue, Z. and Sehgal, A., (2014). A critical period of sleep for development of courtship circuitry and behavior in Drosophila. Science, 344(6181), pp.269-274.
123. Keene, A. C., and Sprecher, S. G. (2012). Seeing the light: photobehavior in fruit fly larvae. Trends Neurosci. 35, 104-110.
124. Keene, A.C., Mazzoni, E.O., Zhen, J., Younger, M.A., Yamaguchi, S., Blau, J., Desplan, C. and Sprecher, S.G. (2011). Distinct visual pathways mediate Drosophila larval light avoidance and circadian clock entrainment. J. Neurosci. 31, 6527-6534.
125. Keller, L. (2009). Adaptation and the genetics of social behaviour. Philos. T. Roy. Soc. B 364, 3209-3216.
126. Kim, D., Alvarez, M., Lechuga, L. M., and Louis, M. (2017). Species-specific modulation of food-search behavior by respiration and chemosensation in Drosophila larvae. Elife 6, e27057.
127. Kim, D., Alvarez, M., Lechuga, L.M. and Louis, M., (2017). Species-specific modulation of food-search behavior by respiration and chemosensation in Drosophila larvae. Elife, 6, p.e27057
128. Kim, S.M., Su, C.Y. and Wang, J.W., (2017). Neuromodulation of innate behaviors in Drosophila. Annual Review of Neuroscience, 40, pp.327-348.
129. Kittel, R.J., Wichmann, C., Rasse, T.M., Fouquet, W., Schmidt, M., Schmid, A., Wagh, D.A., Pawlu, C., Kellner, R.R., Willig, K.I. and Hell, S.W. (2006). Bruchpilot promotes

active zone assembly, Ca2+ channel clustering, and vesicle release. Science 312, 1051-1054.
130. Klapoetke, N.C., Nern, A., Peek, M.Y., Rogers, E.M., Breads, P., Rubin, G.M., Reiser, M.B. and Card, G.M., (2017). Ultra-selective looming detection from radial motion opponency. Nature, 551(7679), p.237.
131. Klump, K.L., (2013). Puberty as a critical risk period for eating disorders: a review of human and animal studies. Hormones and behavior, 64(2), pp.399-410.
132. Kohsaka, H., Okusawa, S., Itakura, Y., Fushiki, A. and Nose, A., (2012). Development of larval motor circuits in Drosophila. Development, growth & differentiation, 54(3), pp.408-419.
133. Kohsaka, H., Zwart, M.F., Fushiki, A., Fetter, R.D., Truman, J.W., Cardona, A. and Nose, A., (2019). Regulation of forward and backward locomotion through intersegmental feedback circuits in Drosophila larvae. Nature communications, 10(1), p.2654.
134. Krishnan, K., Wang, B.S., Lu, J., Wang, L., Maffei, A., Cang, J. and Huang, Z.J., (2015). MeCP2 regulates the timing of critical period plasticity that shapes functional connectivity in primary visual cortex. Proceedings of the National Academy of Sciences, 112(34), pp.E4782-E4791.
135. Landgraf, M., Jeffrey, V., Fujioka, M., Jaynes, J.B. and Bate, M., (2003). Embryonic origins of a motor system: motor dendrites form a myotopic map in Drosophila. PLoS Biol, 1(2), p.e41.
136. Larderet, I., Fritsch, P.M., Gendre, N., Neagu-Maier, G.L., Fetter, R.D., Schneider-Mizell, C.M., Truman, J.W., Zlatic, M., Cardona, A. and Sprecher, S.G., (2017). Organization of the Drosophila larval visual circuit. Elife, 6, p.e28387.
137. Layalle, S., Arquier, N. and Léopold, P., (2008). The TOR pathway couples nutrition and developmental timing in Drosophila. Developmental cell, 15(4), pp.568-577.
138. LeBlanc, J.J. and Fagiolini, M., (2011). Autism: a “critical period” disorder? Neural plasticity, 2011.
139. LeDue, E.E., Mann, K., Koch, E., Chu, B., Dakin, R. and Gordon, M.D., (2016). Starvation-induced depotentiation of bitter taste in Drosophila. Current Biology, 26(21), pp.2854-2861
140. Lee, G., Foss, M., Goodwin, S.F., Carlo, T., Taylor, B.J. and Hall, J.C., (2000). Spatial, temporal, and sexually dimorphic expression patterns of the fruitless gene in the Drosophila central nervous system. Journal of neurobiology, 43(4), pp.404-426.
141. Leitão-Gonçalves, R., Carvalho-Santos, Z., Francisco, A.P., Fioreze, G.T., Anjos, M., Baltazar, C., Elias, A.P., Itskov, P.M., Piper, M.D. and Ribeiro, C., (2017). Commensal bacteria and essential amino acids control food choice behavior and reproduction. PLoS biology, 15(4), p.e2000862.
142. Levelt, C.N. and Hübener, M., (2012). Critical-period plasticity in the visual cortex. Annual review of neuroscience, 35, pp.309-330.
143. Lihoreau, M., Clarke, I. M., Buhl, J., Sumpter, D. J., and Simpson, S. J. (2016). Collective selection of food patches in Drosophila. J. Exp. Biol. 219, 668-675.
144. Lindstedt, C., Miettinen, A., Freitak, D., Ketola, T., López-Sepulcre, A., Mäntylä, E. and Pakkanen, H., (2018). Ecological conditions alter cooperative behaviour and its costs in a chemically defended sawfly. Proceedings of the Royal Society B: Biological Sciences, 285(1884), p.20180466
145. Lipton, A.J., Fujiyoshi, H. and Patil, R.S., (1998), October. Moving target classification and tracking from real-time video. In Applications of Computer Vision, 1998. WACV'98. Proceedings., Fourth IEEE Workshop on (pp. 8-14). IEEE.
146. Lorenz, K., (1935). Der kumpan in der umwelt des vogels. Journal of ornithology, 83(3), pp.289-413.
147. Luna, A. J. F., von Essen, A. M., Widmer, Y. F., and Sprecher, S. G. (2013). Light preference assay to study innate and circadian regulated photobehavior in Drosophila larvae. J Vis. Exp 74, e50237.
148. Marin, O., (2016). Developmental timing and critical windows for the treatment of psychiatric disorders. Nature medicine, 22(11), p.1229.

149. Mast, J. D., De Moraes, C. M., Alborn, H. T., Lavis, L. D., and Stern, D. L. (2014). Evolved differences in larval social behavior mediated by novel pheromones. Elife 3, e04205.
150. Mazzoni, E. O., Desplan, C., and Blau, J. (2005). Circadian pacemaker neurons transmit and modulate visual information to control a rapid behavioral response. Neuron 45, 293-300.
151. McDonald, K.S. and Kirn, J.R., (2012). Anatomical plasticity in the adult zebra finch song system. Journal of Comparative Neurology, 520(16), pp.3673-3686.
152. Meredith, R.M., Dawitz, J. and Kramvis, I., (2012). Sensitive time-windows for susceptibility in neurodevelopmental disorders. Trends in neurosciences, 35(6), pp.335-344.
153. Miroschnikow, A., Schlegel, P., Schoofs, A., Hueckesfeld, S., Li, F., Schneider-Mizell, C.M., Fetter, R.D., Truman, J.W., Cardona, A. and Pankratz, M.J., (2018). Convergence of monosynaptic and polysynaptic sensory paths onto common motor outputs in a Drosophila feeding connectome. eLife, 7, p.e40247.
154. Mirth, C., Truman, J.W. and Riddiford, L.M., (2005). The role of the prothoracic gland in determining critical weight for metamorphosis in Drosophila melanogaster. Current Biology, 15(20), pp.1796-1807.
155. Mirth, C.K. and Riddiford, L.M., (2007). Size assessment and growth control: how adult size is determined in insects. Bioessays, 29(4), pp.344-355.
156. Mirth, C.K. and Shingleton, A.W., (2012). Integrating body and organ size in Drosophila: recent advances and outstanding problems. Frontiers in endocrinology, 3, p.49
157. Mirth, C.K., Tang, H.Y., Makohon-Moore, S.C., Salhadar, S., Gokhale, R.H., Warner, R.D., Koyama, T., Riddiford, L.M. and Shingleton, A.W., (2014). Juvenile hormone regulates body size and perturbs insulin signaling in Drosophila. Proceedings of the National Academy of Sciences, 111(19), pp.7018-7023.
158. Monaghan, P. and Metcalfe, N.B., (1985). Group foraging in wild brown hares: effects of resource distribution and social status. Animal Behaviour, 33(3), pp.993-999.
159. Mosca, T. J., and Luo, L. (2014). Synaptic organization of the Drosophila antennal lobe and its regulation by the Teneurins. Elife 3, e03726.
160. Muraro, N.I., Weston, A.J., Gerber, A.P., Luschnig, S., Moffat, K.G. and Baines, R.A., (2008). Pumilio binds para mRNA and requires Nanos and Brat to regulate sodium current in Drosophila motoneurons. Journal of Neuroscience, 28(9), pp.2099-2109.
161. Murphey, R.K., Froggett, S.J., Caruccio, P., Shan-Crofts, X., Kitamoto, T. and Godenschwege, T.A., (2003). Targeted expression of shibirets and semaphorin 1a reveals critical periods for synapse formation in the giant fiber of Drosophila. Development, 130(16), pp.3671-3682.
162. Nardou, R., Lewis, E.M., Rothhaas, R., Xu, R., Yang, A., Boyden, E. and Dölen, G., (2019). Oxytocin-dependent reopening of a social reward learning critical period with MDMA. Nature, 569(7754), p.116.
163. Nern, A., Pfeiffer, B. D., and Rubin, G. M. (2015). Optimized tools for multicolor stochastic labeling reveal diverse stereotyped cell arrangements in the fly visual system. Proc. Natl. Acad. Sci. 112, E2967-E2976.
164. Neves, G., Cooke, S.F. and Bliss, T.V., (2008). Synaptic plasticity, memory and the hippocampus: a neural network approach to causality. Nature Reviews Neuroscience, 9(1), p.65.
165. Nitabach, M. N., Wu, Y., Sheeba, V., Lemon, W. C., Strumbos, J., Zelensky, P. K., and Holmes, T. C. (2006). Electrical hyperexcitation of lateral ventral pacemaker neurons desynchronizes downstream circadian oscillators in the fly circadian circuit and induces multiple behavioral periods. J. Neurosci. 26, 479-489.
166. Noë, R. (2006). Cooperation experiments: coordination through communication versus acting apart together. Anim. Behav. 71, 1-18.
167. Nordeen, K.W. and Nordeen, E.J., (1992). Auditory feedback is necessary for the maintenance of stereotyped song in adult zebra finches. Behavioral and neural biology, 57(1), pp.58-66.

168. Nottebohm, F., (1969). The “critical period” for song learning. Ibis, 111(3), pp.386-387.
169. Otto, N., Risse, B., Berh, D., Bittern, J., Jiang, X. and Klämbt, C., (2016). Interactions among Drosophila larvae before and during collision. Scientific reports, 6, p.31564.
170. Parnas, M., Lin, A.C., Huetteroth, W. and Miesenböck, G., (2013). Odor discrimination in Drosophila: from neural population codes to behavior. Neuron, 79(5), pp.932-944.
171. Pastuzyn, E.D., Day, C.E., Kearns, R.B., Kyrke-Smith, M., Taibi, A.V., McCormick, J., Yoder, N., Belnap, D.M., Erlendsson, S., Morado, D.R. and Briggs, J.A., (2018). The neuronal gene Arc encodes a repurposed retrotransposon Gag protein that mediates intercellular RNA transfer. Cell, 172(1-2), pp.275-288.
172. Patton, M.H., Blundon, J.A. and Zakharenko, S.S., (2019). Rejuvenation of plasticity in the brain: opening the critical period. Current opinion in neurobiology, 54, pp.83-89.
173. Pfeiffer, B.D., Jenett, A., Hammonds, A.S., Ngo, T.T.B., Misra, S., Murphy, C., Scully, A., Carlson, J.W., Wan, K.H., Laverty, T.R. and Mungall, C., (2008). Tools for neuroanatomy and neurogenetics in Drosophila. Proceedings of the National Academy of Sciences, 105(28), pp.9715-9720.
174. Pöysä, H., (1994). Group foraging, distance to cover and vigilance in the teal, Anas crecca. Animal Behaviour, 48(4), pp.921-928.
175. Pruitt, J.N. and Riechert, S.E., (2009). Frequency-dependent success of cheaters during foraging bouts might limit their spread within colonies of a socially polymorphic spider. Evolution: International Journal of Organic Evolution, 63(11), pp.2966-2973.
176. Punzo, F., (2002). Food imprinting and subsequent prey preference in the lynx spider, Oxyopes salticus (Araneae: Oxyopidae). Behavioural processes, 58(3), pp.177-181.
177. Qiao, H., Keesey, I.W., Hansson, B.S. and Knaden, M., (2019). Gut microbiota affects development and olfactory behavior in Drosophila melanogaster. Journal of Experimental Biology, 222(5), p.jeb192500.
178. Ramdya, P., Lichocki, P., Cruchet, S., Frisch, L., Tse, W., Floreano, D., and Benton, R. (2015). Mechanosensory interactions drive collective behaviour in Drosophila. Nature 519, 233-236.
179. Ramdya, P., Schneider, J., and Levine, J. D. (2017). The neurogenetics of group behavior in Drosophila melanogaster. J. Exp. Biol. 220, 35-41.
180. Rivers, D.B., Thompson, C. and Brogan, R., (2011). Physiological trade-offs of forming maggot masses by necrophagous flies on vertebrate carrion. Bulletin of entomological research, 101(5), pp.599-611.
181. Rohlfs, M. and Hoffmeister, T.S., (2004). Spatial aggregation across ephemeral resource patches in insect communities: an adaptive response to natural enemies? Oecologia, 140(4), pp.654-661.
182. Roper, M., Fernando, C., and Chittka, L. (2017). Insect bio-inspired neural network provides new evidence on how simple feature detectors can enable complex visual generalization and stimulus location invariance in the miniature brain of honeybees. PLoS Comput. Biol. 13, e1005333.
183. Sachse, S., Rueckert, E., Keller, A., Okada, R., Tanaka, N. K., Ito, K., and Vosshall, L. B. (2007). Activity-dependent plasticity in an olfactory circuit. Neuron 56, 838-850.
184. Sachse, S. and Beshel, J., (2016). The good, the bad, and the hungry: how the central brain codes odor valence to facilitate food approach in Drosophila. Current opinion in neurobiology, 40, pp.53-58.
185. Sanes, J. R., and Zipursky, S. L. (2010). Design principles of insect and vertebrate visual systems. Neuron 66, 15-36.
186. Saumweber, T., Rohwedder, A., Schleyer, M., Eichler, K., Chen, Y.C., Aso, Y., Cardona, A., Eschbach, C., Kobler, O., Voigt, A. and Durairaja, A., (2018). Functional architecture of reward learning in mushroom body extrinsic neurons of larval Drosophila. Nature communications, 9(1), p.1104.

187. Sawtell, N.B., Frenkel, M.Y., Philpot, B.D., Nakazawa, K., Tonegawa, S. and Bear, M.F., (2003). NMDA receptor-dependent ocular dominance plasticity in adult visual cortex. Neuron, 38(6), pp.977-985.
188. Scanvion, Q., Hédouin, V. and Charabidzé, D., (2018). Collective exodigestion favours blow fly colonization and development on fresh carcasses. Animal behaviour, 141, pp.221-232.
189. Schausberger, P., Walzer, A., Hoffmann, D. and Rahmani, H., (2010). Food imprinting revisited: early learning in foraging predatory mites. Behaviour, pp.883-897.
190. Scheel, D. and Packer, C., (1991). Group hunting behaviour of lions: a search for cooperation. Animal Behaviour, 41(4), pp.697-709.
191. Schlüter, M., Tavoni, A., and Levin, S. (2016). Robustness of norm-driven cooperation in the commons. In Proc. R. Soc. B (The Royal Society), vol. 283, No. 1822, p. 20152431.
192. Schmucker, D., Clemens, J.C., Shu, H., Worby, C.A., Xiao, J., Muda, M., Dixon, J.E. and Zipursky, S.L., (2000). Drosophila Dscam is an axon guidance receptor exhibiting extraordinary molecular diversity. Cell, 101(6), pp.671-684.
193. Schroll, C., Riemensperger, T., Bucher, D., Ehmer, J., Völler, T., Erbguth, K., Gerber, B., Hendel, T., Nagel, G., Buchner, E. and Fiala, A. (2006). Light-induced activation of distinct modulatory neurons triggers appetitive or aversive learning in Drosophila larvae. Curr. Biol. 16, 1741-1747.
194. Seabold, S., and Perktold, J. (2010). Statsmodels: Econometric and statistical modeling with python. In Proceedings of the 9th Python in Science Conference (Vol. 57, p. 61). Scipy.
195. Seggio, J.A., Possidente, B. and Ahmad, S.T., (2012). Larval ethanol exposure alters adult circadian free-running locomotor activity rhythm in Drosophila melanogaster. Chronobiology international, 29(1), pp.75-81.
196. Seugnet, L., Suzuki, Y., Donlea, J.M., Gottschalk, L. and Shaw, P.J., (2011). Sleep deprivation during early-adult development results in long-lasting learning deficits in adult Drosophila. Sleep, 34(2), pp.137-146
197. Shin, S.C., Kim, S.H., You, H., Kim, B., Kim, A.C., Lee, K.A., Yoon, J.H., Ryu, J.H. and Lee, W.J., (2011). Drosophila microbiome modulates host developmental and metabolic homeostasis via insulin signaling. Science, 334(6056), pp.670-674.
198. Silverman, B. W. (1998). Density estimation for statistics and data analysis. First edition (New York: Routledge).
199. Sizemore, M. and Perkel, D.J., (2011). Premotor synaptic plasticity limited to the critical period for song learning. Proceedings of the National Academy of Sciences, 108(42), pp.17492-17497.
200. Slepian, Z., Sundby, K., Glier, S., McDaniels, J., Nystrom, T., Mukherjee, S., and Condron, B. (2015). Visual attraction in Drosophila larvae develops during a critical period and is modulated by crowding conditions. J. Comp. Physiol. A 201, 1019-1027.
201. Sluckin, W., (2017). Imprinting and early learning. Routledge.
202. Sokabe, T., Chen, H. C., Luo, J., and Montell, C. (2016). A switch in thermal preference in Drosophila larvae depends on multiple rhodopsins. Cell Rep. 17, 336-344.
203. Sokolowski, M. B. (2010). Social interactions in “simple” model systems. Neuron 65, 780-794.
204. Sokolowski, M.B., (1982). Drosophila larval foraging behavior: Digging. Animal Behaviour, 30(4), pp.1252-1253.
205. Sprecher, S. G., Pichaud, F., and Desplan, C. (2007). Adult and larval photoreceptors use different mechanisms to specify the same Rhodopsin fates. Genes Dev. 21, 2182-2195.
206. Sprecher, S. G., Cardona, A., and Hartenstein, V. (2011). The Drosophila larval visual system: high-resolution analysis of a simple visual neuropil. Dev. Biol. 358, 33-43.
207. Stamps, J. A., Yang, L. H., Morales, V. M., and Boundy-Mills, K. L. (2012). Drosophila regulate yeast density and increase yeast community similarity in a natural substrate. PLoS One 7, e42238.

208. Strother, J. A., Nern, A., and Reiser, M. B. (2014). Direct observation of ON and OFF pathways in the Drosophila visual system. Curr. Biol. 24, 976-983.
209. Struhl, G. and Brower, D., (1982). Early role of the esc+ gene product in the determination of segments in Drosophila. Cell, 31(1), pp.285-292.
210. Sugie, A., Hakeda-Suzuki, S., Suzuki, E., Silies, M., Shimozono, M., Möhl, C., Suzuki, T. and Tavosanis, G., (2015). Molecular remodeling of the presynaptic active zone of Drosophila photoreceptors via activity-dependent feedback. Neuron, 86(3), pp.711-725
211. Sumpter, D.J., (2005). The principles of collective animal behaviour. Philosophical transactions of the royal society B: Biological Sciences, 361(1465), pp.5-22.
212. Suster, M.L. and Bate, M., (2002). Embryonic assembly of a central pattern generator without sensory input. Nature, 416(6877), p.174.
213. Svetec, N. and Ferveur, J.F., (2005). Social experience and pheromonal perception can change male–male interactions in Drosophila melanogaster. Journal of Experimental Biology, 208(5), pp.891-898.
214. Svetec, N., Cobb, M. and Ferveur, J.F., (2005). Chemical stimuli induce courtship dominance in Drosophila. Current biology, 15(19), pp.R790-R792.
215. Sykes, P. A., and Condron, B. G. (2005). Development and sensitivity to serotonin of Drosophila serotonergic varicosities in the central nervous system. Dev. Biol. 286, 207-216.
216. Szuperak, M., Churgin, M. A., Borja, A. J., Raizen, D. M., Fang-Yen, C., and Kayser, M. S. (2018). A sleep state in Drosophila larvae required for neural stem cell proliferation. Elife 7, e33220.
217. Takemura, S.Y., Bharioke, A., Lu, Z., Nern, A., Vitaladevuni, S., Rivlin, P.K., Katz, W.T., Olbris, D.J., Plaza, S.M., Winston, P. and Zhao, T. (2013). A visual motion detection circuit suggested by Drosophila connectomics. Nature 500, 175.
218. Takemura, S.Y., Aso, Y., Hige, T., Wong, A., Lu, Z., Xu, C.S., Rivlin, P.K., Hess, H., Zhao, T., Parag, T. and Berg, S., (2017). A connectome of a learning and memory center in the adult Drosophila brain. Elife, 6, p.e26975.
219. Tanaka, N.K., Endo, K. and Ito, K., (2012). Organization of antennal lobe-associated neurons in adult Drosophila melanogaster brain. Journal of Comparative Neurology, 520(18), pp.4067-4130.
220. Tang, H.Y., Smith-Caldas, M.S., Driscoll, M.V., Salhadar, S. and Shingleton, A.W., (2011). FOXO regulates organ-specific phenotypic plasticity in Drosophila. PLoS genetics, 7(11), p.e1002373.
221. Tania, N., Vanderlei, B., Heath, J.P. and Edelstein-Keshet, L., (2012). Role of social interactions in dynamic patterns of resource patches and forager aggregation. Proceedings of the National Academy of Sciences, 109(28), pp.11228-11233.
222. Taylor, M.L., Wigmore, C., Hodgson, D.J., Wedell, N. and Hosken, D.J., (2008). Multiple mating increases female fitness in Drosophila simulans. Animal Behaviour, 76(3), pp.963-970.
223. Technau, G.M., (1984). Fiber number in the mushroom bodies of adult Drosophila melanogaster depends on age, sex and experience. Journal of neurogenetics, 1(2), pp.113-126
224. Tennessen, J.M. and Thummel, C.S., (2011). Coordinating growth and maturation—insights from Drosophila. Current Biology, 21(18), pp.R750-R757.
225. Ting, C.Y., McQueen, P.G., Pandya, N., Lin, T.Y., Yang, M., Reddy, O.V., O'Connor, M.B., McAuliffe, M. and Lee, C.H. (2014). Photoreceptor-derived activin promotes dendritic termination and restricts the receptive fields of first-order interneurons in Drosophila. Neuron 81, 830-846.
226. Tognini, P., Putignano, E., Coatti, A. and Pizzorusso, T., (2011). Experience-dependent expression of miR-132 regulates ocular dominance plasticity. Nature neuroscience, 14(10), p.1237.
227. Tripet, F., Clegg, S., Elnaiem, D. E., & Ward, R. D. (2009). Cooperative blood-feeding and the function and implications of feeding aggregations in the sand fly, Lutzomyia longipalpis (Diptera: Psychodidae). PLoS neglected tropical diseases, 3(8), e503.

228. Tripodi, M., Evers, J.F., Mauss, A., Bate, M. and Landgraf, M., (2008). Structural homeostasis: compensatory adjustments of dendritic arbor geometry in response to variations of synaptic input. PLoS Biol, 6(10), p.e260.
229. Trowbridge, C.D., (1991). Group membership facilitates feeding of the herbivorous sea slug Placida dendritica. Ecology, 72(6), pp.2193-2203.
230. Turchin, P. and Kareiva, P., (1989). Aggregation in Aphis varians: an effective strategy for reducing predation risk. Ecology, 70(4), pp.1008-1016.
231. Valone, T.J., (1989). Group foraging, public information, and patch estimation. Oikos, pp.357-363.
232. Van Vactor Jr, D.L., Cagan, R.L., Krämer, H. and Zipursky, S.L., (1991). Induction in the developing compound eye of Drosophila: multiple mechanisms restrict R7 induction to a single retinal precursor cell. Cell, 67(6), pp.1145-1155.
233. van Versendaal, D., Rajendran, R., Saiepour, M.H., Klooster, J., Smit-Rigter, L., Sommeijer, J.P., De Zeeuw, C.I., Hofer, S.B., Heimel, J.A. and Levelt, C.N., (2012). Elimination of inhibitory synapses is a major component of adult ocular dominance plasticity. Neuron, 74(2), pp.374-383.
234. Venu, I., Durisko, Z., Xu, J. and Dukas, R., (2014). Social attraction mediated by fruit flies' microbiome. Journal of Experimental Biology, 217(8), pp.1346-1352.
235. Vickery, W.L., Giraldeau, L.A., Templeton, J.J., Kramer, D.L. and Chapman, C.A., (1991). Producers, scroungers, and group foraging. The american naturalist, 137(6), pp.847-863.
236. Wasserman, S.M., Aptekar, J.W., Lu, P., Nguyen, J., Wang, A.L., Keles, M.F., Grygoruk, A., Krantz, D.E., Larsen, C. and Frye, M.A., (2015). Olfactory neuromodulation of motion vision circuitry in Drosophila. Current Biology, 25(4), pp.467-472.
237. Watanabe, K., Chiu, H., Pfeiffer, B.D., Wong, A.M., Hoopfer, E.D., Rubin, G.M. and Anderson, D.J., (2017). A circuit node that integrates convergent input from neuromodulatory and social behavior-promoting neurons to control aggression in Drosophila. Neuron, 95(5), pp.1112-1128.
238. Wegman, L.J., Ainsley, J.A. and Johnson, W.A., (2010). Developmental timing of a sensory-mediated larval surfacing behavior correlates with cessation of feeding and determination of final adult size. Developmental biology, 345(2), pp.170-179.
239. Werker, J.F. and Hensch, T.K., (2015). Critical periods in speech perception: new directions. Annual review of psychology, 66, pp.173-196.
240. Wiesel, T.N. and Hubel, D.H., (1963). Single-cell responses in striate cortex of kittens deprived of vision in one eye. Journal of neurophysiology, 26(6), pp.1003-1017.
241. Wolf, A.P., (1995). Sexual attraction and childhood association: A Chinese brief for Edward Westermarck (pp. 147-8). Stanford: Stanford University Press.
242. Wu, Q., Wen, T., Lee, G., Park, J. H., Cai, H. N., and Shen, P. (2003). Developmental control of foraging and social behavior by the Drosophila neuropeptide Y-like system. Neuron 39, 147-161.
243. Yagi, R., Mabuchi, Y., Mizunami, M. and Tanaka, N.K., (2016). Convergence of multimodal sensory pathways to the mushroom body calyx in Drosophila melanogaster. Scientific reports, 6, p.29481.
244. Yanagihara, S. and Yazaki-Sugiyama, Y., (2016). Auditory experience-dependent cortical circuit shaping for memory formation in bird song learning. Nature communications, 7, p.11946.
245. Yoon, B.J., Smith, G.B., Heynen, A.J., Neve, R.L. and Bear, M.F., (2009). Essential role for a long-term depression mechanism in ocular dominance plasticity. Proceedings of the National Academy of Sciences, 106(24), pp.9860-9865.Physiological role
246. Yuan, Q., Xiang, Y., Yan, Z., Han, C., Jan, L. Y., and Jan, Y. N. (2011). Light-induced structural and functional plasticity in Drosophila larval visual system. Science 333, 1458-1462
247. Zheng, Z., Lauritzen, J.S., Perlman, E., Robinson, C.G., Nichols, M., Milkie, D., Torrens, O., Price, J., Fisher, C.B., Sharifi, N. and Calle-Schuler, S.A., (2018). A complete electron microscopy volume of the brain of adult Drosophila melanogaster. Cell, 174(3), pp.730-743.